UNIVERSITEIT VAN PRETORIA
UNIVERSITY OF PRETORIA
YUNIBESITHI YA PRETORIA

The effects of short-term temperature variations on activated sludge settling

by

Werner Herbert Rössle

Submitted in partial fulfilment of the requirements for the degree

of

Doctor in Philosophy in Engineering

in

The Faculty of Engineering, The Built Environment and Information Technology

University of Pretoria
Pretoria
South Africa

Study Leader: Professor W.A. Pretorius

August 2008

ABSTRACT

Settling properties of activated sludge or mixed liquor suspended solids (MLSS) have been studied for more than 75 years at wastewater treatment plants. Temperature, together with MLSS concentration, has been acknowledged as important contributors to MLSS settling variations. Batch MLSS settling tests are performed on a regular basis at most of the plants. The majority of these MLSS settling test reports reflect the complete absence of any form of temperature compensation or even MLSS sample temperature (T_s) recordings.

The objective of this study is to evaluate the effects of short-term temperature variations on MLSS settling parameters. This is done by means of simplified theoretical calculations, followed by operational reactor temperature (T_r) observations, and batch MLSS settling tests. The experimental work concludes with the implementation of an on-line MLSS settling test procedure at a full-scale plant reactor to develop settling models based on diurnal T_r fluctuations. These settling models illustrate that parameter correlations improve when T_r is included in on-line MLSS concentration-based settling models.

The unhindered settling velocity of a single solid biofloc in water is considered in a simplified calculation to estimate the effect of temperature variations on MLSS settling. Over a T_s increase of 20°C, water density and viscosity reductions result in a calculated biofloc settling velocity increase of less than 0.5 m/hr. Similarly, biofloc density, shape, and size changes result in calculated biofloc settling velocity increases of about 11, 10, and 2 m/hr respectively over the 20°C T_s range.

Plant temperature recordings show significant short- to long-term variations. Ambient temperature (T_a) and T_r fluctuate about 20°C and 1.8°C respectively per day, and T_r changes by about 4°C within a week, as measured on-line at local plants during the test period in winter. The aeration method can have a significant impact on T_r. Differences in T_r in adjacent surface and bubble aeration reactors in the same plant were about 5°C. Large enough T_r and T_a variations exist at these local plants to affect MLSS settling test results.

The MLSS settling test cylinder environment and meteorological conditions have a direct influence on T_s during batch settling tests. Direct solar radiation increases the average T_s by 4.3°C, or by 0.15°C per minute, during a 30-minute MLSS settling test duration. This T_s

change leads to a sludge volume index (SVI) change of 63 mℓ/g, at an average SVI decrease of 14.8 mℓ/g per 1°C T_s increase. Changes to other parameters include an initial settling velocity (ISV) increase of about 0.12 m/hr for every 1°C T_s increase, together with a clarified supernatant turbidity increase of about 1.4 formazine nephelometric unit (FNU) for every 1°C T_s increase. T_s adjusts towards T_a before and during a batch MLSS settling test, thereby influencing MLSS settling results. Compensation for T_s variations during routine MLSS settling tests is nevertheless not reported as a common practice. To some extent, this is due to a lack of temperature-controlled MLSS settling test equipment.

An automated MLSS settling meter demonstrates a semi-continuous on-line method to determine settling parameters *in situ* at the operational T_r of a full-scale plant. A basic polynomial fits 11 MLSS settling parameters that indicate in most instances improved MLSS settling at increased T_r. The average SVI decreases by 14.8 mℓ/g for every 1°C T_r increase. Similarly, for every 1°C T_r increase, the maximum settling velocity (u_max) increase is 0.1 m/hr, and the time to reach maximum settling velocity (t_umax) decreases by 2.4 minutes. The incremental 5-minute duration average settling velocities increase over the first 15 minutes of a MLSS settling test, as the MLSS concentration decreases and the T_r increases. This direct incremental settling velocity trend with T_r is reversed between 15 and 30 minutes, as the average 5-minute MLSS settling velocity increases at a reduced T_r.

The inclusion of T_r in MLSS concentration-based settling best-fit correlations with SVI, u_max, and t_umax improves the coefficient of multiple determinations (R^2) by an average of 0.32. Best-fit SVI models with u_max and t_umax have R^2-values of 0.90 and 0.95 respectively. The developed models are only valid for the individual reactor MLSS conditions within the experimental parameter ranges.

The main contribution of this study is to present temperature-based MLSS settling models. These models illustrate that an automated on-line MLSS settling meter is suitable to identify and model temperature related MLSS settling data with minimal experimental effort. A suitable approach is provided to improve the reliability of MLSS settling data, as effects of short-term temperature variations can be practically eliminated from settling test.

Keywords: activated sludge, batch test, biofloc, clarifier, MLSS, model, settling, SVI, temperature, wastewater.

SAMEVATTING

Besinkingskenmerke van geaktiveerde slyk of slykmengselsweefstowwe (SMSS) word al vir meer as 75 jaar by afvalwaterbehandelingsaanlegte bestudeer. Temperatuur, saam met SMSS konsentrasie, word erken as belangrike bydraers tot variasies in SMSS besinkingseienskappe. Lot SMSS besinkingstoetse word op 'n gereelde grondslag by die meeste aanlegte uitgevoer. Die meerderheid SMSS besinkingstoetsverslae toon egter geen vorm van temperatuur kompensasie of SMSS monstertemperatuur (T_s) lesings aan nie.

Die doel van hierdie studie is om die gevolge van korttermyn temperatuur variasies op basiese SMSS besinkingsparameters te evalueer. Die evaluasie is gebaseer op vereenvoudigde teoretiese berekeninge, gevolg deur reaktor bedryfstemperatuur (T_r) observasies, sowel as om lot SMSS besinkingstoetse te doen. Die eksperimentele werk is afgesluit met die implementering van 'n aanlyn SMSS besinkingstoets prosedure by 'n volskaal aanlegreaktor. Wanneer T_r ingesluit word, verbeter besinkingsparameter korrelasies in die konvensionele SMSS konsentrasie-gebaseerde besinkingsmodelle.

SMSS besinking is vereenvoudig deur die vrye besinkingssnelheid van 'n enkele soliede biovlok te bereken, sodat die effek van temperatuur variasies op die lot SMSS besinkingstoets benader kan word. Met 'n T_s verhoging van 20°C sal waterdigtheid en -viskositeit verlagings tot 'n biovlok besinkingssnelheid verhoging van minder as 0.5 m/hr lei. Soortgelyk sal biovlokdigtheid, -vorm, en -grootte veranderings lei tot biovlok besinkingssnelheid verhogings van ongeveer 11, 10 en 2 m/hr respektiewelik.

Aanlegtemperatuur lesings toon betekenisvolle kort- tot langtermyn variasies. Omgewingstemperatuur (T_a) and T_r fluktueer teen ongeveer 20°C en 1.8°C respektiewelik per dag, en T_r verander teen ongeveer 4°C per week, soos plaaslik aanlyn gemeet in winter. Die belugtingsmetode kan 'n beduidende invloed op T_r uitoefen. 'n Verskil van ongeveer 5°C is gemeet in T_r van oppervlak- en borrelbelugting reaktore in dieselfde aanleg. Daar is genoegsame T_r en T_a variasies op aanlegte om SMSS besinkingstoets resultate te beïnvloed.

Omgewings- en meteorologiese toestande by die besinkingstoets silinder het 'n direkte invloed op T_s gedurende lot SMSS besinkingstoetse. Direkte sonbestraling verhoog die gemiddelde T_s met 4.3°C, of teen 0.15°C per minuut, gedurende 'n tipiese 30-minute besinkingstoets periode. Hierdie T_s variasie veroorsaak 'n slykvolume-indeks (SVI)

verandering van 63 mℓ/g, teen 'n gemiddelde SVI verlaging van 14.8 mℓ/g per 1°C T_s verhoging. Veranderinge aan ander besinkingsparameters sluit in 'n aanvanklike besinkingssnelheid (ISV) verhoging van ongeveer 0.12 m/hr vir elke 1°C T_s verhoging, sowel as 'n verhoging van verhelderde bowater turbiditeit van ongeveer 1.4 formasien nephelometriese eenheid (FNU) per elke 1°C T_s verhoging. T_s verander na T_a voor en gedurende 'n lot SMSS besinkingstoets, en beïnvloed sodoende SMSS besinkingsresultate. T_s kompensasie werkswyses vir roetine SMSS besinkingstoetse is nieteenstaande steeds nie algemene praktyk nie, wat gedeeltelik toegeskryf kan word aan die gebrek aan temperatuur beheerbare besinkingstoets toerusting.

'n Outomatiese SMSS besinkingsmeter demonstreer 'n semi-kontinue aanlyn metode om besinkingsparameters te bepaal teen die operasionele T_r van 'n volskaal aanleg. 'n Basiese polinoom pas data van 11 besinkingsparameters om in die meeste gevalle 'n verbeterde SMSS besinkbaarheid by hoër T_r te toon. SVI verlaag teen 14.8 mℓ/g vir elke 1°C T_r verhoging. Vir die 1°C T_r verhoging is die maksimum besinkingssnelheid (u_max) verhoging 0.1 m/hr, en die verlaging in die tyd om u_max te bereik (t_umax) is 2.4 minute. In die eerste 15 minute van 'n besinkingstoets neem besinkingssnelheid toe soos SMSS konsentrasie afneem en T_r toeneem. Die direkte tendens tussen besinkingssnelheid en T_r is omgekeerd in die laaste 15 minute, en besinkingssnelheid neem dan toe by 'n verlaagde T_r.

Die insluiting van T_r in konsentrasie-gebaseerde besinkingsmodelle met SVI, u_max en t_umax verhoog die koëffisiënt van veelvuldige determinasies (R^2) teen 'n gemiddelde van 0.32. SVI modelle met u_max en t_umax het R^2-waardes van 0.90 en 0.95 respektiewelik. Die ontwikkelde modelle is slegs geldig vir die individuele reaktor SMSS kondisies in die eksperimentele parameter gebied.

Die hoofbydrae van hierdie studie is om temperatuur-gebaseerde SMSS besinkingsmodelle te ontwikkel. Hierdie modelle illustreer dat 'n outomatiese SMSS besinkingsmeter geskik is om temperatuur-verwante SMSS besinkingsdata aanlyn te identifiseer en te modelleer met minimum eksperimentele moeite. 'n Geskikte benadering word verskaf om die betroubaarheid van SMSS besinkingsdata te verbeter, omdat invloede van korttermyn temperatuur variasies prakties uitgeskakel word in SMSS besinkingstoetse.

Sleutelwoorde: afvalwater, besinking, biovlok, geaktiveerde slyk, lot toets, model, riool, SMSS, SVI, temperatuur.

TABLE OF CONTENTS

LIST OF TABLES

LIST OF FIGURES

LIST OF EQUATIONS

LIST OF PHOTOGRAPHS

NOMENCLATURE

Symbol / Acronym	Definition	Page when first used
a, b, c, d, e, f, g, h, i, j, k	regression coefficients	87
a, b, c	three periods of settling process	27
a, b, c	plant reactors used in experimental work	40
A, B, C, D, E	five settling stages of MLSS setting profile	27
Ave.	average	87
BNR	biological nutrient removal	1
C	Carbon	144
°C	degree(s) Celsius	18
$CaCO_3$	calcium carbonate	145
C_d	drag coefficient	29
Cl_2	chlorine	148
cm	centimetre	52
COD	chemical oxygen demand	144
d	day(s)	148
d_a	diameter biofloc	29
DO	dissolved oxygen	20
DSVI	diluted sludge volume index	13
e.g.	for example	22
et al.	and others	1
exp, e	exponent	9
ECP	exocellular polymers	143
EPBNR	excess phosphorus biological nutrient removal	148
f	function	9
FOG	fats, oils and grease	145
FNU	formazine nephelometric unit	52
g	gram(s)	146
g	gravitational acceleration constant	29
G	solids flux	9
g/ℓ	gram per litre	9
gSS/ℓ	gram suspended solids per litre	54
$g/m\ell$	gram per millilitre	34
h	settling meter liquid / MLSS interface height	67
hr	hour(s)	73
HRT	hydraulic retention time	146
i, ii, iii, iv	4 methods to acquire G	9
in situ	in natural or original place	23
ISV	initial settling velocity	8
kg	kilogram(s)	150
kHz	kiloHertz	140
kg/m^3	kilogram per cubic metre	29
ℓ	litres	1
LCVFA	long chain volatile fatty acid	144
m	metre(s)	15
mm	millimetre	29
mA	milliAmpere	64
mg	milligram(s)	59

ACKNOWLEDGEMENTS

1   INTRODUCTION

This chapter introduces the concept of temperature dependent MLSS settling tests, and it highlights the lack of temperature compensation or recording for these tests. The experimental focus is established on aspects of MLSS settling, according to the objectives of the study.

1.1   Background

Biological nutrient removal (BNR) processes suffer at times from activated sludge or mixed liquor suspended solids (MLSS) settleability problems (Grady and Filipe, 2000) that disturb the BNR treatment efficiency. Short-term (diurnal) temperature variations in reactor temperature (T_r) have been observed as having an effect on MLSS settleability (Wilén *et al.*, 2006). Scherfig *et al.* (1996) showed that T_r fluctuations are very dependent on local meteorological factors, such as ambient temperature (T_a), wind, and cloud cover. Where MLSS settling properties are traditionally determined batch-wise in 1 litre (ℓ) size cylinders (Gernaey *et al.*, 1998), it is to be expected that unless special care is taken, these meteorological factors will have an effect on the sample temperature (T_s). T_s is usually not reported in batch MLSS settling evaluations that is used to represent BNR MLSS settleability (Ekama *et al.*, 1997).

Based on the temperature dependency of MLSS settling, four aspects of settling evaluations are relevant to this study. These aspects are:

1. the effects of short-term T_s variations on MLSS settling parameters,
2. the T_r and T_a variations in full-scale plants,
3. batch MLSS settling tests under operational conditions, and
4. on-line MLSS settling monitoring at a full-scale plant reactor.

On-line MLSS settling monitoring data contains semi-continuous MLSS settling profiles (Vanrolleghem *et al.*, 1996). The settling profiles form the basis for the temperature dependent MLSS settling models proposed in this study. Settling parameter predictions are subsequently possible with these T_r-based models. These settling models assist with site-specific BNR MLSS settleability management.

1.2   Experimental work

The experimental work follows three distinct stages according to the project scope. The first stage is based on temperature observations at different plant reactors to determine the extent of typical T_r and T_a variations. The second stage includes batch MLSS settling tests to determine settling parameter changes occurring during temperature variations. The final experimental stage consists of on-line MLSS settling evaluations with an automated MLSS settling meter. This stage concludes with statistical calculations to evaluate the temperature-based MLSS settling models obtained from the on-line MLSS settling profiles.

1.3   Project scope

The aim of this project is to determine theoretically and experimentally the effects of short-term temperature variations on MLSS settling parameters. The following five sections address the project scope:

• Literature review on the influence of temperature on MLSS settling (Chapter 2):

The review covers the principles and monitoring of MLSS settling, operational plant temperature conditions, as well as batch and on-line MLSS settling parameter changes related to temperature variations. The aim of the review is to identify effects of short-term temperature variations during MLSS settling, as well as techniques or models that are in use to compensate for these typical temperature variations.

• Theoretical assessment of the influence of temperature and biofloc properties changes on a discrete settling biofloc (Chapter 3):

MLSS settling velocity changes over a temperature range are calculated for water density and viscosity changes, as well as particle density, size, and shape changes. The aim of the basic theoretical assessment is to illustrate potential changes in MLSS settling over a temperature range.

• Temperature survey at plant reactors (Chapter 4):

The extent of temperature (raw sewage, reactor, ambient) fluctuations and observable relationships are established at different plant reactors over short- and long-term periods.

- Batch MLSS settling evaluation based on temperature variations (Chapter 5):

Changes in batch MLSS settling parameters are evaluated according to sample container size, reactor zone sample source, as well as typical container environments found during settling tests, based on short-term temperature variations.

- On-line MLSS settling evaluation based on diurnal temperature variations (Chapter 6):

Diurnal changes in on-line MLSS settling meter data is established, before best-fit models of settling parameters illustrate the impact of T_r inclusion in MLSS concentration-based models. Sludge volume index (SVI) relationships are correlated with the maximum settling velocity (u_max) and the time (t) to reach u_max (t_umax). Finally, simulations of 11 settling parameters with diurnal MLSS concentration and T_r variations in simplified models illustrate the extent of changes in the parameters during temperature variations.

1.4   Conclusions

The purpose of this study is to demonstrate that short-term temperature variations are an essential component of traditional MLSS settling tests. Four temperature-related MLSS settling aspects in this study comprise of a theoretical settling calculation, short- and long-term plant temperature fluctuation identification, batch MLSS settling evaluations, and on-line MLSS settleability monitoring. The development of MLSS settling models and parameter correlations that incorporate temperature concludes the project.

The development of plant specific temperature dependent MLSS settling correlations provides the opportunity to improve traditional MLSS concentration-based settling models. Specialised methods and equipment are required to capture the effects of operational plant temperature variations. Improved MLSS settling models, based on these temperature variations, will provide additional information to assist with the management and design of wastewater treatment plants.

2   LITERATURE REVIEW

This chapter reviews basic MLSS settling tests, operational temperature data, as well as batch and automated MLSS settling tests and parameters, which are applied in the experimental project stage. The purpose of this review is to identify reported correlations, or lack thereof, between MLSS settling parameters and temperature.

2.1   Background

MLSS settling has been investigated for more than 75 years in the wastewater industry (Dick and Vesilind, 1969), during which time numerous reports confirm that temperature influences aspects of MLSS settleability. Werker (2006) classifies dynamic temperature conditions as a dominant environmental factor in wastewater treatment plant processes. These temperature variations are characterised by short-term (diurnal) and long-term (seasonal) cyclic fluctuations (Baetens *et al.*, 1999) that are present at plant reactors. Makinia *et al.* (2005) modelled these fluctuations as basic sinusoidal wave profiles, which follow both cyclic daytime / nighttime and summer / winter heating and cooling stages. These temperature fluctuations lead to physical, chemical, and biological changes in MLSS (Janssen *et al.*, 2002) that will influence the settleability of the MLSS.

Ekama *et al.* (1997) consider indirect effects of temperature fluctuations on MLSS settleability, such as structural changes in biofloc, as more important than direct effects, such as liquid viscosity and density changes. The combined direct and indirect effects of short-term temperature fluctuations on MLSS settleability have not been studied in any detail (Krishna and Van Loosdrecht, 1999). Long-term temperature fluctuations effects on MLSS settling are well described, as seasonal BNR process performance variations and related MLSS settleability changes can usually be easily detected from long-term trends based on routine tests (Osborn *et al.*, 1986).

Information and implementation guidelines for temperature compensation, based on short-term temperature variations during MLSS settling tests, are still lacking (Wilén, 1999). The effects of these short-term temperature variations during basic MLSS settling tests, as represented by empirical settling correlations, need to be quantified and modelled accordingly.

This literature review considers the effects of short-term temperature variations on MLSS settling parameters. The review focuses on four aspects of MLSS settling tests, which are in accordance with the objectives of this project:

1. principles and monitoring of MLSS settling,
2. operational plant temperature conditions,
3. batch MLSS settling tests and temperature variations, and
4. on-line MLSS settling tests and temperature variations.

2.2   Principles and monitoring of MLSS settling

2.2.1   MLSS settling and temperature relationship

The basic ecological unit of MLSS is a biofloc (Bux and Kasan, 1994a). Inside such a biofloc, temperature variations result in physiochemical and microbiological changes (Makinia *et al.*, 2005). Gerardi (2002) recognizes that these physical and biological changes have opposite effects on biofloc settling.

On the one hand, the physical effects of a temperature increase leads to improved (faster) biofloc settling, due to lower water viscosity and density, as well as structural biofloc changes. On the other hand, bacterial activity increases at a higher temperature. Bioflocs absorb or entrap the increased production and accumulation of insoluble biological secretions, such as lipids and oils, and this leads to worse (slower) biofloc settling. Air or gas bubble entrapment, usually from denitrification of anaerobic sludge rich in nitrate (Kazami and Furumai, 2000), decreases this sludge settling velocity further.

These opposing and time-dependent temperature effects change biofloc and MLSS characteristics (Örmeci and Vesilind, 2001). Temperature variations before and during MLSS settling tests will for that reason complicate MLSS settling evaluations.

2.2.2   MLSS settling and MLSS concentration relationship

Throughout the MLSS settling process, the settling velocity of a particle or a singular biofloc depends on its individual characteristics, as well as interactions with other particles or bioflocs (Mazzolani *et al.*, 1998). Figure 2-1, adapted from Ekama (1988),

illustrates in this settling process the relationship between MLSS concentration and interparticle actions or flocculation tendency. MLSS settling and liquid clarification processes are divided into four classes according to the MLSS concentration and interparticle flocculation tendency.

The top sections of the graph (Classes I and II) represent liquid clarification. Single particles settle without interparticle action during Class I, and bioflocs settle with limited interactions during Class II, governed by the flocculation tendency. Hindered MLSS settling follows, represented in the middle section of the graph (Class III) to indicate the switch to zone settling at constant and maximum velocity. The bottom section of the graph (Class IV) represents the reduced settling velocity during transition, before the final compression or thickening leads in time to a stationary settled MLSS (Dupont and Dahl, 1995).
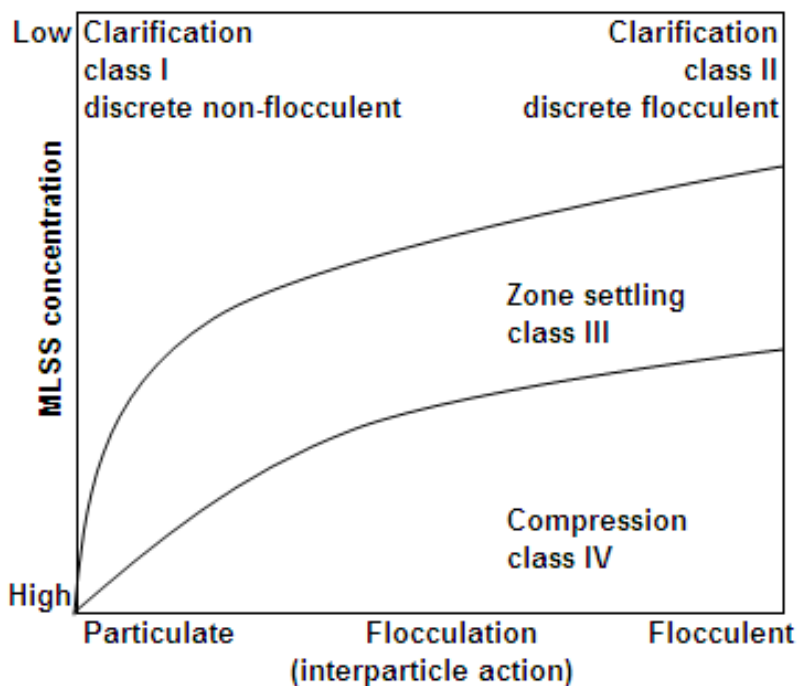
Figure 2-1 MLSS settling behaviour classified as Class I to IV according to MLSS concentration and interparticle actions

Basic mathematical equations illustrate the liquid clarification or Class I MLSS settling process, as well as the associated effects of temperature variations on settling. The resulting force of gravity and frictional shear (Catunda and Van Haandel, 1992) determines the settling velocity of individual particles. Due to the low MLSS

concentration of Class I settling, the particle motion is not affected by other particles, by the settling container wall, or by turbulent currents (Kolmetz *et al.*, 2003). This particle settling in water is temperature dependent according to fundamental correlations. Class I clarification can thus be modelled from basic principles in theoretical models.

Class II to IV flocculent clarification to MLSS compression processes, at increasing MLSS concentration ranges, depend on complex forces in a matrix of interlinked bioflocs (Catunda and Van Haandel, 1992). Keller *et al.* (2002) concluded that the mechanisms of MLSS flocculation (Class II to IV) are still poorly understood. These mechanisms depend on interrelated physical, chemical, and biological factors (Jin *et al.*, 2003) that are all temperature dependent. Stypka (1998) and Biggs *et al.* (2003) confirmed that these processes cannot be presented in a fundamental theoretical model without experimental settleability tests. Class II to IV processes are thus based on empirical settling models.

The four settling classes shown in Figure 2-1 indicate that MLSS settling is dependent on two factors, (i) the MLSS concentration, and (ii) the particle flocculation tendency. Several models have been developed for general and specific use to represent MLSS settleability (Krebs, 1995). According to the literature, the MLSS concentration is the only factor considered in most of these settling models.

2.2.3   MLSS settling parameters: identification and development

Ekama *et al.* (1985) define the MLSS settling profile as the basic measurement of a manual MLSS settling test. Settling parameters that are calculated from this profile include the settled MLSS volume after 30 minutes (SV_{30}), settling indexes such as the SVI, as well as settling velocities occurring during the different stages of the settling process. The magnitude of these settling parameters that represent a well-settling MLSS depends on local plant conditions and process performance requirements.

Cloete and Muyima (1997) specify that settling parameters of a well-settling MLSS represent a fast settling MLSS leaving a clear supernatant, combined with a stable settled MLSS at a reduced volume. The features of such a well-settling MLSS relate to the settling parameter guidelines according to four stages in the MLSS settling profile. These features are summarised in Table 2-1, as adapted from Tandoi *et al.* (2006) and Cloete and Muyima (1997).

Table 2-1 MLSS settleability criteria according to four settling stages

Settling parameter	MLSS criterion
Liquid clarification	SS concentration <= 15 mgSS/ℓ
Reflocculation or lag (stage 1)	Commences after few (usually 2 to 5) min.
ZSV (stage 2)	Well-settling > 3 m/hr
	Light = 2 to 3 m/hr
	Bulking < 1.2 m/hr
Transition (stage 3); Compression (stage 4)	Thickened (no excessive volume), no guideline
Stability	No rising for few (usually 2 to 3) hours
SVI	Well-settling < 100 to 150 mℓ/g
	Light = 100 to 200 mℓ/g
	Bulking > 150 to 200 mℓ/g

For a well-settling MLSS, the stage 1 reflocculation (lag) duration is about 2 to 5 minutes, followed by the stage 2 zone settling velocity (ZSV) proceeding at a constant velocity of more than 3 m/hr. There are no guidelines available for the stage 3 and 4 transition and compression stages, although the compressed MLSS volume should be concentrated to occupy a small volume. The stage 4 compressed MLSS should remain settled for a few hours, without rising or disintegrating. A clarified supernatant suspended solids (SS) concentration of less than 15 mgSS/ℓ indicates sufficient removal of SS from the clarified supernatant.

A SVI lower than about 100 to 150 mℓ/g indicates good MLSS settling, while a higher SVI indicates poor settling (Casey *et al.*, 1995). These high SVI conditions are usually, but not always, associated with a bulking MLSS (Blackbeard *et al.*, 1986). Bulking is a state where the MLSS settling velocity is low and the compression is poor (Novák *et al.*, 1993) Good MLSS settleability can be defined as a fast settling MLSS with a low SVI (Jenkins *et al.*, 1984), based on a small SV_{30}.

Bye and Dold (1998) reviewed the basic settling parameters calculation methods used to obtain settleability data. Table 2-2 lists a summary of these techniques. Three basic calculation techniques between MLSS concentration and initial settling velocity (ISV) are established by (i) direct measurement, (ii) using existing correlations based on indexes

such as SVI, and (iii) using a clarifier operational chart, also based on indexes such as SVI (Hasselblad and Xu, 1996).

Table 2-2 MLSS settling parameters development techniques and use

Step	Action	Method
1	Determine MLSS concentration (X)	Standard Method 2540D (APHA, 1998) or MLSS concentration meter
2	Determine settling profile	Plot of settling volume or interface height vs. time for 30 minute duration
3	Determine SV_{30}	Read from settling profile and calculate settled volume after 30 minutes
4	Determine ISV	Read from settling profile and calculate settling velocity between 2 and 5 minutes
5	Determine ZSV	Read from settling profile and calculate settling velocity at constant slope section
6	Calculate SVI	SV_{30} / X
7	Calculate solids flux (G)	G = ZSV. X
8i	Generate flux curve directly from experimental data	G vs. X (8 to 12 MLSS samples with X range from 2 to 12 g/ℓ)
8ii	Generate flux curve from empirical equation (e.g. $V_s = v_o e^{-nX}$)	Fit ZSV and X by regression to v_o and n $V_s = v_o e^{-nX}$ with V_s and X data
8iii	Generate flux curve from correlations of SVI with v_o and n	v_o = f(SVI), n = f(SVI) $V_s = v_o e^{-nX}$ with V_s and X experimental data
8iv	Obtain G from operational chart	Read off flux by using SVI and X

Kazami and Furumai (2000) report that future MLSS settling research will be focussed to replace the flux curve experimental method (8i in Table 2-2), as the experimental procedure is based on time-consuming and laborious tests. Multiple batch settling tests at a range of MLSS concentrations (at least 8 tests from about 2 to 12 g/ℓ, Ekama *et al*., 1985) are required to generate a flux curve. The preferred method for regular use is to apply correlations to relate MLSS settling velocity to basic measurable settling parameters, such as SVI (8iii or 8iv in Table 2-2). Vanderhasselt and Vanrolleghem (2000) caution, however, against the indiscriminate use of such correlations, as the MLSS settling velocity is influenced by factors not normally incorporated in correlations between MLSS concentration and SVI.

2.2.4 MLSS settling indexes

2.2.4.1 SVI

Mohlman, as cited by Dick and Vesilind (1969), developed the SVI in 1934 to be a basic measure of the physical properties of MLSS. The SVI test is regarded in certain circumstances as an unreliable settling measurement, as the initial MLSS concentration influences the SVI inconsistently (Catunda and van Haandel, 1992). Ekama *et al.* (1985) found SVI comparison to be most unpredictable when the MLSS samples are sourced from different plants at different MLSS concentrations, while Berktay (1998) considered the SVI as unreliable when the MLSS settleability is poor. Poor settleability is usually found in bulking MLSS (Blackbeard *et al.*, 1986) or in settled MLSS with a high SV_{30} (SV_{30} > 400 mℓ/ℓ, Ekama *et al.*, 1985). Schuler and Jang (2007a) summarised the criticism against SVI, by noting that the SVI is a composite, indirect measurement that may not be representative of the four MLSS settling classes taking place in a secondary settling tank.

These and other inadequacies of SVI are categorised in Table 2-3 as five features of the MLSS sample. These features listed in Table 2-3 indicate that SVI test results interpretation depends largely on the experimental procedures implemented for the batch MLSS settling test. The MLSS sample condition, sample modifications, container size, settling parameters required, as well as the test method, all play a role in the calculated SVI test results.

Table 2-3 Reported SVI test deficiencies or limitations

Feature	Deficiency	Reference
MLSS sample condition		
MLSS concentration	SVI highly dependent on MLSS, inconsistent relationship	Dick and Vesilind, 1969
Rheological characteristics	SVI not related to yield strength or to rheological properties	Dick and Vesilind, 1969
Filaments	SVI not well related to filament number or length	Blackbeard *et al.*, 1986
MLSS sample modification		
Temperature	SVI inverse power relationship at 5 to 45°C, inconsistent relationship	Dick and Vesilind, 1969
Stirring	SVI reduces by gentle stirring, removes cylinder wall effects	Dick and Vesilind, 1969; Berktay, 1998
Dilution	SVI reduces by dilution, removes the MLSS concentration effect	Ekama and Marais, 1984
MLSS settling test cylinder		
Cylinder diameter	SVI dependent on cylinder diameter, according to MLSS properties	Dick and Vesilind, 1969
Cylinder depth	SVI dependent on cylinder depth, according to MLSS properties	Dick and Vesilind, 1969
MLSS settling parameters		
Initial settling velocity	SVI not related to ISV	Dick and Vesilind, 1969
Zone settling velocity	SVI not related to ZSV	Ekama and Marais, 1986
Settling profile response	SVI only dependent on one final point on settling profile	Dick and Vesilind, 1969
MLSS settling test method		
Batch method	Frequency of tests usually only once per day	Vanrolleghem and Lee, 2003
On-line method	Equipment not readily available for continuous and automated monitoring	Sekine *et al.*, 1989

Ignorance or confusion continues to exist regarding the most suitable procedure for the SVI test, according to the different methods and equipment used in the reviewed literature. Bye and Dold (1998) contribute this uncertainty in part to the prescribed SVI test procedure (APHA, 1998) that changed in 1980. The basic quiescent MLSS sample settling method was then modified to include slow stirring at 1 to 2 revolutions per minute

(rpm) of the MLSS sample. The SVI test procedure (method 2710D; APHA, 1998) is, strictly speaking, a stirred specific volume index (SSVI) procedure, but it is designated as a SVI. This procedure further states that the T_s of the MLSS sample must be maintained at T_r during a SVI test, without providing implementation guidelines.

Table 2-4 SVI test method according to APHA (1998)

Test component	Method	Remarks from literature
Container size and type	1 ℓ cylinder	Volume and shape (diameter and height) varies
Stirring	1 to 2 rpm	Samples are unstirred or stirred
Temperature	at T_r	No T_s information or T_s compensation or control procedures for changes from T_r
Test duration	30 minutes	Standard 30-min. duration usually not changed
Container material	not stated	Material and wall thickness varies
MLSS sample source	not stated	Taken at BNR reactor outlet

A summary of the variables of the SVI test method (APHA, 1998) is provided in Table 2-4. In literature, the prescribed SVI test method modifications usually involve any combination of three of the six test components, which are (i) container size, (ii) stirring, and (iii) temperature compensation:

(i) The zone settling velocity of MLSS samples (stirred or unstirred) could be affected by the settling container size (diameter and height), depending on the MLSS characteristics. Renko (1996) concludes that a suspension with a low MLSS concentration settles faster in a small diameter cylinder, due to liquid streaming up the cylinder walls. A suspension with a high MLSS concentration settles slower in a small diameter cylinder, as a result of biofloc bridging and support. (ii) Ekama *et al*. (1985) state that gentle MLSS sample stirring reduces cylinder wall effects, short-circuiting, as well as MLSS concentration effects. The MLSS concentration effects reduce mainly due to better biofloc agglomeration during stirring (Vanrolleghem and Lee, 2003). Nevertheless, sample stirring does not completely overcome the effect of MLSS concentration, as demonstrated by Dick and Vesilind (1969) with different MLSS samples. (iii) Details of prescribed equipment and methods to compensate for temperature changes before and during MLSS settling tests are for the most part absent from the available literature.

Bye and Dold (1998) and Lilley *et al.* (1997) confirm that SVI tests for routine use are usually performed at room temperature in a laboratory, and more often than not with an

unstirred MLSS sample. The continued use of the unstirred SVI at room temperature can be attributed to the simplicity and convenience of this SVI method (Schuler and Jang, 2007a), as specialised equipment and procedures for stirring and in particular temperature compensation are not readily available for routine use.

2.2.4.2 Alternative indexes

Ekama *et al.* (1985) and Daigger (1995) promote the replacement of SVI, in process design as well as plant operation and control, by alternative indexes. The most common modifications to the standard SVI include sample stirring or sample dilution, or both. A standard SVI test with sample stirring is named a SSVI. A MLSS sample dilution changes a SVI to a diluted SVI (DSVI). Ekama and Marais (1984) provide guidelines for SVI determinations at a fixed MLSS concentration of 3.5 g/ℓ (unstirred $SVI_{3.5}$ or stirred $SVI_{3.5}$), as well as a DSVI test method.

Table 2-5 Alternative MLSS settling indexes

Index name		Procedure
$SVI_{3.5}$	SVI at standard MLSS concentration of 3.5 g/ℓ	SVI test is performed at a fixed MLSS concentration of 3.5 g/ℓ by sample dilution
SSVI	Stirred specific volume index	Test cylinder is equipped with a slowly rotating stirring device (about 1 rpm)
$SSVI_{3.5}$	Stirred specific volume index at standard MLSS concentration of 3.5 g/ℓ	SSVI test is performed at a fixed MLSS concentration of 3.5 g/ℓ by sample dilution, 2.6 ℓ column
DSVI	Diluted SVI	Sample dilution to obtain a SV_{30} value smaller than 200 or 250 mℓ (Bye and Dold, 1998) after 30 minutes MLSS settling, 1 ℓ cylinder

These alternative settling indexes are summarised in Table 2-5 (adapted from Cloete and Muyima, 1997). The DSVI is performed in a 1 ℓ graduated cylinder, and the $SSVI_{3.5}$ in a 2.6 ℓ column. The recommended depth to diameter ratio for tall columns are prescribed at greater than 9:1, but recommended ratios for 1 ℓ cylinders are absent. Temperature compensation procedures are not supplied in the available literature for the determination of any of the alternative indexes. These settling index test procedures only address MLSS sample stirring, and in some instances the size of the settling container.

The use of alternative indexes, specifically the DSVI, can change the MLSS sample characteristics. Chaignon *et al.* (2002) caution that MLSS sample dilution for the DSVI test, with a supernatant of different ionic strength such as potable water, could lead to deflocculation. Unchlorinated secondary clarified effluent is a suitable dilution medium for the DSVI test (Jeyanayagam *et al.*, 2006). The effects of temperature changes during this MLSS sample dilution with plant effluent are not adequately addressed in available research reports. A DSVI test extends the SVI range (White, 1976), as the dilution reduces the MLSS concentration, but DSVI does not consider the MLSS compression characteristics. White, as cited by Ekama and Marais (1984), proposed the use of the $SSVI_{3.5}$ (at a fixed MLSS concentration of 3.5 g/ℓ), as the SSVI is not always independent of MLSS concentration.

Daigger (1995) cautions that there is not sufficient reference data available to develop improved empirical correlations for these alternative indexes, when compared to the large collection of available SVI data. Operational and research reference data in the literature is generally related to SVI (Mines and Horn, 2004), with fewer case studies using alternative indexes. The effects of temperature variations on these alternative settling indexes are not readily available in the literature. The alternative settling index interpretation depends accordingly on experimental conditions, as is applicable to SVI.

2.2.4.3   Future SVI use with settling parameters

Akça *et al.* (1993) confirm that SVI is still a useful and a valuable indicator of MLSS settling and thickening characteristics. Several South African treatment plants perform SVI tests as the only routine indicator to monitor MLSS settleability (Casey and Alexander, 2001). SVI is also extensively used in various modelling applications. MLSS settling characterization that precedes MLSS settling model selection is often based on SVI (Vanrolleghem *et al.*, 2003), due to SVI data and model availability. Such SVI-based models are used in several applications, amongst others to predict settleability failures (Banadda *et al.*, 2005). Recently, Martínez *et al.* (2006) developed a case-based reasoning tool for MLSS separation, and SVI is included as a quantitative indicator of MLSS settleability. The simplicity of the SVI test is the main reason for its continued extensive use in these various operational and modelling applications (Akça *et al.*, 1993), despite all the publicised shortcomings.

Table 2-6 Experimental conditions for SVI use in settling parameter correlations

Parameter	Cylinder size	T_r, T_s, T_a	Stirred	Reference
Minimum ZSV	1 ℓ	Unknown	No	Bhargava and Rajagopal, 1993
Sonification time	1 ℓ	Unknown	Unknown	Bień *et al*., 2005
Tank bottom SS concentration	1 and 2 m tall columns	Unknown	Unknown	Kazami and Furumai, 2000
Tank average SS concentration	1 ℓ	Unknown	1 rpm	Kim *et al*., 1997
Biological and physico-chemical parameters	Unknown	Unknown	$SSVI_{3.5}$	Sponza, 2004

Several SVI-based parameter correlations, as summarised in Table 2-6, are used for operational process control, design and modelling. SVI is correlated in five different applications, as listed in Table 2-6, to settling velocity, sonification time (ultrasonic floc disintegration time), settled and suspended MLSS concentration, and biofloc properties. SVI is included as an independent variable in all of these correlations, but once again without any temperature related reference information.

2.2.5 SVI and settling velocity correlations

MLSS settling proceeds through different settling velocities (Zhang *et al*, 2006a) during a 30-minute test period. Discrete, zone settling, and compression settling velocities are three separate processes taking place. The zone settling velocity is considered as a key parameter, due to its use in design and operational MLSS settling control.

Most empirical ZSV models include MLSS concentration as the only independent variable, although a variety of mathematical expressions with calibrated constants are used (Smollen and Ekama, 1984). The exponential Vesilind function is the most widely used model, and it links the maximum MLSS settling velocity (the ZSV) to the MLSS concentration (Grijspeerdt *et al*., 1995) as follows:

$$V_s = v_o . e^{-n.X}$$

where V_s represents ZSV, X represents the initial MLSS concentration, and v_o and n are MLSS-specific settling constants.

The MLSS settling constants v_o and n define settling characteristics (Daigger and Roper, 1985). These constants require calibration to reactor process conditions and MLSS properties for each individual plant reactor (Bergh, 1996). The ZSV is also named constant- (Bhargava and Rajagopal, 1993), hindered- (Dupont and Dahl, 1995), highest- (Gernaey *et al.*, 1998), relative- (Bergh, 1996), or maximum settling velocity (Lynggaard-Jensen and Lading, 2006). The v_o constant is also named initial settling velocity (Lynggaard-Jensen and Lading, 2006). The use of numerous terms indicates that detailed experimental MLSS settling information is required to ensure parameters are interpreted correctly.

Catunda and Van Haandel (1992) found that parameter values that characterise MLSS settleability exhibit considerable oscillations around average values. This noticeable scatter in experimental settling results is frequently reported (Kristensen *et al.*, 1994). Daigger and Roper (1985) found likewise a great deal of experimental settling data scatter, and they had to separate SVI data in four SVI ranges to improve correlations.

Table 2-7 Experimental conditions for SVI use in settling velocity correlations

Parameter	Empirical equation	Reference	Cylinder	T_r, T_a, T_s	Stirred
Settling velocity, V_s	$V_s = 7.80e^{-[0.148 + 0.00210.(SVI)].X}$	Daigger and Roper (1985)	1 ℓ	Unknown	1 rpm
Settling velocity, V_s	$V_s = (17.4e^{-0.00581.SVI} 3.931).\exp(-(-0.9834.e^{-0.00581.SVI} +1.043).X)$	Härtel and Pöpel (1992)	Not stated, equation was compiled from various data sources		
Settling velocity, V_s	$V_s = (28.1 (SVI)^{-0.2667}).\exp(-(0.177+0.0014.SVI).X)$	Akça *et al.* (1993)	Not stated, equation was compiled from various data sources		

Empirical correlations between ZSV and SVI attempt to make MLSS settling predictions easier. The SVI-based settling velocity correlations listed in Table 2-7 illustrate the additional uses of SVI in MLSS settling correlations, as well as the continued lack of temperature related reference data.

None of the previous studies explicitly addresses temperature fluctuations as a possible contributing factor to variations in the empirical MLSS settling correlations results. The extent of temperature variations under operational and laboratory test conditions must be determined to consider the possible impact of temperature on MLSS settling.

2.3   Operational plant temperature conditions

2.3.1   Overview

Various T_r models have recently been developed. Wells *et al*. (2005) describe several model improvements to allow plant designers and operators to predict reactor and plant effluent temperature variations. These models are developed in order to design treatment plant structures to avoid low T_r conditions, or to reduce the heat load from the final effluent discharge to rivers during cold winter months (Makinia *et al.*, 2005). These T_r-based model developments are for the most part unrelated to MLSS settleability, as correlations between modelled T_r fluctuations and MLSS settleability variations have not been considered in the available literature.

2.3.2   Modelling temperature variations

Makinia *et al*. (2005) present reviews of several dynamic T_r models that predict temperature fluctuations in full-scale reactors. Several energy contributions of heat gains and losses that influence this T_r are summarised in Table 2-8, according to model components provided by Gillot and Vanrolleghem (2003) and Makinia *et al*. (2005).

These T_r models illustrate the extent of temperature variations possible at a treatment plant. Table 2-8 indicates that, although the raw sewage plant inlet temperature (T_{raw}) component is the largest single contributor to T_r, the combined site-specific conditions have a larger influence on T_r. The contribution of energy components can change on a short- and a long-term basis, according to local conditions. For example, cloud cover and

shading have a direct effect on the contribution from solar radiation (Scherfig *et al.*, 1996).

Table 2-8 Typical range of energy contributions to influence T_r

Energy transfer phenomena	Temperature change [°C/day]
Significant energy contributions:	
Sensible heat (inflow)	0.5 to 3.5 decrease or increase
Solar radiation	0.5 to 2.5 increase
Surface evaporation	0.5 to 2.5 decrease
Process energy (exothermic biochemical reactions)	0.5 to 2.0 increase
Atmospheric radiation	0.5 to 1.0 decrease
Insignificant energy contributions:	
Precipitation (rain / snow on surface)	<0.2 decrease or increase
Mechanical energy (aerators / mixers)	<0.1 increase
Geothermal energy (basin wall convection / conduction)	<0.05 decrease or increase

An overview of temperature data for raw wastewater, reactors, secondary settling tanks, as well as the surrounding environment (ambient), provide an indication of the expected range of operational temperature variations. These variations will contribute towards the change from T_r to T_s during batch MLSS settling tests, as well as temperature-based MLSS settling changes in reactors and secondary settling tanks.

2.3.2.1 Ambient temperature

Observations by Banks *et al.* (2003) confirm that short-term T_a fluctuations follow diurnal sinusoidal wave profiles. These T_a profiles are mirrored, with a lag period, by changes in temperatures of affected water bodies, such as plant T_r. There will be damping effects present in these T_r profiles with increased depth, if the reactor content is not well mixed.

Sinusoidal wave profiles are also present in long-term (seasonal) T_a changes, as illustrated in Figure 2-2. The meteorological data for Johannesburg, South Africa, provides an average diurnal T_a fluctuation of 12°C, based on monthly averages over a 30-year period (South African Weather Service, 2007). The average fluctuation moves from an average daily minimum of 10°C to an average daily maximum of 22°C, as illustrated in Figure 2-2. The lowest and highest recorded T_a is -8°C and 35°C respectively, as measured in winter (June) and summer (January).
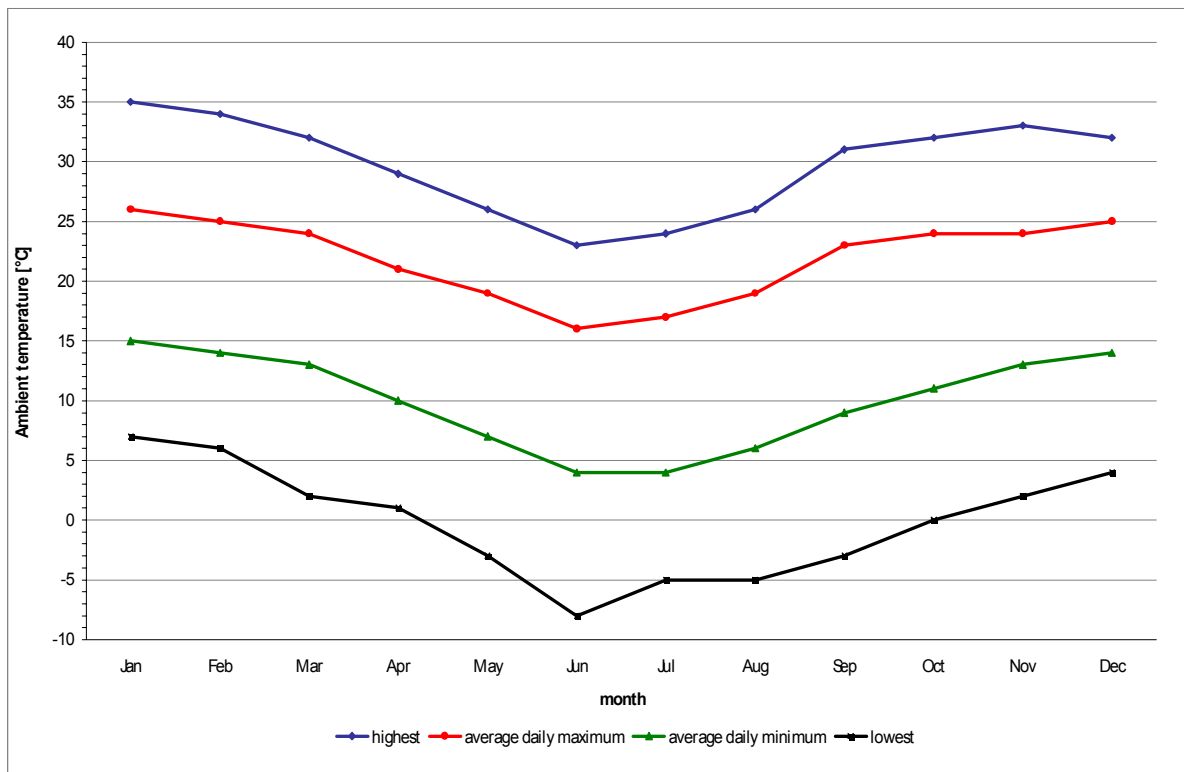
Figure 2-2 Annual T_a profiles for Johannesburg, South Africa

2.3.2.2 Raw wastewater temperature

There is limited information available about the short-term and long-term changes in T_{raw}. These T_{raw} variations are due to cyclic domestic water uses and industrial processes, with additional contributions from industrial process unit shut-downs and start-ups (Morgan-Sagastume and Allen, 2003), as well as seasonal climate changes. Short-term meteorological conditions should also influence T_r, but this could not be confirmed from the available literature. T_{raw} variations are plant specific, but T_{raw} data is usually not required for plant performance monitoring.

Wahlberg *et al.* (1996) demonstrate the extent and influence of unique plant specific T_{raw} variations with a case study. An average winter T_r reduced subsequently in spring by 2°C, from 10.3°C to 8.3°C, due to the colder snowmelt inclusion in a wastewater plant inflow. A guideline for industrial effluent contributions to sewer networks limit the maximum discharge temperature to 45°C (IWPC, 1977), although T_{raw} was at that stage not related to T_r.

2.3.2.3 Reactor temperature

The long-term average T_r fluctuation for design calculations in South Africa has been approximated as 8°C (WRC, 1984), based on a minimum and maximum T_r of 14 and 22°C respectively. Osborn *et al*. (1986) reported the same seasonal T_r measurements, of 14 and 22°C, for a plant in Johannesburg. Long-term T_r variations of up to 13°C have been detected in European plants, such as 7 to 20°C for the Klaby plant in Sweden (Ingildsen, 2002), as well as 9 to 22°C for the Katwoude plant in the Netherlands (Janssen *et al.*, 2002). These long-term T_r fluctuations are subject to individual plant conditions and seasonal meteorological conditions.

Psychrophilic, mesophilic, and thermophilic bacteria function in low (0 to 15°C), medium (15 to 40°C), and high (40 to 75°C) temperature ranges respectively (Droste, 1997). No single organism will grow over all three temperature ranges, although MLSS bacteria can tolerate short-term exposure to high temperatures (Archibald and Young, 2004). Temperature exerts a selective pressure to create medium- to long-term microbiological population shifts (Erdal, 2002). Most municipal wastewater treatment plants operate in the psychrophilic or lower mesophilic temperature range, while industrial effluent plants such as pulp and paper mills operate in the higher mesophilic or thermophilic range (Archibald and Young, 2004). Long-term MLSS settleability evaluations outside the operational T_r range can therefore produce inconsistent settling test results, to some extent due to microbial population shifts.

Bubble or diffused air aeration reactors have higher T_r than comparable surface aeration reactors, due to the addition of warm compressed air that can reach 85°C at source (Maqueda *et al.*, 2006). Pitman (1991) observed that a plant with a bubble aeration system produced MLSS with excellent settling properties, at maximum 60 mℓ/g DSVI, against DSVI values of up to 300 mℓ/g at two nearby plants equipped with mechanical surface aeration systems. Parker (2004) contributed this kind of improved settleability to the superior air and dissolved oxygen (DO) distribution of bubble aerators. The influence of higher T_r in bubble aeration reactors on MLSS settleability is not well documented in the available literature.

Scherfig *et al*. (1996) observe frequent T_r drops of 2 to 3°C over a few days when winter weather patterns in Europe change rapidly. The diurnal T_r fluctuation is in the range 0.5 to

1.0°C (Makinia *et al.*, 2005). The temperature change from the reactor inlet to outlet is reported at about -1.0 to 0.5°C in winter, compared to 0.5 to 1.5°C in summer. These T_r variations are once again subject to individual plant conditions.

2.3.2.4 Secondary settling tank temperature

The formation of concentration and thermal density currents in secondary settling tanks are created by SS concentration and temperature differences (De Clercq *et al.*, 2003). These temperature differences are as small as 0.2°C. Taebi-Harandy and Schroeder (2000) experimentally confirmed these small temperature differences, as well as related settleability changes. The MLSS inflow from the reactor, the MLSS in the settling tank, the return activated sludge (RAS), the clarified effluent from the tank, as well as the top surface effluent layer, all exhibit different temperatures that can be related to T_a (Tadesse *et al.*, 2004). Density currents cause short-circuiting (Kim *et al.*, 2003) as MLSS inflow moves over dead space (when warmer and lighter) or under dead space (when colder and heavier) inside a secondary settling tank.

Denitrification in a secondary settling tank is regulated by the NO_3^- / NO_2^- concentration and the sludge residence time (Azimi and Horan, 1991). There is furthermore a correlation between temperature and the denitrification rate, as the buoyancy of gas bubbles increases by 15% for a MLSS temperature increase of 10°C (Ekama *et al.*, 1997). Sarioglu and Horan (1996) determined that the gas bubble size is dependent on temperature. At lower temperatures (<15°C), the small gas bubbles result in a critical nitrogen concentration (rising sludge) of 13 to 16.5 mgN/ℓ that decreases to about 8 to 13 mgN/ℓ at higher temperatures. Settled MLSS stability is therefore temperature dependent.

Solar radiation (Schutte, 2006) and changing wind patterns (Van Der Walt, 1998) create diurnal temperature changes in secondary settling tanks. Kim *et al*. (2006) modelled the effect of these diurnal temperature fluctuations on MLSS settling flow patterns. A positive heat flux is created by daytime solar radiation once T_a is about 2°C warmer than the tank MLSS influent. This temperature increase results in density currents and cascading flow patterns. Conversely, a negative heat flux is created by nighttime and winter surface cooling once T_a is 2°C cooler than the tank MLSS influent. This temperature decrease results in buoyant flow, a surface current and significant short-circuiting. Jokela and Immonen (2002) studied the impact of the lower winter water

temperatures (3 to 12°C) on activated sludge clarification in a chemical-industry wastewater treatment plant. They observed sludge settling deterioration and ultimate sludge carry-over during variable and lower temperatures. These results confirm the general hypothesis of the direct link between MLSS settleability and temperature.

The temperature dependent MLSS settling process in a secondary settling tank is simulated by manual batch MLSS settling tests. For these tests, the temperature impact on MLSS samples in containers will vary according to procedures and equipment used.

2.4 Batch MLSS settling tests and temperature variations

Batch MLSS settling tests should preferably be carried out on-site as soon as possible after a MLSS sample is collected (Ho *et al.*, 2006). The immediate testing of MLSS samples ensures the sample is fresh (Ekama, 1988). Wilén (1999) recommends that T_s is as close as possible to T_r during settling tests, as storage (specifically at 4°C) results in a reduction in microbial activity and a larger tendency of the MLSS to deflocculate. Neither T_s nor T_a is as a rule regulated or monitored during batch MLSS settling tests. Research reports mention occasionally that a settling test is performed at a laboratory or room temperature (Chaigon *et al.*, 2002). Constant room temperatures are in such cases assumed, if not specified (Grijspeerdt and Verstraete, 1997; Hercules *et al.*, 2002).

Most research reports disregard the requirement to create uniform temperature conditions throughout the MLSS settling container content. Tchobanoglous *et al.* (2003) caution against T_s variations inside large settling columns. For this reason, Clements (1976) insulates settling columns with polystyrene to minimise changes to T_s. Simon *et al.* (2005) specifies a maximum 2°C difference between T_s and T_a to minimise the effects of convection on samples during MLSS settling. These references appear to be the only reports in the available literature to address the control of T_s inside settling containers.

Different types and sizes of containers are used for batch MLSS settling tests. Tchobanoglous *et al.* (2003) describe these containers as 1 or 2 ℓ graduated cylinders or 2 ℓ settlometers (usually wider than 2 ℓ graduated cylinders), as well as larger settling columns. These columns vary in size, from 1.8 m (Bye and Dold, 1999) to 3 m (Clements, 1976) tall. The basic 30-minute batch MLSS settling test in such a container is the short-

term simulation of reactor MLSS settleability. The reactor MLSS settles subsequently in a downstream secondary settling tank.

2.5   On-line MLSS settling tests and temperature variations

It is not realistic to measure MLSS settling in an operational secondary settling tank (Forster and Dallas-Newton, 1980), as the liquid / MLSS interface blanket height changes according to the hydraulic load on the settling tank. An *in situ* MLSS settling test approach is recommended, which suggests on-line MLSS settling measurements at the reactor. Rasmussen and Larsen (1997) state that such semi-continuous on-line methods can identify variations in MLSS settling properties that are not easily detected with batch settling tests.

Vanrolleghem and Lee (2003) find the scarcity of on-line instrumentation for MLSS settling monitoring in wastewater treatment plants surprising. They blame this monitoring deficiency on the lack of fundamental insights in the determination of MLSS settling factors. Grijspeerdt *et al.* (1995) recognise that specific research from the early 1990s attempts to develop reliable on-line MLSS settling sensors. This technological progress results in the development and implementation of novel sensors, suitable for aspects of on-line settleability monitoring and control.

2.6   Summary

The MLSS settling process depends on the MLSS concentration and the flocculation tendency of SS particles. The flocculation tendency is governed by complex physical, chemical, and biological interactions. Temperature has opposite effects on these physical and biological changes, and MLSS settleability changes are therefore difficult to predict.

Several parameters represent the MLSS settleability, with SVI still regarded as the most widely used parameter, in spite of several limitations. Alternative indexes have been developed, but SVI is still preferred for routine and modelling use, mainly due to the simplicity and convenience of the experimental test procedure. The lack of reported temperature data in MLSS settling test results, although required by standard methods,

suggests that temperature compensation is not performed during these experimental procedures.

Existing plant temperature models include energy components that contribute to create site-specific T_r profiles. These T_r profiles usually mirror with lag short- and long-term T_a fluctuations. MLSS settling is very sensitive to meteorological conditions at full-scale secondary settling tanks. It is obvious that these conditions, specifically temperature, wind, and sunshine, will have a similar significant influence on batch MLSS settling test results. Inadequate information was found in the available literature on the use of batch settling equipment with temperature compensation facilities to manage changes from T_r to T_s, due to the influence of T_a.

Automated MLSS settling meters are suitable equipment for on-line MLSS settleability evaluations. Surprisingly, the reported on-line settling meter applications over diurnal T_r fluctuations excluded temperature-based settling models. On-line monitoring of MLSS settling during these diurnal temperature fluctuations provides as a result an opportunity to correlate possible relationships between MLSS settling parameters and temperature.

2.7 Conclusions

The review of the literature, relating temperature to MLSS settling, indicates that there is a lack of reported MLSS settling data subject to short-term temperature fluctuations. The following conclusions are based on the literature survey:

• Unhindered single particle settling can be represented by theoretical equations. The temperature variation effect on particle settling velocity can be calculated from these equations. Hindered MLSS settling requires though empirical correlations that are developed from experimental data. Unhindered or hindered MLSS settling correlations that incorporate T_s or T_r are not available from the literature survey.

• MLSS settling parameters are determined from basic batch MLSS settling tests, based on standard methods that require the implementation of temperature compensation. Details of methods or equipment suitable for temperature compensation are not obtained from the literature survey.

- Reactor temperature models are available for short- and long-term temperature fluctuation simulations. The literature survey indicates that MLSS settling aspects are not incorporated in these reactor temperature models.

- SVI is still the most prevalent settling index used by operators, although the deficiencies, amongst others a significant temperature reliance, has been reported for more than 75 years. T_r recordings and T_s compensation procedures during batch MLSS settling tests are absent from the reported literature. Suitable settling equipment details, to compensate for short-term temperature effects, are also not readily available.

- Numerous settling models provide relationships between SVI and MLSS settling velocity. It appears from the literature survey that temperature compensation is absent from these MLSS settling models.

- A small number of on-line MLSS settling meters have been developed and successfully tested in pilot and full-scale reactors. These settling meters have, however, not been utilised to identify MLSS settling parameter relationships based on short-term temperature fluctuations.

MLSS settling dependence on temperature variations are sufficiently demonstrated in the literature survey to merit proceeding with the rest of the research program, as represented by the research aims.

2.8   Research aims

The purpose of this study is to demonstrate that short-term temperature variations are an essential component of traditional MLSS settling determinations. Consequently, this research focuses on four aspects, owing to their relevance to MLSS settling tests and monitoring, combined with the identified lack of operational temperature information from the literature survey:

- The theoretical impact of temperature on unhindered biofloc settling will be calculated. The changes in unhindered biofloc settling velocity over a temperature range will

illustrate the extent of possible MLSS settling velocity changes due to temperature variations.

- The magnitude of short- and long-term temperature variations will be established with an operational plant survey. Significant T_r variations will confirm the need to determine the impact of T_r fluctuations on MLSS settling parameters.

- Batch MLSS settling tests will establish the sensitivity of settling parameters to environmental conditions. The extent of settling parameter variations will indicate if the current lack of temperature compensation or reference temperature data in MLSS settling tests require future equipment and procedure improvements.

- On-line MLSS settling evaluations will be conducted to establish the effect of diurnal T_r fluctuations on MLSS settling parameters. The temperature-based settling parameter correlations will be compared to traditional MLSS concentration-based correlations to evaluate the impact of T_r inclusion. T_r-based settling parameter modelling will be based on best-fit and simplified curve-fitting procedures to illustrate the effects of short-term T_r variations on MLSS settling.

The above-mentioned four main research aims are individually addressed in the subsequent four chapters.

3 THEORETICAL FRAMEWORK

This chapter illustrates the effects of temperature changes on the Class I liquid clarification process. Basic theoretical principles are used to calculate settling velocity changes of an unhindered biofloc in water under variable temperature conditions.

3.1 Background

Theoretical MLSS settling models are required to calculate the influence of temperature on MLSS settling. The MLSS settling processes progress through 3 settling periods, as illustrated in Figure 3-1 (adapted from Ekama *et al.*, 1997). The first period (a) represents the start of the settling process at a uniform initial MLSS concentration (A). The second period (b) represents four interrelated MLSS settling processes (B, C, D, E). Liquid clarification (B), MLSS zone settling (C), MLSS transition (D), and MLSS compression (E) take place concurrently during this second period. The last period (c) represents the end of the MLSS settling processes, when the sample contains a clarified supernatant (B) and a settled MLSS (E).
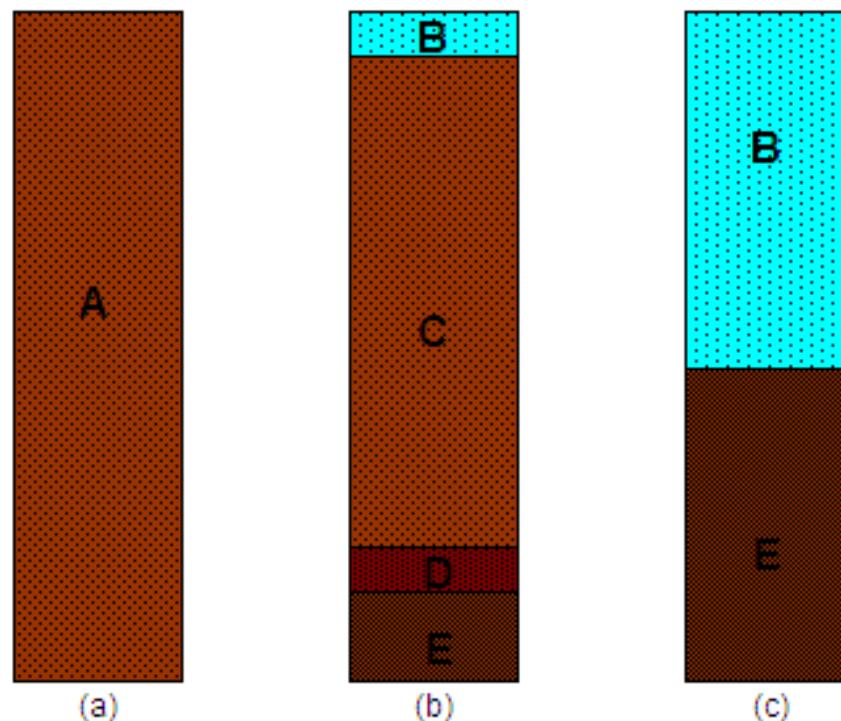
Figure 3-1 Unhindered (B) and hindered (C, D, E) settling of MLSS sample (A) in a container for three periods (a, b, c) of settling process

The hindered MLSS settling stages A and C to E are represented by simple empirical to complicated settling models based on fundamental mechanisms (Stypka, 1998). The liquid clarification stage B is represented by basic theoretical principles to describe the settling velocity of a spherical solid particle in liquid across a temperature range. In such a theoretical model, a solid particle represents a biofloc. A shape factor modifies the spherical particle to represent a non-spherical solid biofloc. This simplification excludes additional biofloc characteristics, such as porosity and biological components.

A simplified theoretical model, based on discrete, unhindered solid biofloc settling, hence represents MLSS settling. This simplified model expresses the settling velocity changes of the modified biofloc due to the effect of temperature variations on the water and biofloc characteristics.

The aim of this chapter is to illustrate the influence of temperature variations on the settling velocity of a simplified biofloc.

3.2   Materials and methods

3.2.1   Modelling approach

A simplified theoretical model illustrates the biofloc settling velocity changes over an extended operational temperature range. Variations in water viscosity and density, as well as in the key biofloc properties density, size, and shape (Scuras *et al.*, 1998), are used in the biofloc settling velocity calculations.

3.2.2   Discrete biofloc settling theory

Stokes' settling model equation (Cho *et al.*, 1993) calculates the unhindered settling velocity of a solid spherical biofloc in the laminar flow regime. Yuan (2001) derives Stokes' equation in detail from basic force relationships. A shape factor (Φ) is included to simulate the effect of the non-spherical biofloc shape (Gregory and Zabel, 1990) in the calculation of the biofloc settling velocity (u), valid when Re < 1, and Re = $24\Phi/C_d$:

$$u = (\rho_a - \rho_w)\ g\ d_a^2 / (18\mu\Phi),$$

where g is the gravitational constant, Re is the Reynolds number, and C_d is the empirical drag coefficient.

Water temperature has a direct impact on the physical state of water (Weast, 1985), in terms of the absolute water viscosity (μ) and the water density (ρ_w). Water temperature influences the physical state of the biofloc (Gerardi, 2002), in terms of the biofloc density (ρ_a), the biofloc size expressed as diameter (d_a), and Φ. The parameters representing the water and biofloc properties are varied over a range of values, as listed in Table 3-1, to determine the unhindered biofloc settling velocity changes. Average values, as indicated, are used in the simulations during the variation of each parameter.

Table 3-1 Simulation ranges used for water and biofloc characteristics

Parameter	Average value used in simulations	Start of simulation	End of simulation
Temperature	-	5°C	25°C
Water viscosity	-	1.523E-3 Ns/m^2	9.41E-4 Ns/m^2
Water density	998.89 kg/m^3	999.94 kg/m^3	997.08 kg/m^3
Biofloc density	1014 kg/m^3	1005.5 kg/m^3	1022.5 kg/m^3
Biofloc size	800 μm (0.8 mm)	10 μm (0.01 mm)	1410 μm (1.4 mm)
Biofloc shape	15	20	1

The water viscosity and water density variation is fixed from 1.523E-3 Ns/m^2 to 9.41E-4 Ns/m^2, and 999.94 kg/m^3 to 997.08 kg/m^3 respectively, due to the relationship with temperature over the range of 5 to 25°C (Weast, 1985). Biofloc size varies from small microflocs of 10 to 20 μm diameter (Wilén, 1999) to macroflocs up to 1400 μm diameter (Kim *et al.*, 2006), with an average diameter size range of 10 to 1000 μm (Andreadakis, 1993). Biofloc density varies from a lower range of 1015 to 1034 kg/m^3 (Andreadakis, 1993) to between 1020 and 1062 kg/m^3 (Yuan, 2001; Etterer and Wilderer, 2001). A low biofloc density range of 1005.5 to 1022.5 kg/m^3 is used to limit the rapid settling velocity increase of an single biofloc. The biofloc shape factor (Gregory and Zabel, 1990) ranges from 1 for a spherical particle up to and greater than 20 for a non-spherical biofloc.

3.2.3   Data presentation

The Microsoft Excel (Excel, 2007) curve fitting function is used to represent water density and water viscosity data in graphical format on 2-dimensional (2-D) graphs. The

coordinate system consists of the horizontal x_1-axis representing the property parameter of water as the dependent variable, and the vertical y_1-axis representing the discrete biofloc settling velocity as the response variable.

The two-input data table function of the Microsoft Excel is used to calculate the 3-dimensional (3-D) correlations. The correlations are calculated between changes in temperature (represented by water viscosity and density), the biofloc property (density, size, or shape), and the biofloc settling velocity, according to the data range in Table 3-1. The results from the calculated data are represented by the surfaces on the 3-D graphs. The bands of colour indicate changes in the settling velocity ranges, as listed in the legend box placed next to the graph. The horizontal x_1-axis and x_2-axis indicate the biofloc property and the temperature-based viscosity as the two dependent variables. The vertical y_1-axis represents the calculated discrete biofloc settling velocity as the response variable.

The coefficient of multiple determinations (R^2), as calculated by Microsoft Excel, measures the proportion of variation in the data points that are represented by the regression model. A value of R^2 equal to one means that the curve passes through every data point, while a value of R^2 equal to zero means that the regression model does not describe the data any better than a horizontal line passing through the average of the data points (DataFit, 2005).

3.3   Results and discussion

3.3.1   Temperature effect on water viscosity

The relationship between water temperature and water viscosity (Weast, 1985) is represented by an inverse polynomial equation with a R^2-value of 0.9994, as shown in Figure 3-2. The water viscosity decreases by 000058 Ns/m^2, from 1.523E-3 to 9.41E-4 Ns/m^2, as the water temperature increases from 5 to 25°C.
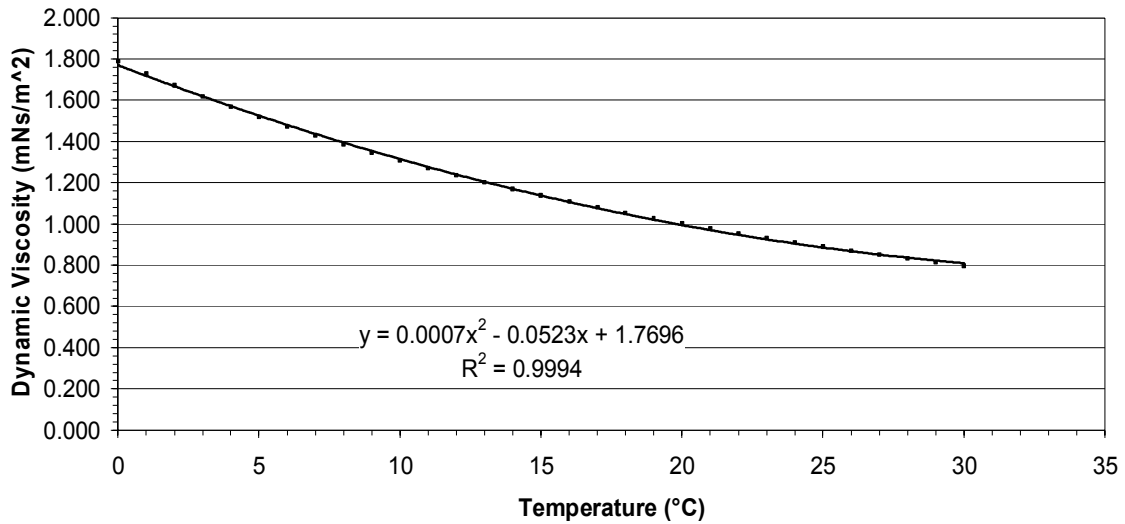
Figure 3-2 Water viscosity as a function of water temperature

3.3.2 Temperature effect on water density

The relationship between water temperature and water density (Weast, 1985) is represented by an inverse polynomial equation with a R^2-value of 0.9996, as shown in Figure 3-3. The water density decreases by 2.87 kg/m3, from 999.94 to 997.08 kg/m^3, as the water temperature increases from 5 to 25°C.
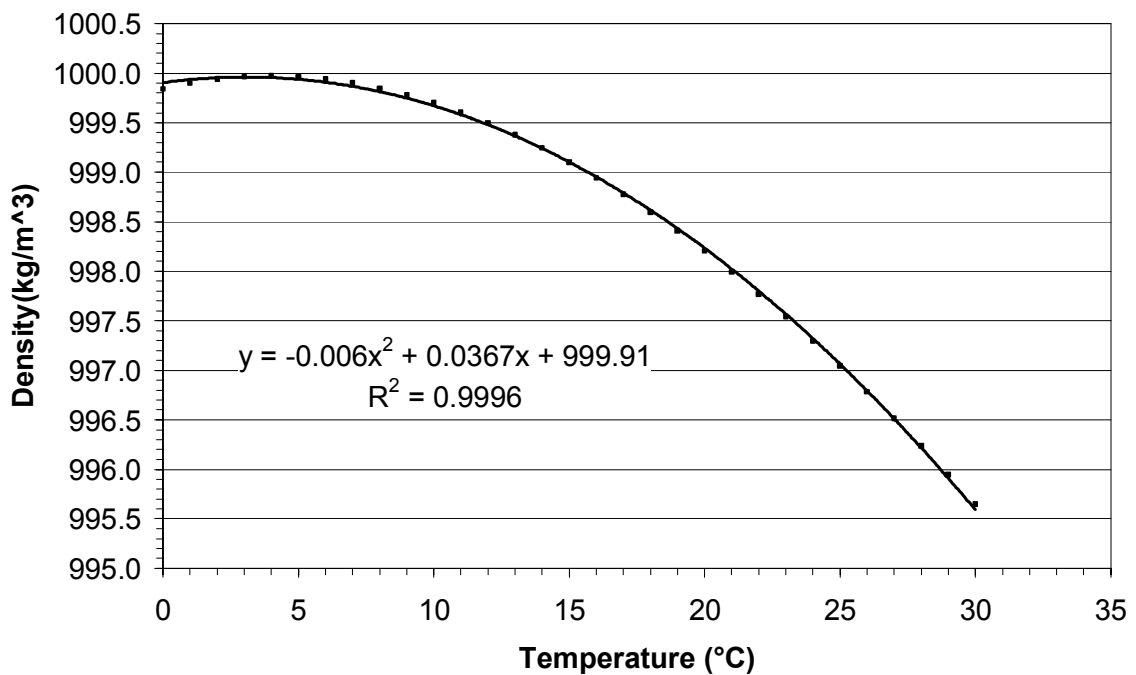
Figure 3-3 Water density as a function of water temperature

3.3.3 Settling response to water density and viscosity change

The discrete biofloc settling velocity changes due to water viscosity and water density variations over the 20°C temperature range. The change in the discrete settling velocity is graphically evaluated, to compare the different impacts of temperature related water viscosity and density variations.

The effect of a density variation on discrete biofloc settling velocity is illustrated in Figure 3-4, with a 20% velocity increase over the 20°C range. The discrete biofloc settling velocity increases by 0.14 m/hr, from 0.69 to 0.83 m/hr, due to the density decrease from 999.94 to 997.08 kg/m^3. The effect of viscosity variations on discrete biofloc settling velocity is also illustrated in Figure 3-4, with a corresponding 62% velocity increase. The discrete biofloc settling velocity increases by 0.43 m/hr, from 0.69 to 1.1 m/hr, due to the viscosity decrease from 1.523E-3 to 9.41E-4 Ns/m^2. The discrete biofloc settling velocity increases by 0.65 m/hr, from a minimum 0.69 to a maximum 1.34 m/hr, due to the combined water viscosity and density decrease of 000058 Ns/m^2 and 2.87 kg/m^3 respectively.
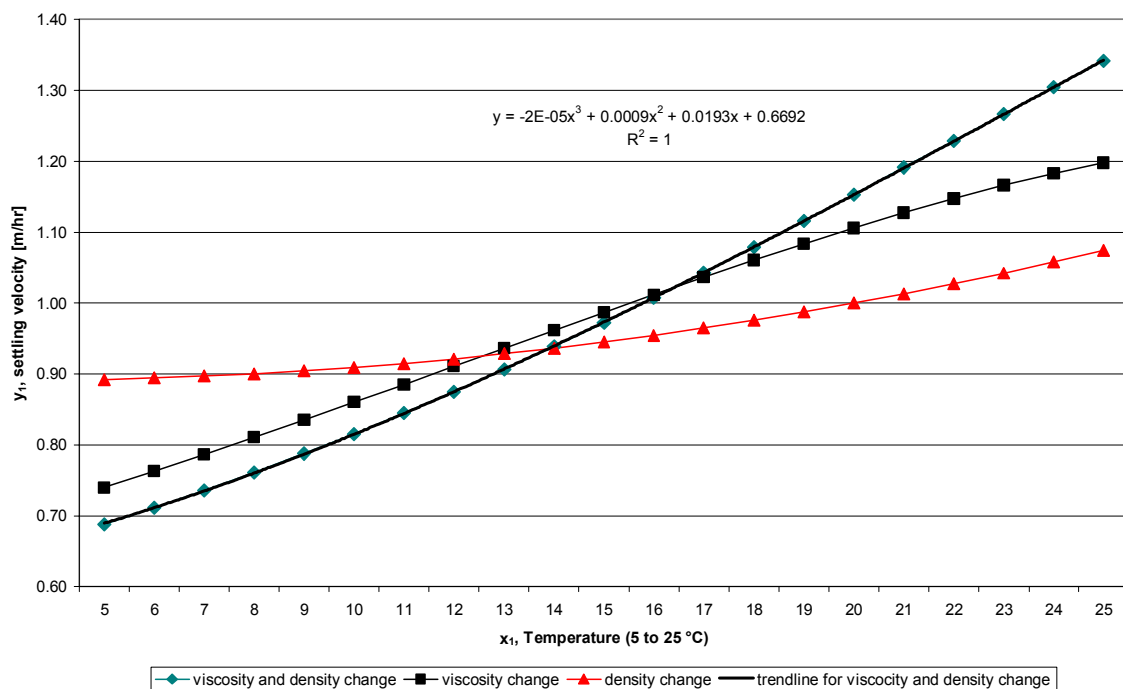
Figure 3-4 Biofloc settling velocity in water as a function of water viscosity and density

The effect of a water temperature increase over 20°C is represented by the water viscosity decrease of 0.00058 Ns/m^2 (from 0.000152 Ns/m^2 to 0.00094 Ns/m^2) and a water density decrease of 2.87 kg/m^3 (from 999.94 to 997.08 kg/m^3), to illustrate the temperature dependent settling velocity change due to biofloc density, size, and shape variations.

3.3.4 Settling response to biofloc density change

Discrete biofloc settling velocity changes, due to the combined effect of biofloc density change and temperature variation, are illustrated on the x_1-, x_2-, and y_1-axes of Figure 3-5. The settling velocity increases at the low temperature (5°C) by 15.4 m/hr, from 0.27 to 15.64 m/hr. This velocity increase originates from a biofloc density increase of 17 kg/m^3, from 1005.5 to 1022.5 kg/m^3. The settling velocity increases by 26.06 m/hr further at the higher temperature (25°C), as indicated from 0.7 to 26.76 m/hr. The velocity increase originates from the same biofloc density increase of 17 kg/m^3, from 1005.5 to 1022.5 kg/m^3.
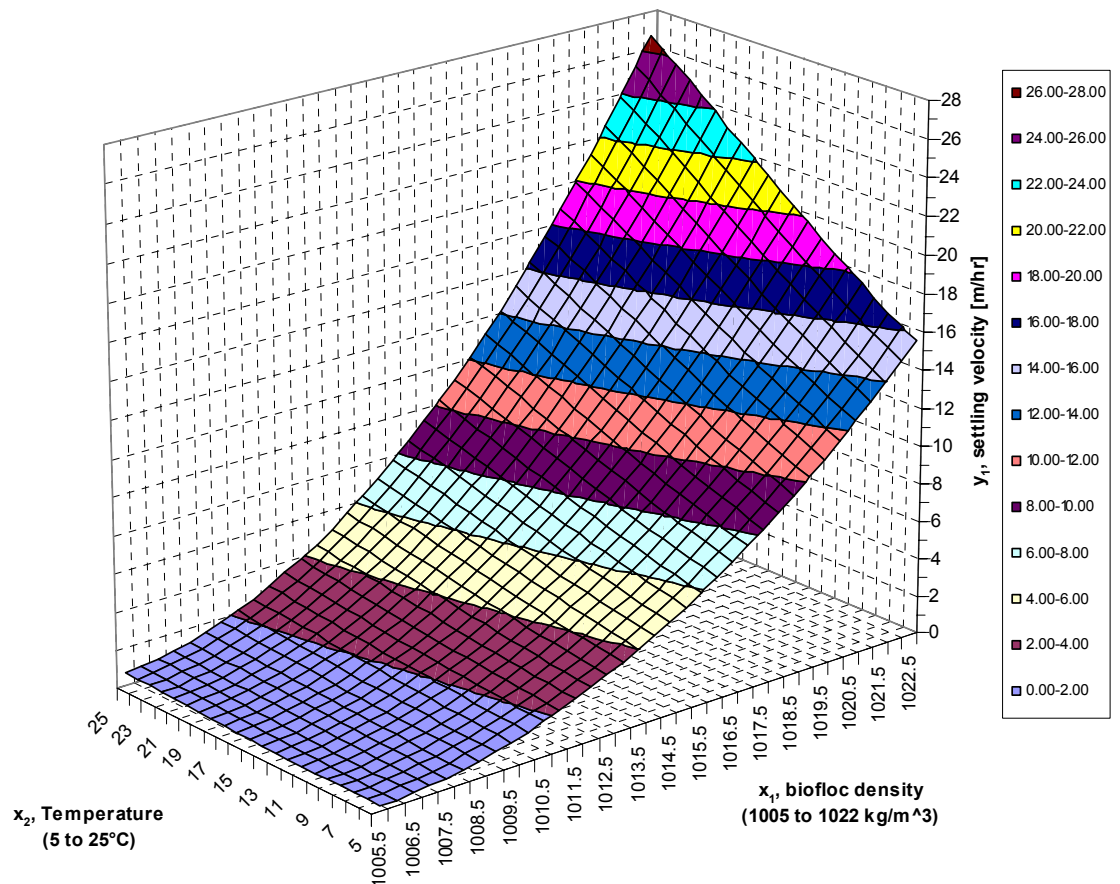
Figure 3-5 Biofloc settling velocity as a function of temperature and biofloc density

The settling velocity also increases due to a temperature increase, as illustrated on the x_2- and y_1-axes of Figure 3-5. The biofloc settling velocity increases at the low biofloc density of 1005.5 kg/m^3 by 0.43 m/hr, from 0.27 to 0.70 m/hr, due to a temperature increase of 20°C. The settling velocity increases by 11.12 m/hr further at the high biofloc density of 1022.5 kg/m^3, as indicated from 15.64 to 26.76 m/hr. The velocity increase originates from the same temperature increase of 20°C.

The discrete biofloc settling velocity increases further for a denser biofloc at a higher temperature. The settleability improves more at higher temperatures, when compared to the lower temperatures. This result is in agreement with a full-scale plant studies performed by Jang and Schuler (2006), and Schuler and Jang (2007b). These studies indicate that settleability improves with a biomass density increase, at an average SVI decrease of about 30 to 40 mℓ/g for each 0.01 g/mℓ (10 kg/m^3) density increase.

3.3.5 Settling response to biofloc size change

Discrete biofloc settling velocity changes, due to the combined effect of biofloc size change and temperature variations, are illustrated on the x_1-, x_2-, and y_1-axes in Figure 3-6. The settling velocity increases at the low temperature (5°C) by about 2.39 m/hr, from 0.0001 to 2.396 m/hr. This velocity increase originates from a biofloc size increase of about 1.4 mm, from 0.01 to 1.4 mm. The settling velocity increases by about 4.89 m/hr more at the higher temperature (25°C), as indicated from 0.0002 to 4.89 m/hr. The velocity increase originates from the same biofloc size increase of about 1.4 mm, from 0.01 to 1.41 mm.

The discrete settling velocity also increases due to a temperature increase, as illustrated on the x_2- and y_1-axes of Figure 3-6. The settling velocity increases for the small biofloc with a 0.01 mm diameter by only 0.0001 m/hr, from 0.0001 to 0.0002 m/hr, due to a temperature increase of 20°C. The discrete biofloc settling velocity increases by 2.49 m/hr further for the larger biofloc with a 1.41 mm diameter, as indicated from 2.40 to 4.89 m/hr. The velocity increase originates from the same temperature increase of 20°C.
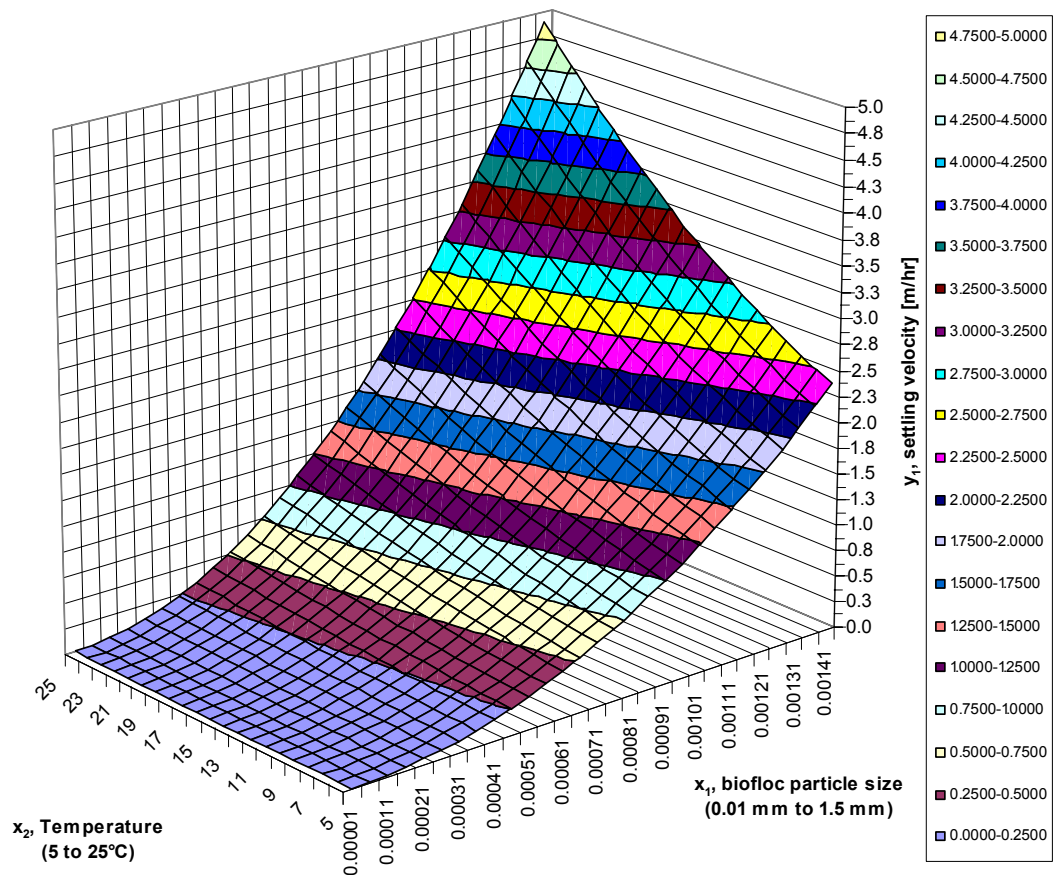
Figure 3-6 Biofloc settling velocity as a function of temperature and biofloc size

The discrete biofloc settling velocity increases therefore more for a larger biofloc at higher temperatures. The settleability improves more at higher temperatures, when compared to lower temperatures.

3.3.6 Settling response to biofloc shape change

Discrete biofloc settling velocity changes, due to the combined effect of biofloc shape change and temperature change, are illustrated on the x_1-, x_2-, and y_1-axes in Figure 3-7. The biofloc settling velocity decreases at the low temperature (5°C) by 9.78 m/hr, from 10.30 to 0.52 m/hr, due to a biofloc shape factor increase of 19, from 1 for a sphere to 20 for an irregular shaped biofloc. The biofloc settling velocity decreases by about 19.997 m/hr more at the high temperature (25°C), as indicated from 21.04 to 1.05 m/hr. The velocity decrease originates from the same biofloc shape factor increase of 19, from 1 to 20.
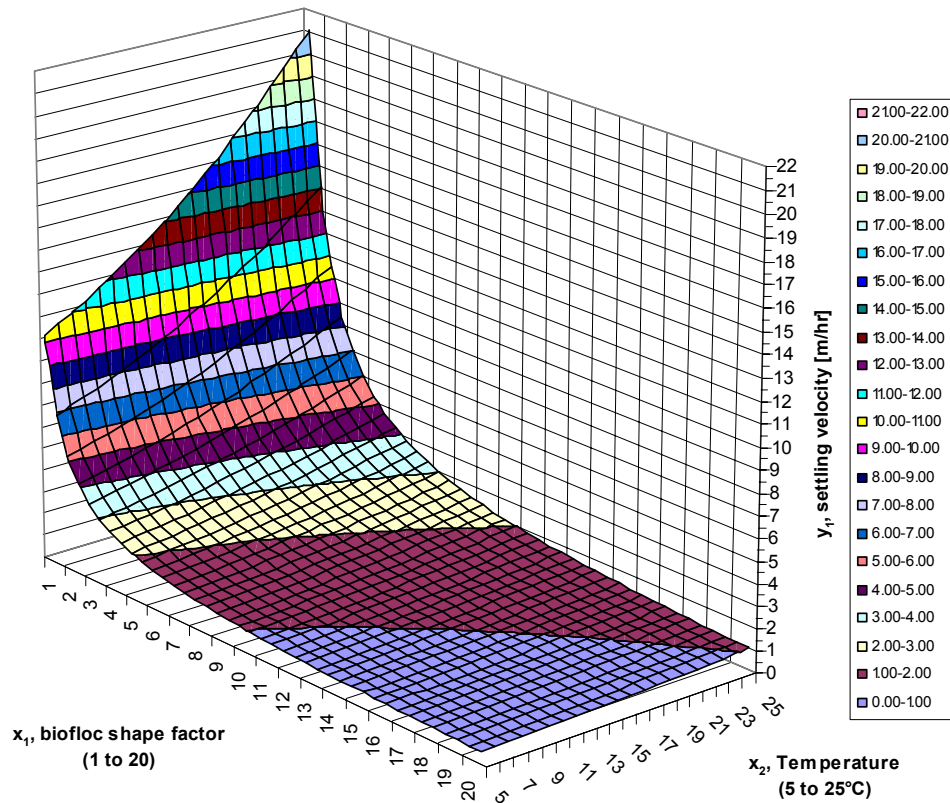
Figure 3-7 Biofloc settling velocity as a function of temperature and biofloc shape

The discrete settling velocity also increases due to a temperature increase as illustrated on the x_2- and y_1-axes of Figure 3-7. The biofloc settling velocity for the spherical biofloc increases by 10.74 m/hr, from 10.30 to 21.04 m/hr, due to a temperature increase of 20°C. The biofloc settling velocity for an irregular shaped biofloc, with a shape factor of 20, increases by only 0.53 m/hr, from 0.52 to 1.05 m/hr. The velocity decrease originates from the same temperature increase of 20°C.

The discrete biofloc settling velocity increases further for a more regular shaped biofloc, confirming results by Grijspeerdt and Verstraete (1997). The settleability improves more at higher temperatures, when compared to lower temperatures.

3.4   Summary

The Stokes model provides an indication of the unhindered settling velocity change of a simplified solid biofloc in water under influence of a temperature variation. The

temperature variation changes the effect of water (viscosity and density) and biofloc properties (density, size, and shape) on the settling velocity of the biofloc.

The predicted discrete biofloc settling velocity changes, originating from variations in water and biofloc properties, are summarised in Table 3-2. The discrete biofloc settles in all instances faster at the higher temperature of 25°C. The highest settling velocities are predicted for bioflocs with the largest density, followed by bioflocs with shape changes towards a sphere, and lastly by a larger size biofloc.

Table 3-2 Biofloc discrete settling velocity link to temperature and biofloc characteristics

Parameter	Parameter range	Settling velocity at 5°C [m/hr]	Settling velocity at 25°C [m/hr]
Biofloc density	1005.5 kg/m^3	0.27	0.70
	1022.5 kg/m^3	15.64	26.76
Biofloc size	1.4 mm	2.40	4.89
	0.01 mm	0.00001	0.00002
Biofloc shape	1 [-]	10.30	21.04
	20 [-]	0.52	1.05

The predicted discrete biofloc settling velocities are only valid for a solid biofloc. Additional physical changes such as porosity, and biological changes such as composition modifications, are disregarded in this evaluation. The predicted settling velocities represent only an indication of possible settling variations due to temperature fluctuations.

Hasar *et al*. (2004) identified temperature and MLSS concentration as the largest contributors to MLSS flow behaviour in a sequencing batch reactor (SBR). MLSS viscosity decreased logarithmically with a temperature increase, along with an exponential increase for a MLSS concentration increase. The basic biofloc settling calculations support these reported experimental findings, demonstrating that temperature plays a significant role in MLSS settleability.

3.5   Conclusions

The calculated unhindered settling velocity of a biofloc over a 20°C temperature range variation changes due to water viscosity and density changes, as well as biofloc density, shape, and size changes. The following conclusions are applicable for the settling biofloc:

• A water viscosity change increases the biofloc settling velocity by 0.4 m/hr, against a water density change that increases the biofloc settling velocity by 0.1 m/hr. The effect of water viscosity changes on settleability is more distinct than the effect of water density changes.

• Biofloc density is the biofloc characteristic with the largest influence on settleability in terms of settling velocity. The settling velocity increased for the denser biofloc by 11 m/hr across a 20°C increase.

• Biofloc shape is the biofloc characteristic with the second largest influence on settleability in terms of settling velocity. The settling velocity increased for the spherical biofloc by 10 m/hr across a 20°C increase.

• Biofloc size is the biofloc characteristic with the third largest influence on settleability in terms of settling velocity. The settling velocity increased for the larger biofloc by 2 m/hr across a 20°C increase.

These preliminary calculations confirm that temperature is an important dependent variable in MLSS settling. The calculations illustrate significant MLSS settling velocity changes over a temperature range variation. The next chapter will illustrate typical short- and long-term temperature variations found in a selection of operational treatment plants.

4   TEMPERATURE OBSERVATIONS

Temperature variations from an exploratory survey at five reactors are presented in this chapter. The extent of short- and long-term temperature variations illustrates typical operational temperature variation ranges. This temperature data complements the limited published information obtained from the literature survey, as well as the temperature-based settling calculations from the previous chapter.

4.1   Background

T_r is subject to short-term (hourly to diurnal) and long-term (weekly and monthly to seasonal) variations (Wahlberg *et al.*, 1996). Makinia *et al.* (2005) modelled these T_r variations as sinusoidal wave profiles that follow cyclic nighttime and winter cooling stages, between daytime and summer heating stages. The long-term T_r fluctuations are related to T_a fluctuations, which vary according to the geographical position of the plant. T_r extends from a minimum of 5 to 10°C during winter in Northern Europe and Canada to a maximum of over 30°C during summer in Asiatic countries (Oldham and Rabinowitz, 2002; Tandoi *et al.*, 2006). Long-term T_r fluctuations have a direct influence on MLSS settling. Improved MLSS settling is recorded during warmer summer months, followed by transition periods during spring and autumn (Kruit *et al.*, 2002), with poorer MLSS settling evident during colder winter months.

These long-term T_r variations govern several aspects of the biological processes, such as the rate of reactions (Krishna and Van Loosdrecht, 1999), the growth rate of all bacteria and in particular nitrifying bacteria (Barnard, 1974), as well as the selective development of specific microorganism populations (Grady and Filipe, 2000). The theoretical reaction rates for most of these biological processes double for each 10°C temperature increase up to a maximum temperature (Dochain and Vanrolleghem, 2001). Some full-scale process rates could be less temperature sensitive (Pöpel and Fischer, 1998) due to inhibiting factors.

These long-term T_r variations also influence the physical properties of MLSS. As MLSS is mainly composed of water and bioflocs (Wilén *et al.*, 2006), the physical properties relate to water characteristics such as density and viscosity, as well as biofloc

characteristics such as density, size, and shape. Short-term T_r variations influence the physical properties of MLSS, as demonstrated in the previous chapter.

Short-term T_r fluctuations are not routinely used as an operational process performance parameter. Diurnal T_r fluctuation effects on MLSS settleability are therefore not recorded or correlated to process performance. The average daily T_r of 14°C in winter and 22°C in summer for South African weather conditions are usually used as T_s for modelling exercises (WRC, 1984). The extent of MLSS T_s changes due to the influence of T_a, as well as the final difference from T_r, after a time delay due to MLSS sample collection, transfer, storage, and settling during batch tests, has not been reported in any detail in the available literature.

The aim of this chapter is to establish a typical range of plant temperature fluctuations. Differences between T_r and T_a illustrate temperature variations that can be expected between plant reactors and settling test containers under the influence of T_a.

4.2   Materials and methods

4.2.1   Experimental approach

T_r readings are recorded with hand-held or on-line thermometers at five different BNR reactors. On-line readings are continuously recorded and stored with data loggers to capture T_r profiles. These profiles are required to establish the extent of short-term temperature variations found in batch and automated MLSS settling evaluations.

4.2.2   Temperature data collection

4.2.2.1   Plant reactors used for temperature observations

Batch and on-line temperature data was collected at five BNR reactors at two wastewater plants, as indicated in Table 4-1. The size of the reactors and the aeration method are listed, as these reactor attributes could influence T_r and the extent of diurnal T_r profiles.

Plant 1 contains two full-scale reactors (1a and 1b) with surface aeration systems, as well as a pilot plant (1c) with submerged bubble aeration. Plant 2 is located about 80 km from

plant 1. Plant 2 includes adjacent surface aeration (plant 2a) and bubble aeration (plant 2b) reactors. This plant configuration offers the opportunity to identify the effects of the aeration methods on full-scale T_r.

Table 4-1 Sizes of five BNR reactors in two plants used in temperature observations

Plant	Reactor	BNR reactor size [m^3]	Aeration method
1	a	25550	Surface
1	b	15000	Surface
1	c	1.8	Bubble
2	a	45500	Surface
2	b	31796	Bubble

4.2.2.2 Short- and long-term temperature variation

On-line DO concentration meters (Royce Model 9100D; Royce, 1999) in plant 1 and 2 aerobic reactors include built-in temperature sensors. This temperature function is used to record once-off T_r readings during winter and spring at plant 1a, 2a, and 2b reactors.

These on-line DO concentration meters measure T_r continuously at plant 1b reactor. A similar DO meter was placed in the raw sewage inflow channel of plant 1 to record T_{raw}.

Data loggers (Fourier MicroLog Plus; Fourier, 2007) record the on-line data to produce diurnal T_r profiles. These data loggers contain internal temperature sensors to record T_a. Each logger produces separate T_a and T_r profiles.

4.2.2.3 Temperature data presentation

Microsoft Excel is used to plot and trend T_a, T_r, and T_{raw} profiles in graphical format in 2-D graphs. The coordinate system consists of the horizontal x_1-axis representing the time over several days or 24 hours, and the primary y_1- and secondary y_2-axes represent the temperature data.

4.3 Results and discussion

4.3.1 Long-term temperature variation

Long-term T_r variations that were recorded at wastewater treatment plants are summarised in Table 4-2. This data is based on manual readings that are listed in Table 11-1 in Appendix A. Winter T_r of surface aeration plants 1a and 2a differ by about 2°C due to geographical and local conditions. The bubble aeration plant 2b T_r is about 5°C warmer at 17 to 18°C in winter, when compared to the T_r of the adjacent surface aeration plant 2a. Spring T_r increases by about 8°C for the surface aeration reactors of plant 1a and 2a, and by 5°C for the bubble aeration reactor of plant 2b.

Table 4-2 Seasonal and daytime temperature variations: surface and bubble aeration

Plant reactor	winter morning T_r [°C]	winter afternoon T_r [°C]	spring morning T_r [°C]	spring afternoon T_r [°C]
Reactor 1a	14.2	15.0	21.6	22.0
Reactor 2a	12.1	12.7	20.6	20.5
Reactor 2b	17.7	18.0	22.8	23.0

This T_r survey confirms the extent of long-term T_r variations. The large T_r difference of more than 5°C between surface and bubble aeration at adjacent reactors of 2a and 2b has significant design and operational implications for temperature dependent BNR processes, as well as for aspects of MLSS settleability.

The T_r between morning and afternoon conditions changes by less than 1°C at all three reactors. This indicates that MLSS samples collected from the reactor during this period of the day will have a relatively constant temperature, with variations of less than 1°C in T_r. The lower afternoon T_r of 20.5°C at reactor 2a is due to a rain event. Continuous T_r profiles are preferred to identify temperature variations that might not be detected with individual readings. The T_s should also be related to T_r for batch MLSS settling tests, as different T_a can lead to changes in T_s before and during the settling tests.

The T_{raw} of plant 1 was monitored together with T_a for 42 days in spring, as shown in Figure 4-1. The T_{raw} fluctuates by 4.3°C over a range from 16.3 to 20.6°C. The cyclic T_a profile shape is similar to T_{raw} over the 42-day period, with a total change of 27°C

measured from 12 to 39°C. The placement of the small data logger enclosure in direct sunshine contributed to this extended T_a range. The T_{raw} and T_a trends follow different slopes, with T_{raw} increasing as T_a is decreasing. These trends confirm that T_{raw} is influenced by local factors other than T_a, making it difficult to predict T_{raw} profiles from T_a data.
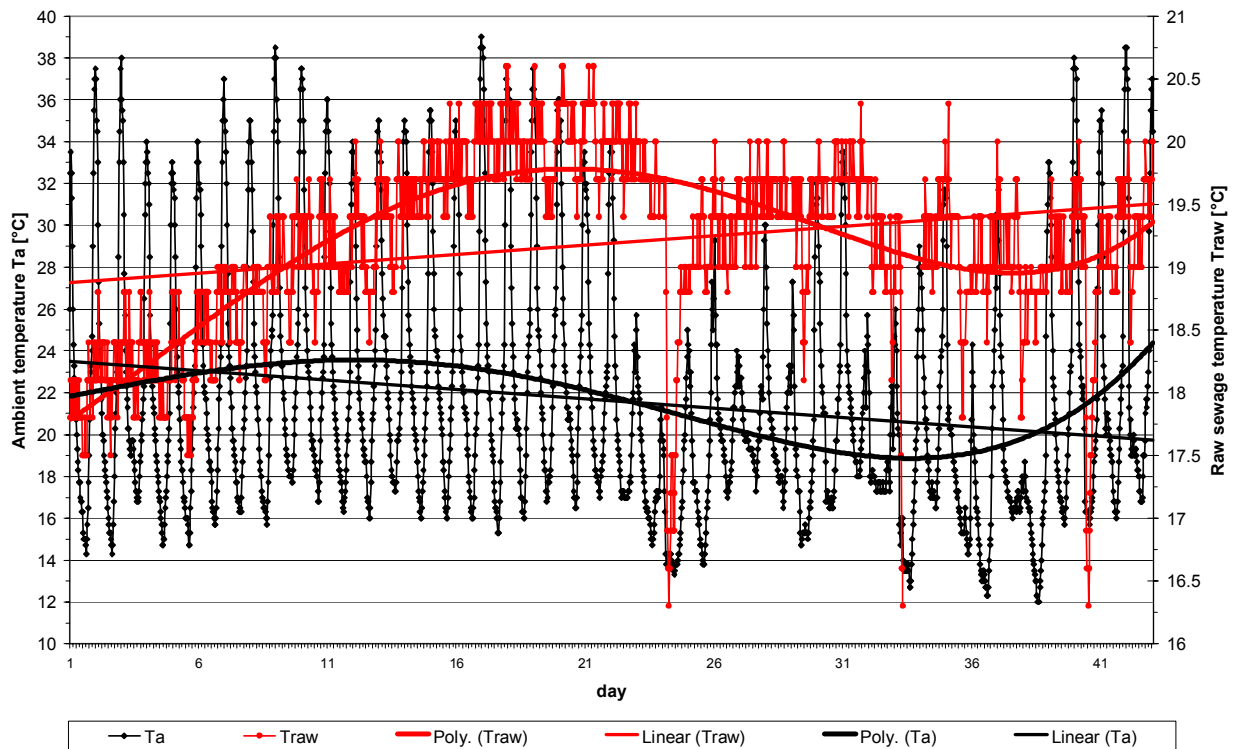
Figure 4-1 T_{raw} and T_a profiles over 42 days, plant 1

The T_r of plant 1a was monitored together with T_a for 19 days in spring, as shown in Figure 4-2. The T_r fluctuates by 2.8°C over a range from 17.2 to 20.0°C. The cyclic T_a profile shape is similar at a total change of 24.7°C, covering a range from 8.3 to 33°C. The T_r and T_a trends follow similar slopes, confirming that T_a directly influences T_r. The T_a fluctuations are mirrored by changes in the T_r. These substantial T_r changes of a few degrees Celsius occurring over several days are thus related to T_a changes.
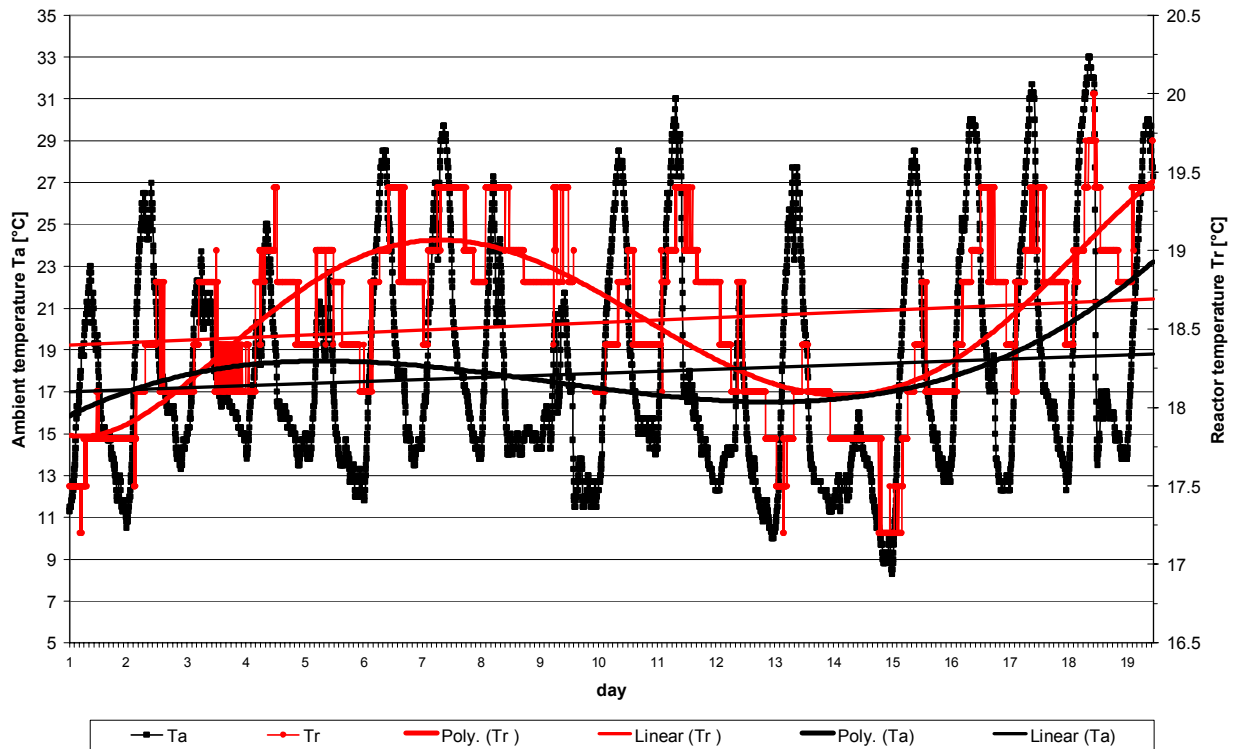
Figure 4-2 T_r and T_a profiles over 19 days, plant reactor 1a

The T_r and T_a recordings for the other two reactors at plant 1 over 10 days in spring show distinct diurnal temperature fluctuation trends. It illustrates and confirms the noticeable relationship between T_r and T_a, as shown in Figure 4-3. The T_r profile is connected by rising trend channels on the minimum and maximum daily T_r points, while the average T_r increase is shown with a linear trend line.

These trend channels indicate that the average T_r can change by approximately 4°C within 10 days at the local plants. The diurnal T_r fluctuation range increases from about 16.5 to 18°C to about 19.0 to 20.5°C, while the average linear T_r trend changes by 2.75°C, from 17.25 to 20°C. The constant slope of the trend channels illustrates that the diurnal T_r profile fluctuation stays relatively constant at about 1.5°C.

The temperature profile in Figure 4-3 also shows that the T_a increases from a diurnal variation range of about 12 to 32°C to about 16 to 30°C. The diurnal T_r variation of about 1.5°C is more constant than the diurnal T_a fluctuation that changes from about 20 to 14°C within a few days. The relationship between T_r and T_a is not constant, indicating that other factors and local conditions influence this relationship. These profiles are in good

agreement with profiles provided by Scherfig *et al*. (1996), where similar rapid temperature changes over a few days were reported.
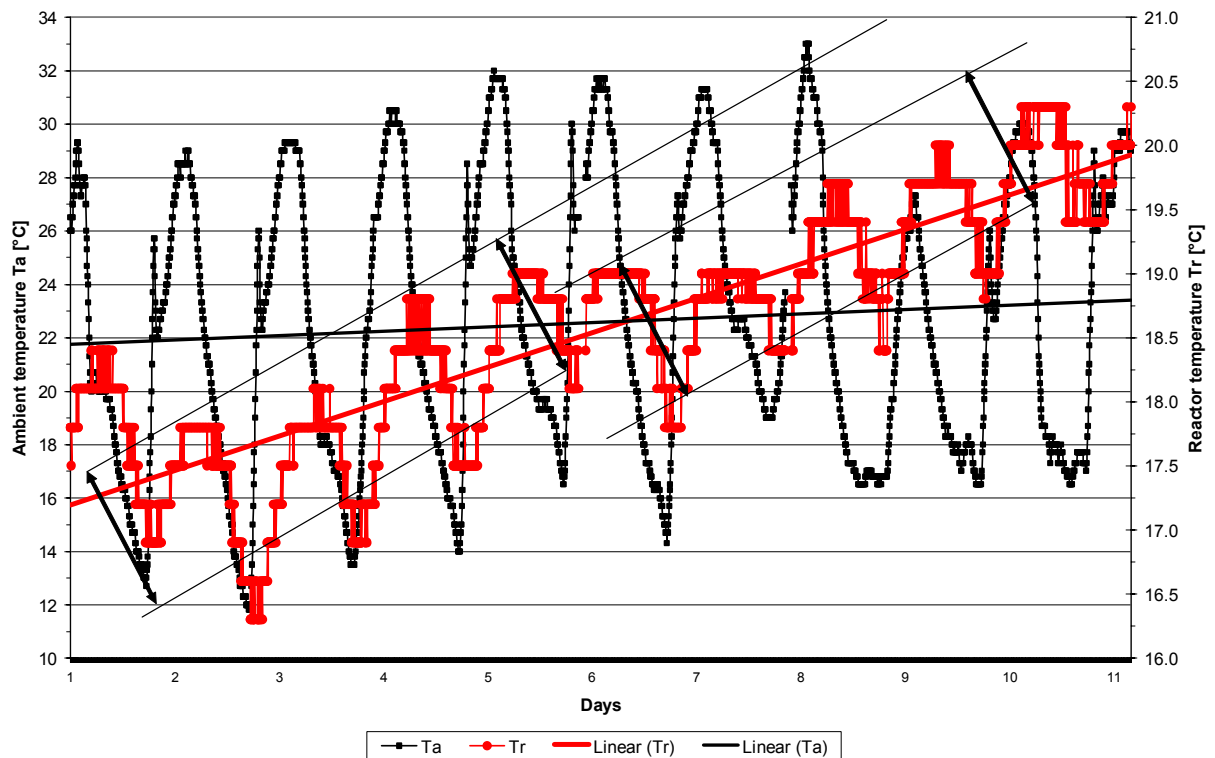
Figure 4-3 T_r and T_a profiles over 10 days, plant reactor 1b

The T_r and T_a recordings for the plant reactor 1c over an 11 day period during winter indicate more distinctive diurnal temperature fluctuation trends. It confirms the direct relationship between T_r and T_a for a smaller sized reactor, as shown in Figure 4-4. Rising trend channels on the minimum and maximum daily T_r points illustrates the T_r profile, and the average T_r increase is shown with a linear trend line.

The trend channels indicate that the average T_r can change by approximately 2°C within 10 days. The T_r diurnal fluctuation range decreases correspondingly from about 13 to 20°C to about 11 to 18 °C, corresponding directly to the changes in the T_a. The steady slope of the rising trend channels shows that the diurnal T_r profile fluctuation stays constant at about 7°C.

The profile in Figure 4-4 shows that T_a decreases from a diurnal variation range of about 4 to 20°C to about 2 to 18°C. The diurnal reactor temperature variation of about 7°C follows the T_a diurnal fluctuation of about 16°C closely, due to the small reactor size.
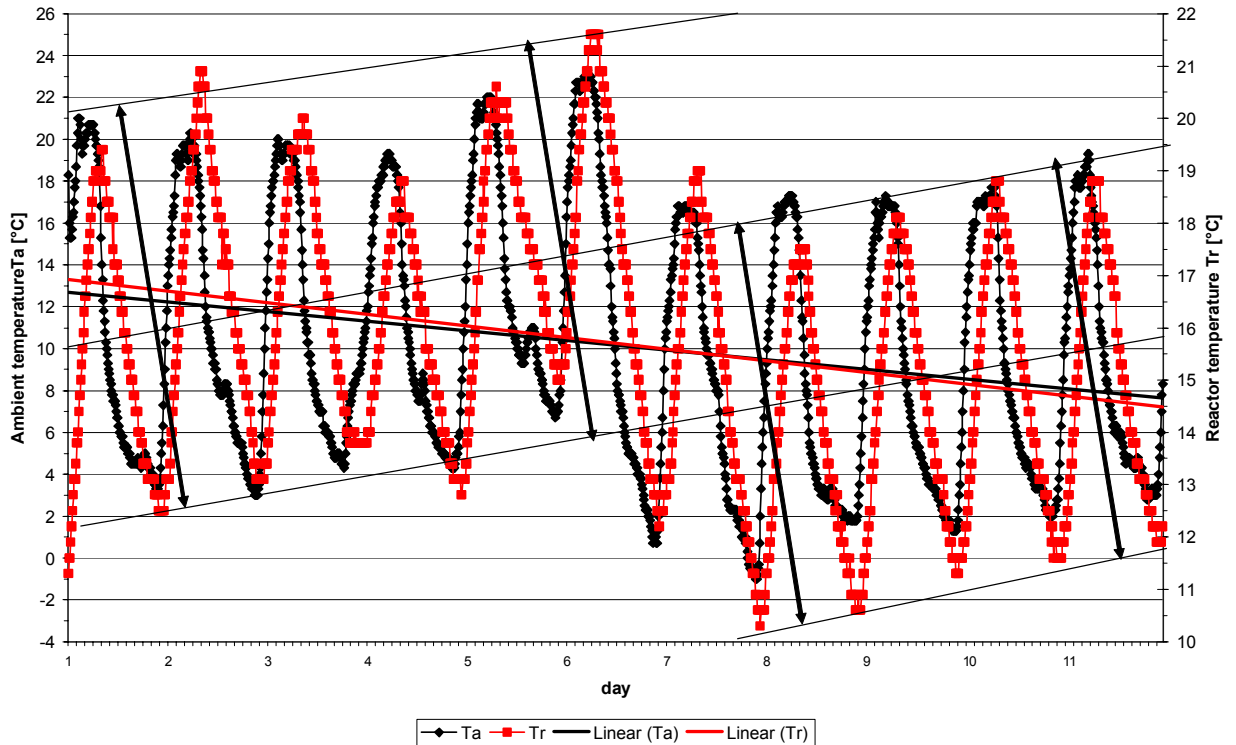
Figure 4-4 T_r and T_a profiles over 11 days, plant reactor 1c

4.3.2 Short-term temperature variations

The diurnal temperature variations for plant 1c in spring and plant reactor 1b in winter, as displayed in Figure 4-5 and Figure 4-6 respectively, illustrate the direct diurnal relationship between T_a and T_r. The T_a fluctuations are mirrored by changes in T_r, with a lag, which confirms the experimental observations of Banks *et al.* (2003).

A T_{raw} diurnal profile for plant 1 during winter, with a fluctuation of less than 1°C, is shown in Figure 11-1 in Appendix B. This profile indicates that the raw sewage temperature does not follow the diurnal T_a profile. T_{raw} cannot be represented by typical sinusoidal wave profiles, as found in cyclic T_a and T_r fluctuations.

The T_a and T_r fluctuations for a spring day are represented by polynomials with $R^2 = 0.925$ and 0.918 respectively. The minimum T_a of 14°C occurs at about 06:00, and the maximum T_a of 31.8 °C follows at about 15:30. The plant 1b minimum and maximum T_r are indicated from the data points as constant from about 05:00 to 10:00 at 17.5°C and 19:00 to 24:00 at 19°C respectively. These horizontal deviations from the sinusoidal wave profile are generated by the limited minimum recording limit of 0.3°C of the on-line thermometer logger. A 2-day profile is provided in Figure 11-15 in Appendix E for reference purposes, to illustrate the T_r response to T_a fluctuations. Two polynomial equations represent the T_a and T_r correlations with respective R^2 of 0.78 and 0.91.

$$Ta \quad y = 6E\text{-}08x^4 - 4E\text{-}05x^3 + 0.0079x^2 - 0.4466x + 22.202$$
$$R^2 = 0.9247$$

$$Tr \quad y = -1E\text{-}09x^4 + 3E\text{-}07x^3 + 0.0001x^2 - 0.0239x + 18.68$$
$$R^2 = 0.9177$$
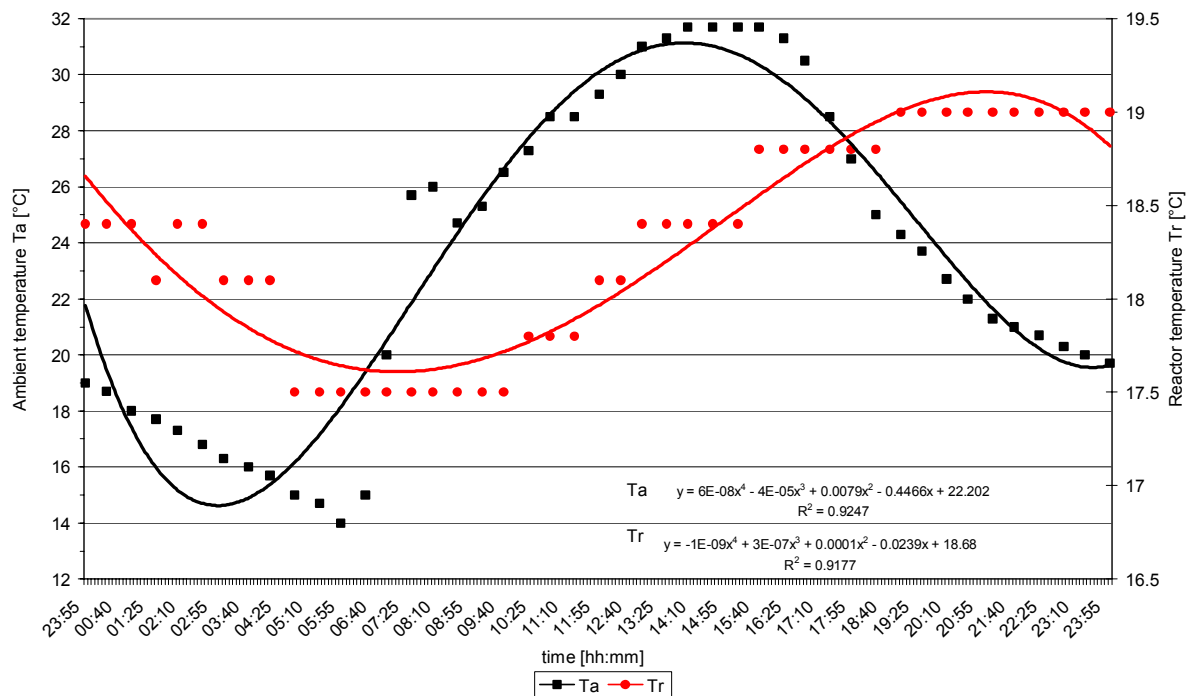
Figure 4-5 Diurnal T_r and T_a profile, plant reactor 1b

The T_a and T_r fluctuations are represented by polynomials with $R^2 = 0.904$ and 0.918 respectively. The plant reactor 1c T_r profile lags behind the T_a profile by only 2.5 hours. The minimum T_r of 10.9°C occurs at about 08:30, and the maximum T_r of 17.2 °C is recorded at about 21:00.
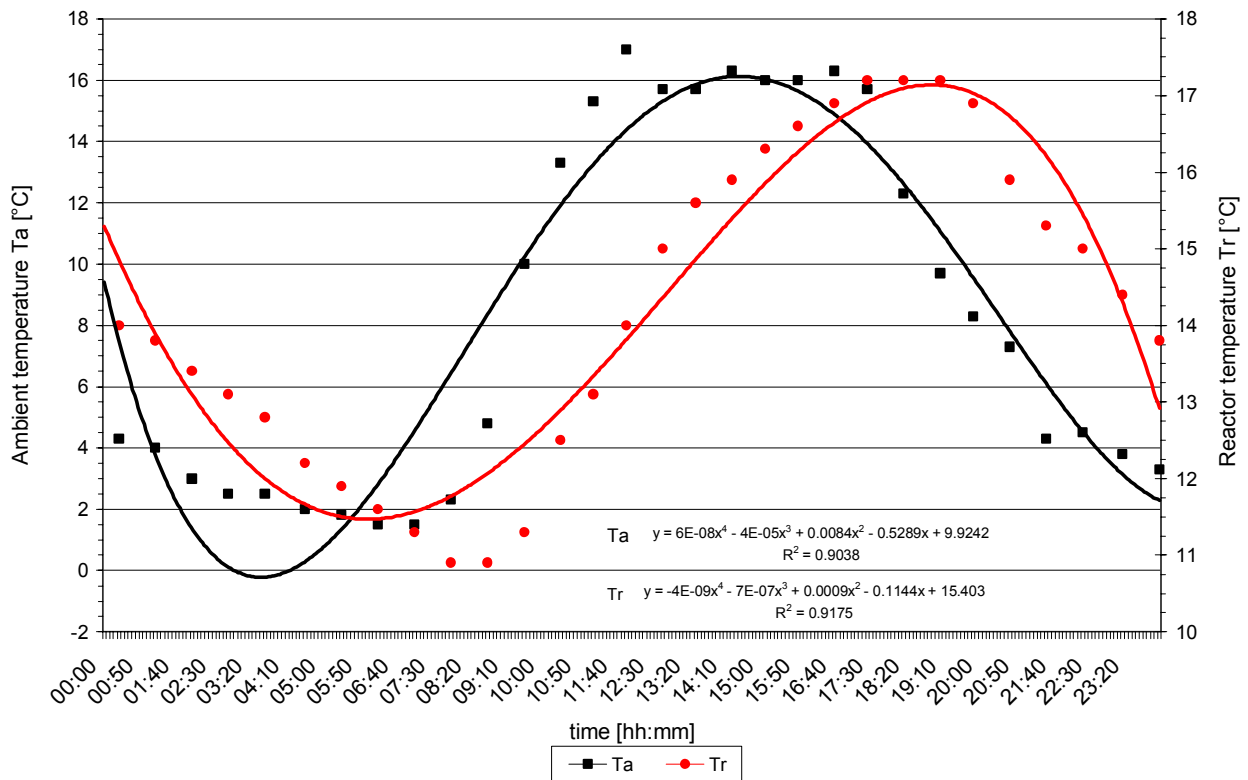
Figure 4-6 Diurnal T_r and T_a profile, plant reactor 1c

4.4   Summary

Long-term T_r variations of about 8°C are recorded from winter to spring. Reactors with surface and bubble aeration at the same plant indicated T_r differences in excess of 5°C. The increase in T_r in a full-scale plant during a week in spring has been identified at about 4°C, although the diurnal short-term T_r fluctuation of about 1.5°C stays relatively constant. This diurnal T_r variation follows a diurnal T_a variation of 14 to 32°C in spring. The winter T_a varies from 1 to 17°C, leading to an accentuated diurnal T_r fluctuation of about 7.2°C in a small pilot plant. The identified temperature variations are summarised as follows:

- Winter surface and diffused aeration systems T_r difference: 5°C,
- Winter to spring surface aeration T_r increase: 8°C,
- Winter T_a fluctuation: minimum of 1°C to maximum of 17°C,
- Spring T_a fluctuation: minimum of 14°C to maximum of 32°C,
- Monthly T_{raw} fluctuation: 4.3°C,

- Weekly T_r (full-scale) fluctuation, spring: minimum of 16.5°C to maximum of 20.5°C,
- Weekly T_r (pilot plant) fluctuation, winter: minimum of 11°C to maximum of 20°C,
- Diurnal T_r (full-scale) fluctuation in a day: 1.5°C,
- Diurnal T_r (pilot plant) fluctuation in a day: 7.2°C, and
- Diurnal T_{raw} fluctuation: <1°C.

Oldham and Rabinowitz (2002) review the application of BNR technology for cold climates in several parts of the world. The key elements in these designs are the BNR responses to low T_r conditions (presumably with surface aeration reactors). Comparable long-term low T_r conditions were identified in this temperature observation study. Reviews of BNR technology in the literature usually exclude MLSS settleability response data to these low T_r conditions.

4.5 Conclusions

The aim of this chapter is to identify operational temperature fluctuations at plant reactors. The following conclusions are based on manual temperature readings and continuous temperature profiles obtained from different reactors:

- Long-term T_{raw} changes cannot be contributed or directly related to T_a variations,
- Significant seasonal, weekly, and diurnal T_r fluctuations are recorded at plant reactors,
- Significant T_r differences were identified between surface and bubble aeration systems,
- The average T_r changes rapidly over a few days at a full-scale reactor, due to changes in T_a, as well as additional factors,
- The short-term diurnal T_r fluctuation at a full-scale reactor stays constant at 1.5°C during variations, and
- The large T_r fluctuations in a pilot plant reactor demonstrates the direct and rapid influence that meteorological conditions such as T_a has on the MLSS temperature in small containers, as found in pilot plant reactors and test cylinders.

If batch MLSS settling T_s changes significantly from these recorded T_r levels, the batch settling test results and settling parameters will be subject to variations. Batch MLSS settling test results depends on the manner in which T_r is considered during sample handling, before and during MLSS settling tests.

5   BATCH MLSS SETTLING EVALUATION

Traditional batch MLSS settling tests are evaluated in this chapter. The settling results illustrate the effects of temperature variations on aspects of manual MLSS settling tests in an operational plant environment.

5.1   Background

The MLSS settling and clarification processes are not evaluated continuously in an operational secondary settling tank (Gernaey *et al*., 1998). These processes are therefore simulated on laboratory scale in a test cylinder, as represented by the qualitative graphical description in Figure 5-1 (adapted from Kazami and Furumai, 2000).

A MLSS sample from a reactor is placed in a transparent test cylinder to start a batch settling test. The settling MLSS / liquid interface level is recorded for the duration of the settling interval. This settling interval consists of four settling stages: (1) reflocculation or lag, (2) zone settling, (3) transition, and (4) compression (or processes A, C, D, E). The clarification stage (process B) progresses simultaneously on top of the interface.
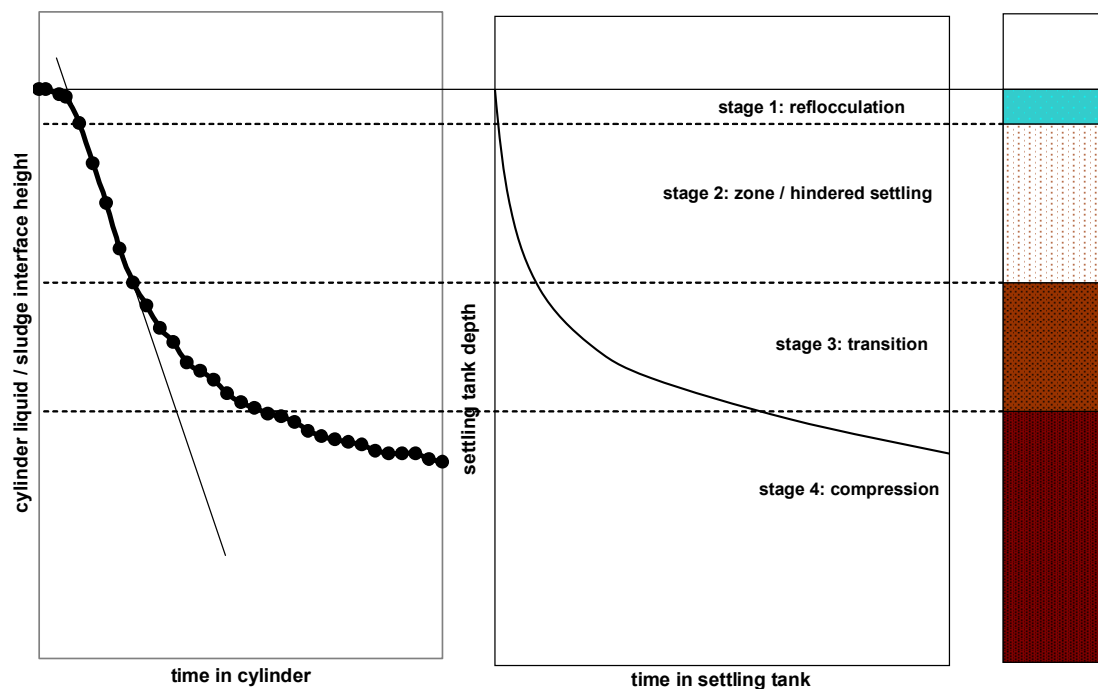
Figure 5-1 MLSS settling profiles in a cylinder and a secondary settling tank

MLSS settling tests are usually performed in a laboratory that is not located near the plant reactor. Therefore, there are time delays between the collection of MLSS samples from the reactor until the start of batch MLSS settling tests. The T_s adjusts during sample collection, transfer, storage, and settling towards the prevailing T_a.

The MLSS settling test procedures (APHA, 1998) are summarised in Table 5-1. The cylinder size, sample stirring provision, and temperature control are the most important experimental conditions that require special equipment. The recommended equipment for SV_{30} and SVI tests are stirred 1 ℓ cylinders that are temperature controlled at T_r. The ZSV test requires larger stirred columns, which must also be temperature controlled at T_r.

Table 5-1 Batch MLSS settling tests procedures (APHA, 1998)

Parameter & method	Container	Temperature control	Stirring	MLSS concentration
SV_{30}, 2710C	1ℓ transparent cylinder	Yes, at T_r	Yes, < 4 rpm	Not required
SVI, 2710D	1ℓ transparent cylinder	Yes, at T_r	Yes, < 4 rpm	standard method 2540D
ZSV, 2710E	>1 m high column >10 cm diameter	Yes, at T_r or a evaluation temperature	Yes	Not required

Parker *et al*. (2000) recommend that the purposes of batch MLSS settling tests are identified before experimental methods are finalised. If the test purpose is only preliminary diagnostic work, several relationships are available between ZSV as a function of MLSS concentration and SVI. For more reliable research work to determine ZSV, the standard methods (APHA, 1998) prescribe a settling test using a long column with temperature control facilities. Unstirred MLSS settling tests in graduated cylinders are considered as an approximation to determine SV_{30}, SVI, and ZSV. If these test purposes and methods are not considered, MLSS settling tests can lead to the misuse of settling parameters for unsuitable purposes (Dick and Vesilind, 1969), especially when large temperature effects are present.

The aim of this chapter is to use basic batch MLSS settling tests to illustrate how variations in settling parameters obtained from unstirred MLSS settling tests are related to the following aspects:

- settling parameter change in different size test cylinders,
- settling parameter change throughout the three zones of a BNR reactor, and
- settling parameter change during temperature variations.

5.2   Materials and methods

5.2.1   Experimental approach

The extent of calculated MLSS settleability changes as reported in Chapter 3, over observed operational temperature ranges as reported in Chapter 4, needs to be experimentally verified. Batch MLSS settling tests are used to determine the impact of three operational test conditions on MLSS settling parameters.

The three test conditions investigated are (i) container size, (ii) BNR reactor zone sample source, and (iii) sample environmental conditions. The settling parameters representing MLSS settleability are SVI, ISV, and supernatant turbidity.

Preliminary tests verify the suitability of a MLSS concentration meter used during temperature variations, the effect of a 1 and 2 ℓ cylinder and the MLSS sample location in a BNR reactor on settling parameters, as well as the impact of extended sample heating and cooling on MLSS settleability.

5.2.2   Settling measurement equipment

Transfer pipettes are used to draw supernatant samples from the cylinders for turbidity measurements. Turbidity is determined with a spectrophotometer (Merck Spetroquant Nova 60; Merck, 2007) calibrated in FNU (Formazine Nephelometric Unit). A hand-held MLSS concentration meter (Royce Model 711) is used for additional MLSS concentration measurements in reactor zones and batch MLSS samples. The T_s of MLSS samples are measured with a hand-held digital thermometer (Testo 925; Testo, 2007), equipped with a 60 cm immersion probe to detect the temperature in the middle of the cylinder.

5.2.3 Settling profile determination

Batch MLSS settling tests are performed in unstirred 2 ℓ graduated cylinders. The four stages of MLSS settling during the 30-minute test, which are (1) reflocculation, (2) zone settling, (3) transition, and (4) compression, are indicated in Figure 5-2 according to profile slope changes (adapted from Ekama *et al.*, 1997). At the start of MLSS settling process, the reflocculation during stage 1 leads after a lag period to the formation of a MLSS / liquid interface that begins to descend, and a changing settling profile slope is formed. Once this settling interface reaches maximum settling velocity, the linear portion of the profile indicates maximum or zone settling velocity in stage 2. A reduction in settling velocity leads to another change in the profile slope, to indicate transition in stage 3. Compression in stage 4 starts with a more stable slope that continues until the settling test duration is completed, or the MLSS / liquid interface is stationary.
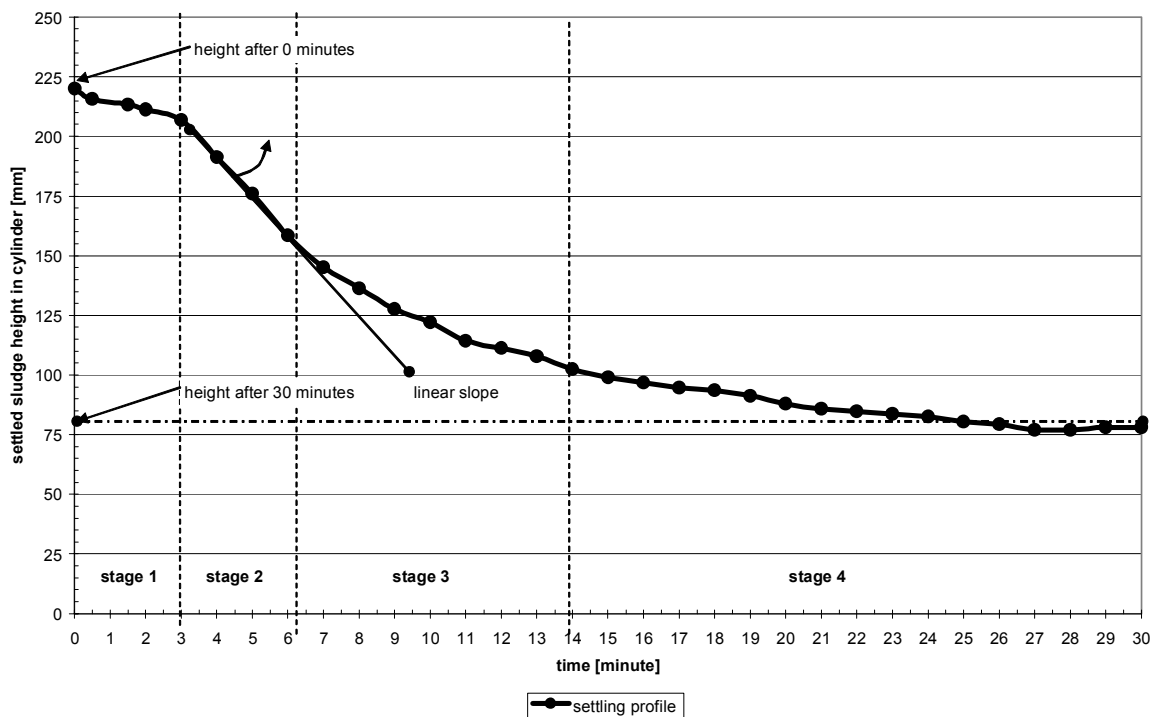
Figure 5-2 Batch MLSS settling profile with 4 settling stages

The ZSV (or u_max) is calculated from the maximum linear slope, and the time to reach ZSV (or t_umax) is determined from the start of the linear slope, as indicated in Figure 5-2. SV_{30} is obtained from the interface height or volume of settled MLSS after 30 minutes, after which SVI is calculated from this SV_{30} and the measured initial MLSS concentration.

5.2.4 Temperature impact on MLSS concentration meter reading

MLSS concentration meter measurements are based on the principle of light scattering caused by the presence of bioflocs (Vanrolleghem *et al.*, 2006). It is not known to what extend commercial MLSS concentration meter readings vary due to changes in temperature-dependent physical biofloc characteristics. MLSS samples in 2 ℓ containers are therefore heated or cooled, and restirred to measure T_s and MLSS concentrations. The measured MLSS concentrations are plotted against T_s. The Microsoft Excel curve fitting function is used to identify trends to indicate if MLSS meter readings are significantly altered by T_s variations, which may exclude the use of such meters in this study.

The MLSS concentration instrument readings decrease slightly with a T_s increase, as summarised in Table 11-2 in Appendix C. The average decrease of 14 mgSS/ℓ per 1°C T_s increase is negligible. The MLSS concentration meter is considered suitable for experimental use within the operational temperature variation range of a few degrees Celsius, as the meter reading change is less than 140 mgSS/ℓ per 10°C T_s change.

5.2.5 Settling container size

MLSS settling results in different sized containers (1 ℓ, 2 ℓ graduated cylinders, and 20 ℓ drum) are compared to determine if settling variations are evident over the MLSS concentration range. Dimensions of the graduated cylinders and the plastic drum are listed in Table 5-2. For a well-settling MLSS, even a 1 ℓ cylinder with a narrow diameter (about 60 mm) should not cause cylinder wall effects (Bhargava and Rajagopal, 1993).

Table 5-2 Batch MLSS settling tests container size

Container	Length / Width [mm]	Diameter [mm]	Height [mm]
1 ℓ	N/A	60.0	355
2 ℓ	N/A	76.8	432
20 ℓ	210 / 250	N/A	405

5.2.6 Reactor zone samples

Thirty-five sets of 2 ℓ grab MLSS samples are periodically taken from the anaerobic zone, anoxic zone, and four successive aerobic zone sections (numbered 1 and 2 from

start, 3 and 4 from end of zone) of a pilot plant BNR reactor consisting of cascading 200 ℓ drums. The piping configuration (bottom inlet, top outlet) and continuous mixing ensure zone samples are representative. MLSS concentration, DO concentration, as well as T_r are measured in all the zones. Batch MLSS settling tests are performed and settling profiles are tabulated. Clarified supernatant samples are collected to measure the turbidity. SV_{30} are obtained from the settling profiles to calculate SVI. ISV are then calculated from the settled MLSS height differences over the settling period of 2 to 5 minutes.

The reactor zone conditions in Table 11-3 in Appendix D indicate relatively stable process conditions. The DO concentrations of the anaerobic and anoxic zones are low (below 0.1 mg/ℓ), while the DO concentrations are above 2.0 mg/ℓ in most sections of the aerobic zone. The MLSS concentration is an average of about 3500 mg/ℓ, with a standard variation of less than 300 mg/ℓ. The MLSS sample settling tests are usually performed at similar conditions (middle of day), which is reflected in low standard deviations in reactor zone temperatures. The higher temperature of about 1°C in the aerobic zone 1 is due to the temporary installation of a heater probe in an attempt to control the T_r of the reactor.

5.2.7 Additional preliminary tests: extended heating and cooling

Preliminary extended heating and cooling test results are summarised in Table 11-4 in Appendix D. The results indicate that MLSS settling changes due to temperature variations are not linear. Larger settleability changes are evident at lower temperatures.

Several studies (Çetin and Sürücü, 1990; Krishna and Van Loosdrecht, 1999; Morgan-Sagastume and Allen, 2003; Zhang et al., 2006b) reported poorer MLSS settling at elevated temperatures. SVI values increased (up to 540 mℓ/g) at long-term elevated temperatures as high as 35 to 45°C. These extreme temperature conditions resulted in deflocculation and reduced MLSS settling properties, as confirmed experimentally by Wilén et al. (2006) at 30 to 45°C, as well as at 4°C. Some of these MLSS settling studies were performed at industrial wastewater plants, as well as during long-term temperature variations. These observations illustrate the importance of proper reference conditions during MLSS settling evaluations. Empirical settling models are not valid outside the experimental temperature boundaries. This preliminary test confirmed that MLSS settleability is not directly related to temperature variations outside these experimental boundaries.

5.2.8   Sample conditioning methods

To change environmental conditions, 1 ℓ and 2 ℓ cylinders are placed in direct sunlight or in shade. The rest of the experimental method is identical to previous procedures.

5.3   Results and discussion

5.3.1   Impact of container size on MLSS settling

Container size does not play a significant role in settling of MLSS samples from the local reactor, when judged by the average variation in settling parameters listed in Table 5-3. The raw experimental data is tabulated in Table 11-5 and trends are displayed in Figure 11-2 to Figure 11-13 in Appendix D. For the average MLSS concentration of 4203 mg/ℓ, the average SVI, ISV, and supernatant turbidity from the three settling tests for the 1 ℓ and 2 ℓ cylinders differ by only 4 mℓ/g, 0.14 m/hr, and 2 FNU respectively. The smaller 1 ℓ cylinder samples heated up slightly faster, due to solar radiation, during the 30-minute settling tests. The faster sample heating in the 1 ℓ cylinder resulted in a small T_s difference of 0.3°C between the 1 ℓ and 2 ℓ cylinder samples after 30 minutes.

Table 5-3 Impact of container size on MLSS settling

Container [ℓ]	T_{s30} [°C]	SVI [mℓ/g]	ISV [m/hr]	Turbidity [FNU]
1	23.5	108	0.70	19
2	23.2	111	0.84	21
20	20.6	126	0.64	15

The settling results of the 20 ℓ sample differ slightly from the 1 ℓ and 2 ℓ samples. The limited area exposed to solar radiation in the large 20 ℓ container causes a slower T_s increase, compared to the 1 and 2 ℓ cylinders. At the lower T_s in the 20 ℓ container, the SVI is slightly higher and the ISV and supernatant turbidity slightly lower. The SVI, ISV, and turbidity change in the 20 ℓ container points directly towards the significant T_s impact on MLSS settleability. Wall effects and biofloc bridging effects are not present in the large 20 ℓ container. The reduced settleability (in terms of SVI and ISV) of the 20 ℓ sample is therefore related to T_s differences between small and large containers.

The SVI, ISV, and supernatant turbidity variations in the 1 ℓ, 2 ℓ, and 20 ℓ containers are small enough to accept that the 2 ℓ cylinder is suitable for the MLSS settling evaluations performed during the remainder of the experimental work. This verification ensures the container size is not a factor in 2 ℓ batch settling and 2 ℓ on-line settling test (based on the use of well-settling MLSS samples).

5.3.2 Impact of reactor zone on MLSS settling

Settling parameters are influenced differently as MLSS moves through the three BNR reactor zones. The SVI, ISV, and supernatant turbidity data is summarised in Table 11-3 in Appendix D, and illustrated in Figure 5-3. The SVI improves slightly after entering the aerobic reactor zone, but the ISV in essence stays unchanged through the three reactor zones. Supernatant turbidity reduces noticeably in all three reactor zones. This leads to a MLSS clarification improvement through successive zones in the BNR reactor.
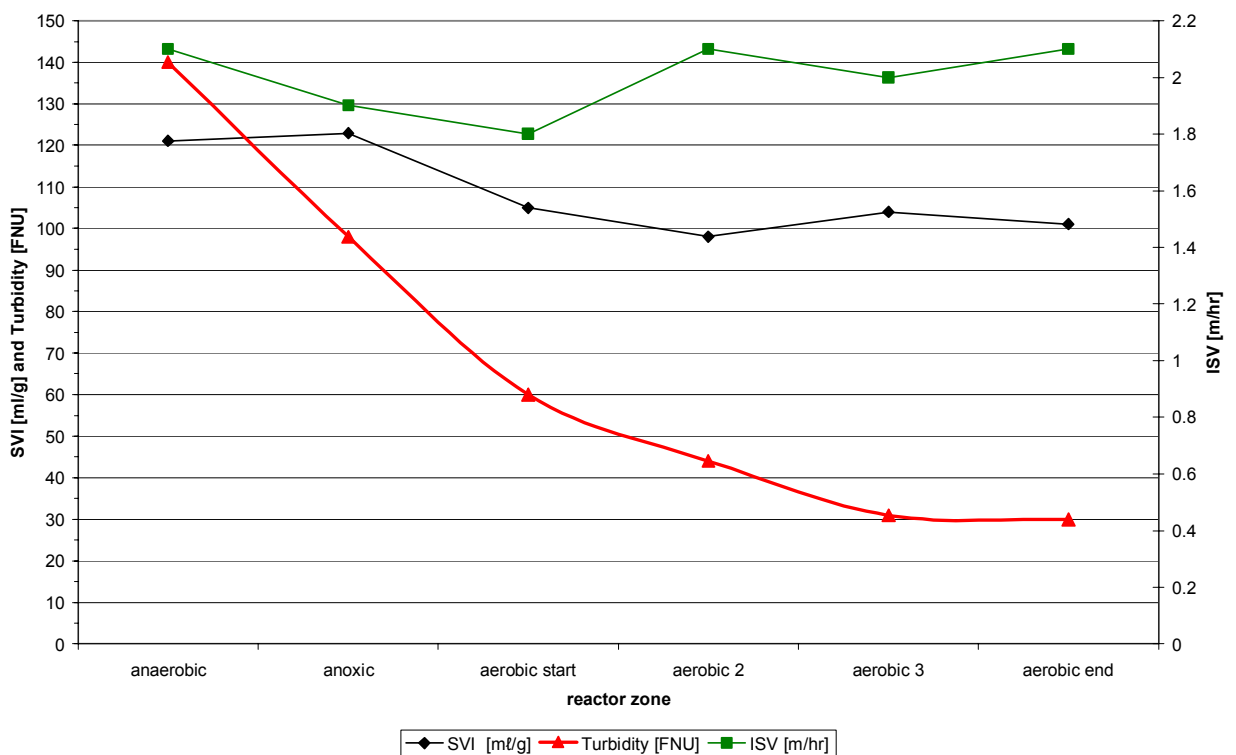
Figure 5-3 Settling parameters changes throughout three BNR reactor zones

The SVI improves from an average of 122 mℓ/g from the non-aerated anaerobic to anoxic zones, to an average of 102 mℓ/g in the four aerobic zones. The first aerobic section MLSS has a slightly higher SVI of 105 mℓ/g, against the average of 101 mℓ/g for the

MLSS in the other three aerobic sections. There is an immediate SVI improvement from the unaerated anoxic zone to the first aerobic zone. The standard deviation of SVI of 31 mℓ/g in the anaerobic to anoxic zones reduces to 11 mℓ/g in the four sections of the aerobic zone, which indicates a more stable SVI under aeration. The shift, from unaerated to aerated conditions, results in a small improvement in SVI, with an average SVI reduction measured at 19 mℓ/g.

ISV stays constant at an average of 2.0 m/hr from the anaerobic to anoxic zone, to 2.0 m/hr in the four sections of the aerobic zone. The average standard deviation of 0.6 m/hr stays constant throughout the reactor zones, for comparable settling velocity conditions in all reactor zones. The shift from unaerated to aerated conditions does not change the ISV significantly, with changes of about 0.3 m/hr measured between adjacent reactor zones.

Settled sewage mixes with RAS to create an anerobic zone at the reactor inlet, forming a MLSS with the highest supernatant turbidity of 140 FNU. This turbidity decreases by 42 FNU to 98 FNU in the anoxic zone, as the zone retention time and aerated a-recycle MLSS introduced into the anoxic zone appears to assist with MLSS flocculation to reduce supernatant turbidity. The turbidity reduces then by 38 FNU to 60 FNU in the first section of the aerobic zone. The turbidity reduction from the anaerobic zone to the start of the aerobic zone is 69%. The turbidity reduces subsequently slightly by 16 and 13 FNU in the second and third section of the aerobic zone, to 44 and 31 FNU respectively. No additional turbidity reduction is detected in the last section of the aerobic zone.

It appears that once a minimum aeration period is reached, extended aeration is not beneficial for further supernatant turbidity reduction. These results illustrate hydraulic residence time requirements in reactors and settling tanks, as simulated for MLSS settling by the 30-minute settling test duration. Ekama *et al.* (1997) found that an 1200 second (20 minute) flocculation duration is sufficient in full-scale settling tanks. The simulated 30-minute batch MLSS settling test is thus appropriate to determine the extent of supernatant clarification.

MLSS deflocculates when exposed to anaerobic conditions (Wilén *et al.*, 2000), as found in the anaerobic reactor zone. Reflocculation occurs relatively fast in the downstream reactor zones or under quiescent conditions in the stilling chamber of the secondary

settling tank. The SVI or settling velocity changes due to temperature variations in the different reactor zones is unknown from the available literature. This preliminary survey with 35 MLSS samples from six sections of a BNR reactor indicated the following changes to three MLSS settling parameters:

- SVI improves slightly in the aerobic reactor,
- ISV is relatively constant throughout reactor zones, and
- Supernatant turbidity reduces throughout BNR reactor zones.

5.3.3 Impact of container environment on MLSS settling

MLSS settling curves represent individual plant reactor conditions, and settling characteristics of MLSS is accordingly unique (Stypka, 1998). MLSS settling models, such as the Takács model (Takács *et al.*, 1991), require calibration with site-specific MLSS settling characteristics (Wilén, 2006) obtained from individual reactors.

The container environment plays a significant role in MLSS settling at an average MLSS concentration of 4203 mg/ℓ, as summarised in Table 5-4. The raw data is tabulated in Table 11-5 in Appendix D, and trends are displayed in Figure 11-2 to Figure 11-13 in Appendix D. The average SVI, ISV, and supernatant turbidity for three tests with the 1 ℓ and 2 ℓ cylinders differ significantly by about 50%, due to the placement of the cylinders in the sun or shade.

Table 5-4 Impact of container environment temperature on settling (T_r 19.6°C, T_a 17.9°C)

Cylinder [ℓ]	Position	T [°C] after 30 min	SVI [mℓ/g]	Change [mℓ/g/1°C]	ISV [m/hr]	change [m/hr/1°C]	Turbidity [FNU]	change [FNU/1°C]
1	Sun	23.5	108	N/A	0.70	N/A	19	N/A
	Shade	19.1	174	-15	0.04	0.15	14	1.2
2	Sun	23.2	111	N/A	0.84	N/A	21	N/A
	Shade	19.1	171	-14.6	0.44	0.10	14	1.7

SVI decreases with 1 ℓ and 2 ℓ samples are 15.0 mℓ/g and 14.6 mℓ/g per 1°C T_s increase respectively. The corresponding ISV increases are 0.15 m/hr and 0.10 m/hr per 1°C T_s

increase respectively. The corresponding supernatant turbidity increases are 1.2 FNU and 1.7 FNU per 1°C T_s increase respectively. The average SVI decrease, the ISV increase, and the supernatant turbidity increase are therefore 14.8 mℓ/g, 0.12 m/hr, and 1.42 FNU per 1°C T_s increase respectively.

Local effects of solar radiation on sample placements in the shade or direct sunlight result in a temperature difference of about 4.3°C over 30 minutes. This large T_s variation confirms the important effect of solar radiation intensity on water bodies, as observed by Tadesse *et al*. (2004). The large variations in excess of 50% in SVI, ISV, and supernatant turbidity indicate the importance of sample environmental conditions control, as well as temperature compensation and recordings before and during batch MLSS settling tests.

5.4 Summary

Several aspects of batch MLSS settling tests procedures influence results. The three aspects of settling procedures evaluated in this study consist of (i) container size, (ii) reactor zone sample origin, and (iii) container environment.

• Container size (1 ℓ, 2 ℓ or 20 ℓ) does not change the SVI, ISV, or supernatant turbidity of the plant specific MLSS samples significantly.

• MLSS samples from the three BNR reactor zones do not exhibit large variations in SVI or ISV, but the clarified supernatant turbidity improves throughout successive BNR reactor zones.

• Temperature-dependent MLSS settling variations are not linear over an extended T_s range. A larger MLSS settleability deterioration change is evident at lower T_s.

• Temperature variations during sample handling have significant impacts on MLSS settling. An average SVI decrease of 14.8 mℓ/g per 1°C T_s increase, an ISV increase of 0.12 m/hr per 1°C T_s increase, combined with a supernatant turbidity increase of 1.7 FNU per 1°C T_s increase, were measured during 30-minute MLSS batch settling tests, at a total T_s variation of about 4.3°C.

• No temperature dependent settling trends are identified across the BNR reactor from these standard MLSS batch settling tests. This indicates the insensitivity of conventional settling equipment and traditional methods to attempt to perform temperature dependent batch MLSS settling tests over small operational T_r ranges.

5.5   Conclusions

The general conclusions to summarise experimental results are as follows:

• Temperature has a significant impact on MLSS settling, with a SVI decrease of 14.8 mℓ/g per 1°C T_s increase, an ISV increase of 0.12 m/hr per 1°C T_s increase, combined with a clarified supernatant turbidity increase of 1.7 FNU per 1°C T_s increase. At higher temperatures within the operational T_s range, MLSS settling improves, and supernatant clarification deteriorates.

• Temperature dependent MLSS settling variations are not linear, with larger MLSS settleability deterioration evident at lower temperatures, when compared to small MLSS settleability changes at higher temperatures outside the operational T_s range.

• There is an immediate, but relatively small, improvement in MLSS settleability, in terms of SVI, when anaerobic MLSS is aerated.

• There is a continuous improvement in supernatant clarification, according to the turbidity reduction, when anaerobic MLSS transfers through successive reactor zones. Aeration results in supernatant turbidity reduction until a mimimum turbidity is reached.

• Existing conventional batch settling equipment and traditional basic procedures are not suitable to effortlessly identify temperature dependent MLSS settling changes over small operational T_r ranges.

The significant effects of short-term temperature changes on batch MLSS settling test results creates the need for more advanced MLSS settling monitoring techniques. On-line MLSS settling is such a technique, where temperature compensation is incorporated in the settling sampling and test method.

6 ON-LINE MLSS SETTLING EVALUATION

On-line MLSS settling profiles are evaluated in this chapter. Profiles are obtained from an automated MLSS settling meter to calculate temperature and MLSS concentration-based settling parameters. The improved MLSS settling models illustrate the effects of including short-term temperature fluctuations in the determination of settling parameters.

6.1 Background

The capacity and performance of a secondary settling tank relates to the velocity at which MLSS separates and settles to the bottom of the tank (Jeyanayagam *et al.*, 2006). MLSS concentration and MLSS settling velocity measurements are thus required to perform a batch MLSS settleability evaluation. On-line instrumentation is available to perform these manual measurements on an automated basis. Gernaey *et al.* (1998) consider the development and use of such on-line MLSS settling meters as a major improvement on batch MLSS settleability tests.

MLSS concentration is the main factor that contributes to variations in the MLSS settling process (Reardon, 2005). Numerous additional settleability factors are summarised for reference purposes in alphabetical order in Table 11-7 to Table 11-12 in Appendix G. These factors create suitable conditions for the formation of a well-settling MLSS. The most essential factors include a sufficient sludge age in the BNR reactor, combined with suitable DO concentrations in the different reactor zones, as well as a wastewater feed containing adequate substrates (De Clercq *et al.*, 2007).

Temperature is a settleability factor that affects several aspects of MLSS settling (Morgan-Sagastume and Allen, 2003). Temperature modifies water density and water viscosity (Clements, 1976), as well as the surface and composition characteristics of the individual bioflocs (Gerardi, 2002). These temperature-based MLSS settling changes are highly variable, due to operational T_r variations. The short-term T_r variations follow diurnal T_a fluctuations, while long-term T_r variations follow seasonal T_a fluctuations (Wahlberg *et al.*, 1996).

On-line MLSS settling meters are ideally suited to monitor and collect MLSS settling data over these diurnal T_r fluctuations. There are three main developments reported on the

implementation of automated MLSS settling equipment. (i) One of the first reported MLSS settling meters was developed in Japan (Sekine *et al.*, 1989) in the late 1980s for batch settling tests. This MLSS settling meter is able to measure SVI, compression velocity, as well as ISV. (ii) A second unit was developed in Belgium (Vanderhasselt *et al.*, 1999b) in the 1990s for on-line MLSS settling tests. This settling meter includes a stirrer to measure SSVI. Vanrolleghem *et al.* (1996) reports that this meter is designed with a sample dilution function to measure DSVI. (iii) Wahlberg (2004) developed a settling meter that is patented as an apparatus, as well as an integrated method, to measure and manipulate MLSS settling, compression and flocculating characteristics.

Simon *et al.* (2005) and Lynnggaard-Jensen and Lading (2006) recently described a novel settling meter sensor that consists of a sample chamber intended for direct submersion into a reactor. This sensor is equipped with an array camera and photo sensor to measure the MLSS settling interface over 30 minutes. These reports indicate that substantial research and development is directed to automate aspects of the traditional batch MLSS settling test.

The aim of this chapter is to model temperature dependent MLSS settling parameters. The parameters are obtained from semi-continuous MLSS settling profiles that are generated during diurnal T_r fluctuations with the use of an automated on-line MLSS settling meter.

6.2   Materials and methods

6.2.1   Experimental approach

On-line MLSS settling tests are performed at a full-scale BNR reactor outlet. Van Huyssteen *et al*. (1990) describe this plant in some detail. The on-line settling tests are required to confirm that the range of temperature related full-scale MLSS settling changes are comparable to settling parameter changes identified during the preliminary batch MLSS settling tests, as reported in Chapter 5.

The automated on-line MLSS settling meter generates about 40 successive MLSS settling profiles per 24-hour day. The settling data and profiles, in electronic format, are used to calculate settling parameters. A statistical computer software program evaluates these parameter correlations to obtain temperature dependent MLSS settling models. A

practical approach is therefore provided to improve the reliability of MLSS settling parameters, as effects of short-term temperature variations before and during MLSS settling tests can be virtually eliminated.

6.2.2 MLSS settling meter configuration

The custom-built MLSS settling meter automates the monitoring and recording of batch MLSS settling tests. The settling meter monitoring method is based on a vertical moving single point infrared light detector that consists of a light source and receiver. The light detector follows the descending liquid / MLSS interface along a transparent cylinder filled with MLSS. The program logic controller (PLC) records the height of the light detector in electronic format during the MLSS settling period, thereby generating a settling profile.
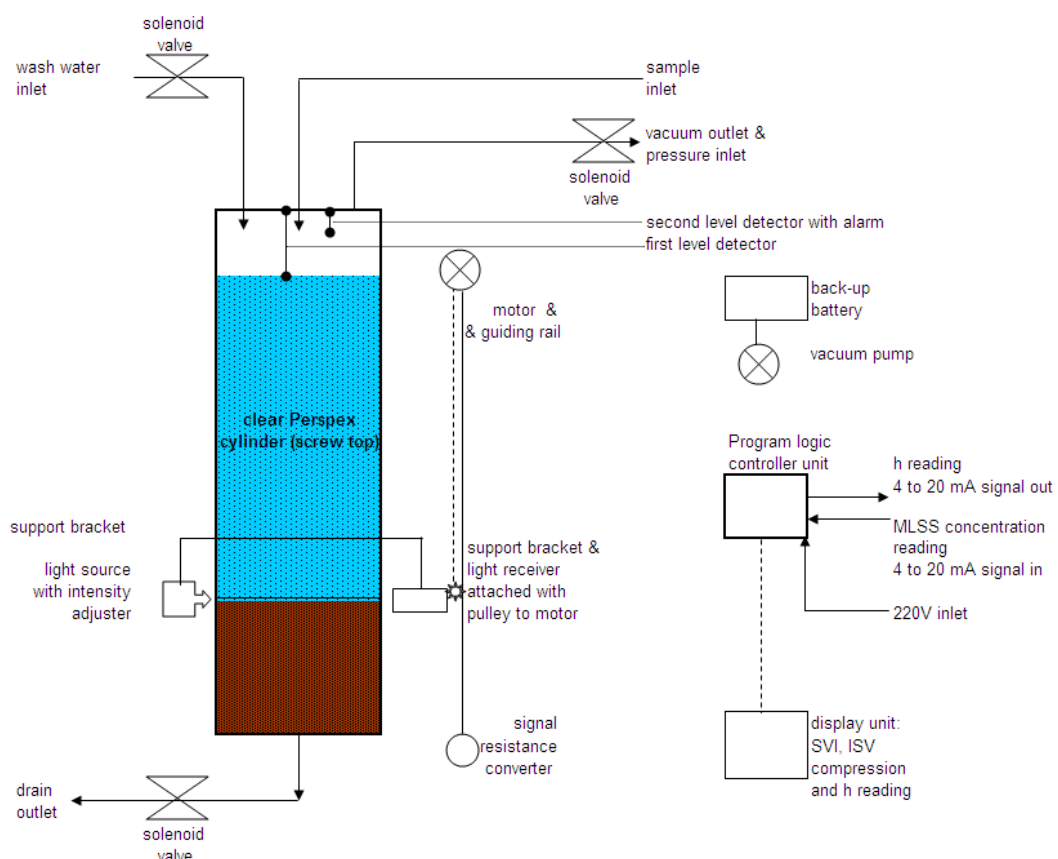
Figure 6-1 Schematic diagram of main components of the MLSS settling meter

Three requirements of the MLSS settling meter are: (i) to obtain MLSS samples without subjecting bioflocs to excessive turbulence, (ii) to trend successive 30-minute MLSS

settling profiles together with T_r and MLSS concentration data, and (iii) to operate fully automated and without supervision.

Figure 6-1 illustrates the main components of the MLSS settling meter. A vacuum driven sample suction system transfers the MLSS sample from the reactor basin into the cylinder. The vacuum system also pressurises the cylinder after each settling test to drain the cylinder, and to flush out any stagnant MLSS sample trapped in the transfer pipe. The vacuum system ensures the MLSS sample is not exposed to excessive pump shear during sample transfer. A wide cylinder is used to prevent or reduce wall effects during settling. The clear Perspex cylinder has a working volume of 2 ℓ, with a height of 360.9 mm, an internal diameter of 84.0 mm, and a wall thickness of 3.5 mm.

The MLSS sample transfer is rapid and the cylinder fills up within a few seconds. The MLSS sample discharge into the cylinder creates enough turbulence to ensure the sample mixes homogenously. The settling test starts immediately after a maximum level detector stops the sample transfer. The scanner moves downward to follow the settling liquid / MLSS interface level during the 30-minute test duration. The light sensor activates almost instantaneously as the MLSS settles, due to the scanner light source signal that the detector receives through the transparent clarified supernatant. The sensor stops moving down once the scanner light source signal is lost, due to the opaque settled MLSS. The sensor moves downward in about 4 mm increments, which is the minimum distance that the geared drive unit of the sensor can move.

The PLC records the MLSS interface level after each minute of the 30-minute settling period. The PLC calculates the initial settling velocity (minutes 2 to 5 of the 30-minute test) and the SVI. These parameter values appear on a digital display unit after each settling cycle. The settling meter has a manual termination function to cancel a test and to restart the complete settling cycle.

The settling meter is relatively mobile and simple to commission. The meter start-up requires a 220 V power source, a potable wash water supply, a 4 to 20 mA signal input from the reactor MLSS concentration meter, as well as a MLSS sample source. The MLSS concentration reading is not essential for the MLSS settling meter operation, as it is only used for the SVI display and SVI calculation. The settling meter and components

are installed in a fully enclosed weatherproof cabinet, to eliminate or reduce meteorological effects, such as wind, rain, solar radiation, and T_a changes. Photograph 1 in Appendix F shows the general arrangement of the MLSS settling meter components. The automated operation sequence to create one MLSS settling profile consists of the following three steps:

Step 1: MLSS sample preparation

• cylinder drain valve opens,

• cylinder chamber pressurises to force out previous MLSS sample through bottom drain and to flush top MLSS sample inlet line, adjustable duration of 5 seconds,

• potable wash water cleaning cycle to spray inner cylinder walls, adjustable duration 4 seconds,

• cylinder chamber pressurises to force out wash water through bottom drain, adjustable duration 5 seconds,

• cylinder drain valve closes,

• cylinder chamber under vacuum to extract MLSS sample from reactor basin into cylinder,

• vacuum stops when cylinder maximum level sensor at 2 ℓ capacity is detected,

• external initial reactor MLSS concentration reading obtained for SVI calculation, and

• external logger T_r is recorded.

Step 2: MLSS settling test

• 30 minute counter starts,

• MLSS settling interface height is recorded every minute for 30 minutes according to level of light detector,

• height reading capture at 120 seconds,

• height reading capture at 300 seconds, PLC calculates, displays ISV (2 to 5 minutes),

• height reading capture at 1500 seconds,

• height reading capture at 1790 seconds, PLC calculates, displays compression velocity (25 to 30 minutes), and

• final height capture according to light detector level at 30 minutes, PLC calculates, displays SVI.

Step 3: MLSS sample removal

- light detector moves upwards to the start position at maximum cylinder height level, and

- step 1 restarts after a total of 46 minutes (16-minute adjustable period between tests), except if the manual override function is turned on at any stage to return to start of step 1.

A two-channel data logger (Microlog Plus; Fourier, 2007) captures the settling meter height profiles. The logger data is recorded in a Microsoft Excel compatible format to ensure manual download to a computer.

6.2.3 MLSS settling meter velocity data collection method

The settled MLSS height (h) variations over 30-minute settling test duration are obtained from the original MLSS settling profiles, as illustrated in Figure 6-2. The stage 1 lag or reflocculation time, stage 2 ZSV or u_max, stage 3 transition, and stage 4 compression are indicated on successive settling profiles.
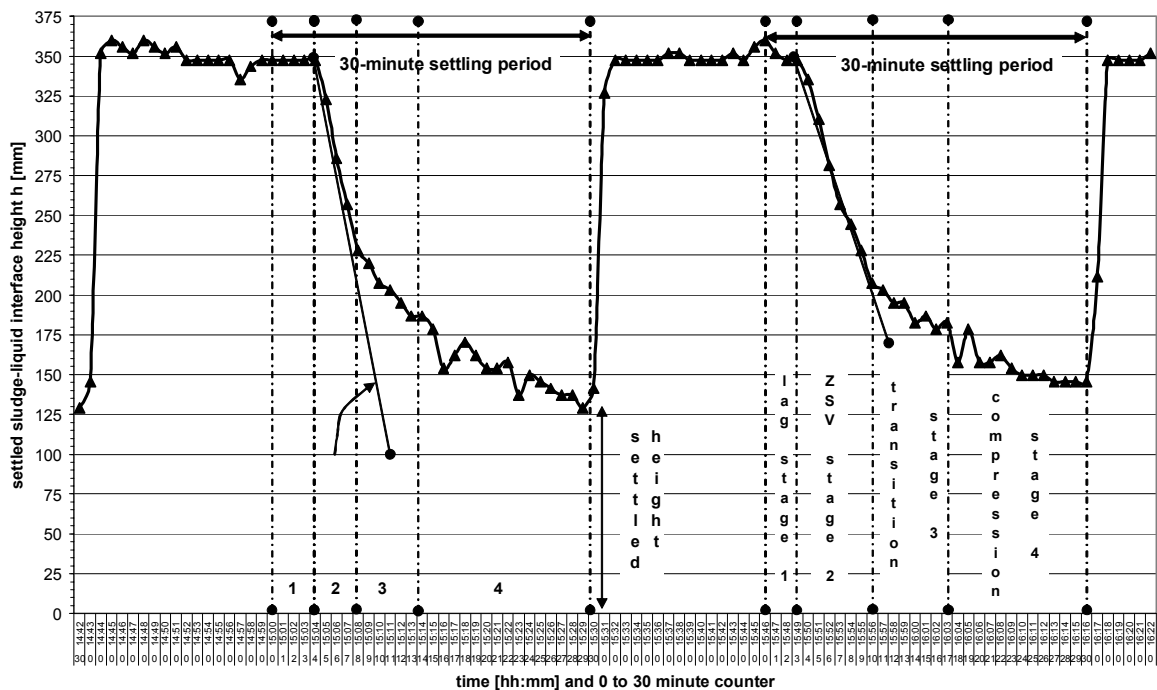
Figure 6-2 Two consecutive on-line MLSS settling profiles recorded by the settling meter

The MLSS settling parameters are computed from these settling profiles with the use of a Microsoft Excel spreadsheet as follows:

- lag time before settling of liquid / MLSS interface starts (stage 1),
- ISV from period 2 to 5 minutes of MLSS settling,
- u_max from the linear negative slope (stage 2),
- t_umax from when u_max commences (start of stage 2),
- SV_{30} from the settled MLSS height after 30 minutes (end of stage 4), and six incremental 5-minute MLSS settling velocities over 30 minutes: u1, u2, u3, u4, u5, u6.

6.2.4 MLSS settling meter velocity data collection boundaries

The on-line MLSS meter generated 85 settling profiles for the full-scale plant. The experimental data range boundaries for these profiles are listed in Table 6-1. The MLSS concentration and T_r variations at the full-scale plant are recorded from 4489 to 4923 mgSS/ℓ, and from 17.2 to 19.0°C respectively.

Table 6-1 Experimental data range for on-line MLSS settling evaluation

Parameter	Full-scale reactor condition
n	85
Minimum T_r [°C]	17.2
Maximum T_r [°C]	19.0
Minimum MLSS concentration [mg/ℓ]	4489
Maximum MLSS concentration [mg/ℓ]	4923

6.2.5 Data presentation

6.2.5.1 Data logger transfer and calculations

A data logger (Microlog Plus; Fourier, 2007) equipped with an internal thermometer measures and records T_r. The logger has an external 4 to 20 mA signal input facility that is used to store the settling meter h data. A similar data logger is used to record T_r from the built-in thermometer of the DO concentration meter (ATI Model B15\60; ATI, 2007). An additional data logger (Alog MCS131LCD; MC Systems, 2007) stores the on-line

data from the DO and MLSS concentration meters. The data collection proceeds as follows:

- The DO concentration meter data logger produces a data table of readings of date [dd-mm-yyyy], time [hh:mm] in 5 minute increments, and DO concentration [mg/ℓ] in 0.1 mg/ℓ increments. The data tables are transferred into Excel spreadsheets.

- The MLSS concentration meter data logger produces a data table of readings of date [dd-mm-yyyy], time [hh:mm] in 5 minute increments, and MLSS concentration [mg/ℓ] in 0.1 mg/ℓ increments. The data tables are transferred into Excel spreadsheets.

- The MLSS settling meter data logger produces a data table of readings of date [dd-mm-yyyy], time [hh:mm:ss] in 1 minute increments, and height [mm] in 0.1 mm increments. The data tables are transferred into Excel spreadsheets.

- The thermometers data produces data tables of readings of date [dd-mm-yyyy], time [hh:mm] in 5 minute increments, T_a from the internal ambient temperature sensor in 0.3°C increments and T_r from the DO concentration meter temperature sensor [°C] in 0.3°C increments. The data tables are transferred into Excel spreadsheets.

The Excel spreadsheet containing the settling meter height data is the reference sheet for all calculations. An example of a settling data graph is provided in Figure 11-14 in Appendix E. Data in the spreadsheet is not filtered to remove noise. Bergh (1996) describes experimental noise as fluctuations in measurements that originate from the process or measuring devices used.

The cylinder height readings [mm] are converted to cylinder volume values [mℓ]. The DO and T_r readings are averaged over each 30-minute settling period, and the initial MLSS concentration reading is used to calculate SVI. The MLSS settling profile over 30 minutes is used to calculate the 11 MLSS settling parameters: SVI [mℓ/g], u_max [m/hr], u_ave [m/hr], t_umax [minute], h [mm] and the six incremental u1 to u6 five-minute settling velocities [m/hr].

The reference Microsoft Excel spreadsheet is used to list the date, time, DO concentration, MLSS concentration, SV_{30}, SVI, t_umax, u_max, u_ave, h, and u1 to u6. The two dependent variables, MLSS concentration and T_r, are transferred together with the 11 settling parameters into the DataFit (2005) statistical computer program.

6.2.5.2 Empirical settling correlations and statistical comparisons

The MLSS settling data is used to generate 2-D best-fit correlations between the MLSS concentration and the 11 MLSS settling parameters. The same settling data is then used to generate 3-D best-fit correlations with MLSS concentration, T_r, and the 11 MLSS settling parameters. To evaluate the impact of T_r inclusion, the improvement in correlations can be statistically determined by comparing R^2-values. R^2 is the most widespread coefficient used to assess MLSS settling models (Ozinsky and Ekama, 1995).

There are 298 single independent 2-D regression models and 242 3-D non-linear regression models pre-defined in DataFit (2005). These pre-defined models allocate best-fit correlations for the settling data according to R^2-values. This automatic ranking function of DataFit identifies the best-fit correlations.

The DataFit package generates 3-D plots of the regression models, where the dependent variables are allocated to the x_1- and x_2-axes, and the response variables to the y-axis. In the graphical display of the non-linear regressions, bullets above and below the surfaces indicate the data points, and the surfaces with colour bands indicate the regression result ranges. The built-in regression analysis function of Microsoft Excel analyzes the rest of the experimental MLSS settling data.

6.3 Results and discussion

The mathematical relationships between settleability parameters are approximated as basic polynomial functions, to show trends that adequately describe MLSS settling behaviour. The on-line MLSS settling results are presented in the following sections:

- settling parameters diurnal profiles (h, MLSS concentration, SVI)
- settling parameters best-fit model
  - dependent variables: MLSS concentration and T_r
  - response variables: SVI, u_max, and t_umax
- settling parameter model correlations (SVI with u_max and t_umax)
- settling parameters simplified models
  - dependent variables: MLSS concentration and T_r
  - response variables: SVI, u_max, t_umax, u_ave, h, u1, u2, u3, u4, u5, u6

6.3.1 h and T_r diurnal variation

The recorded data points and fitted trends for the diurnal T_r and settled MLSS height variations are shown in Figure 6-3. The x_1-axis indicates the 24-hour diurnal period, the primary y_1-axis indicates T_r, and the secondary y_2-axis indicates the on-line MLSS settling meter h reading.
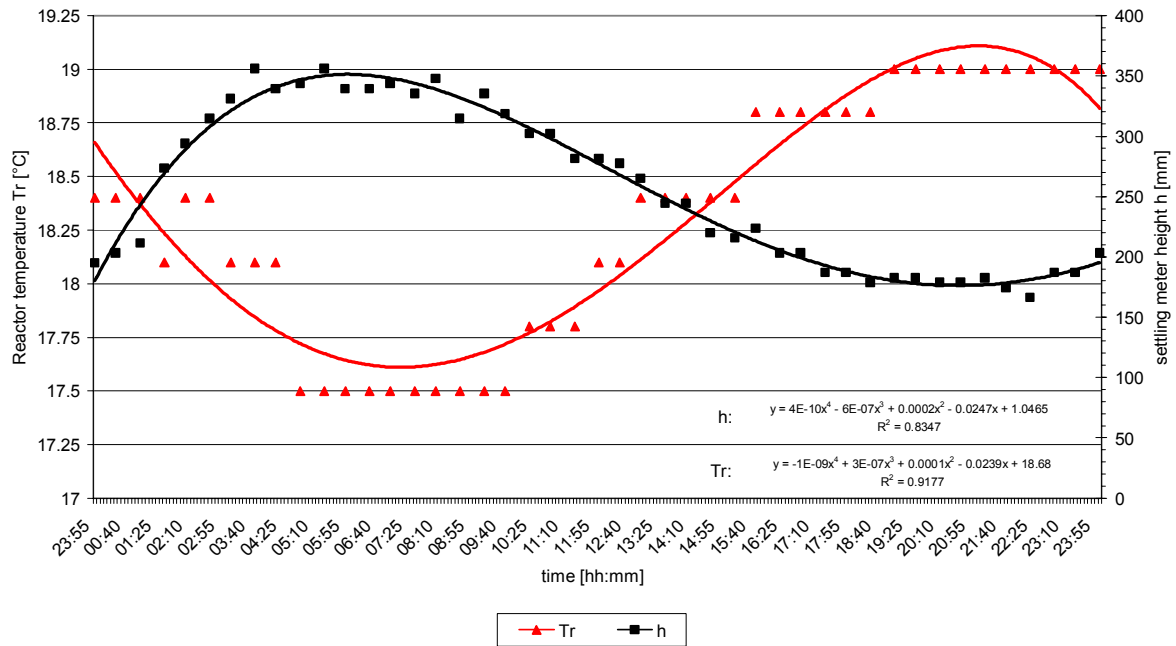
Figure 6-3 Data and fitted curves of temporal variations in T_r and h

The full-scale plant T_r fluctuated by about 1.5°C per typical day in spring. The T_r profile changed from 17.5 to 19.0°C, and the h profile changed from about 350 to 170 mm, as shown in Figure 6-3. These T_r and h profiles follow sinusoidal wave profiles, as represented by the fitted curves with R^2 of 0.92 and 0.83 respectively. From the on-line MLSS settling tests, the MLSS settling meter height reading illustrated the inverse relationship between T_r and the 30-minute settled MLSS height in a settling test cylinder.

6.3.2 MLSS concentration and T_r diurnal variation

The recorded data points and fitted trends for the diurnal T_r and MLSS concentration variations for the full-scale plant are shown in Figure 6-4. The x_1-axis indicates the 24-hour diurnal period, the primary y_1-axis indicates T_r and the secondary y_2-axis indicates the on-line MLSS concentration reading. Two 2-day profiles, with T_r and MLSS concentration correlations R^2 of 0.91 and 0.90 respectively, are provided in Figure 11-16 in Appendix D for reference purposes.

MLSS $\quad y = 0.0001x^3 - 0.067x^2 + 7.187x + 4660.7$
$\quad R^2 = 0.937$

$T_r \quad y = -5E\text{-}07x^3 + 0.0003x^2 - 0.0329x + 18.802$
$\quad R^2 = 0.9104$
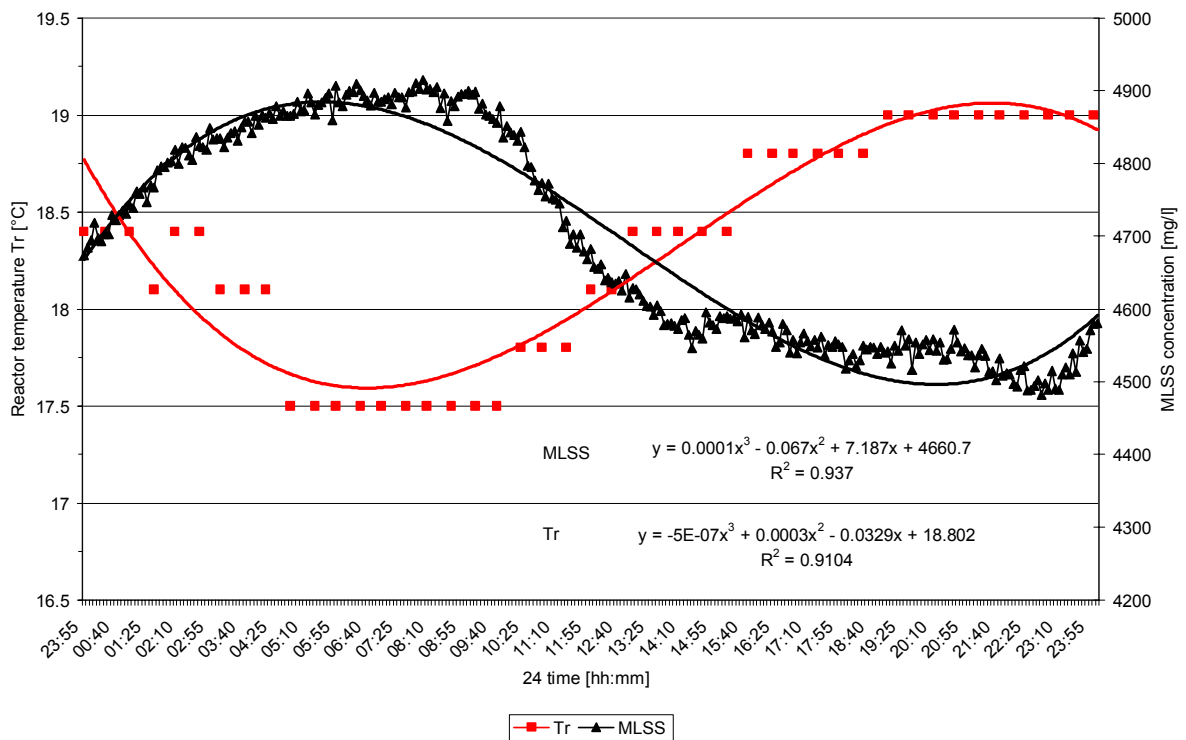
Figure 6-4 Data and fitted curves of temporal variations in T_r and MLSS concentration

The full-scale plant average MLSS concentration varies by about 400 mg/ℓ per day. The diurnal MLSS loading variations, originating from the plant and reactor inflow, as well as the secondary settling tank RAS flow, cause MLSS concentration variations (Otterpohl and Freund, 1992). This MLSS concentration profile was relatively smooth over the 24-hour period, as shown in Figure 6-4. The T_r and MLSS concentration profiles follow a sinusoidal wave profile, as represented by fitted curves with R^2 of 0.92 and 0.94 respectively.

6.3.3 SVI and T_r diurnal variation

The calculated SVI, recorded data points for the diurnal T_r, and fitted trends for the full-scale plant, are shown in Figure 6-5. The x_1-axis indicates the 24-hour diurnal period, the primary y_1-axis indicates T_r, and the secondary y_2-axis indicates the calculated SVI reading. Two 2-day profiles, with SVI and T_r correlations R^2 of 0.92 and 0.91 respectively, are provided in Figure 11-17 in Appendix D for reference purposes.
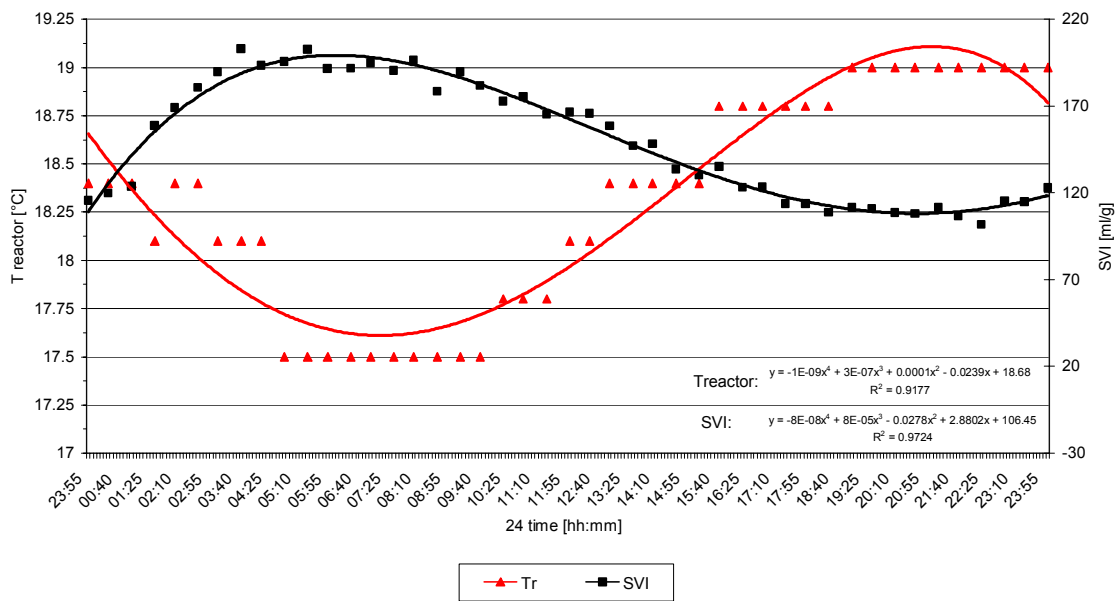
Figure 6-5 Data and fitted curves of temporal variations in T_r and SVI

The full-scale plant average SVI varies by about 100 mℓ/g per day. This variation was caused by the diurnal MLSS concentration and T_r fluctuation. The SVI profile was relatively smooth over a daily 24-hour period, as shown in Figure 6-5. The T_r and SVI trends follow sinusoidal wave profiles, as represented by fitted curves with R^2 of 0.92 and 0.97 respectively.

Two 2-day profiles, with SVI and MLSS concentration correlations R^2 of 0.92 and 0.90 respectively, are provided in Figure 11-18 in Appendix D for reference purposes.

6.3.4 Model fitting: SVI dependence on MLSS concentration and T_r

The SVI dependence on MLSS concentration and T_r is statistically evaluated with individual and combined correlations in 2- and 3-D models.

6.3.4.1 SVI link to MLSS concentration

The recorded data points and a fitted trend for the on-line MLSS concentration and calculated SVI are shown in Figure 6-6. The x-axis indicates MLSS concentration, and the y-axis indicates SVI. The best-fit curve for SVI related to MLSS concentration from full-scale data is represented by a polynomial with a R^2 of 0.69, as shown in Figure 6-6.

Figure 6-6 SVI related to MLSS concentration

The direct relationship between SVI as the response variable and MLSS concentration as the dependent variable is confirmed by the polynomial, since SVI increases according to the best-fit curve as MLSS concentration increases. The calculated SVI data scatter was visible from 97 to 203 mℓ/g throughout the MLSS range of 4489 to 4923 mg/ℓ. The data scatter is in agreement with earlier observations of experimental MLSS settling data and calculated SVI ranges, as presented in models by Daigger and Roper (1985) and Catunda and Van Haandel (1992). There are therefore other significant factors present that are not incorporated in the traditional SVI regression models based only on MLSS concentration. Ambient and reactor temperature fluctuations, and the related change in sample temperature, are such factors that can account for some of the scatter in SVI data.

6.3.4.2   SVI link to T_r

The recorded data points and a fitted trend for the on-line T_r and calculated SVI are shown in Figure 6-7. The x-axis and the y-axis indicate the T_r and SVI respectively. The best-fit curve for SVI related to T_r for full-scale plant data is represented by a 6th order polynomial, based on a very low R^2 of only 0.38.
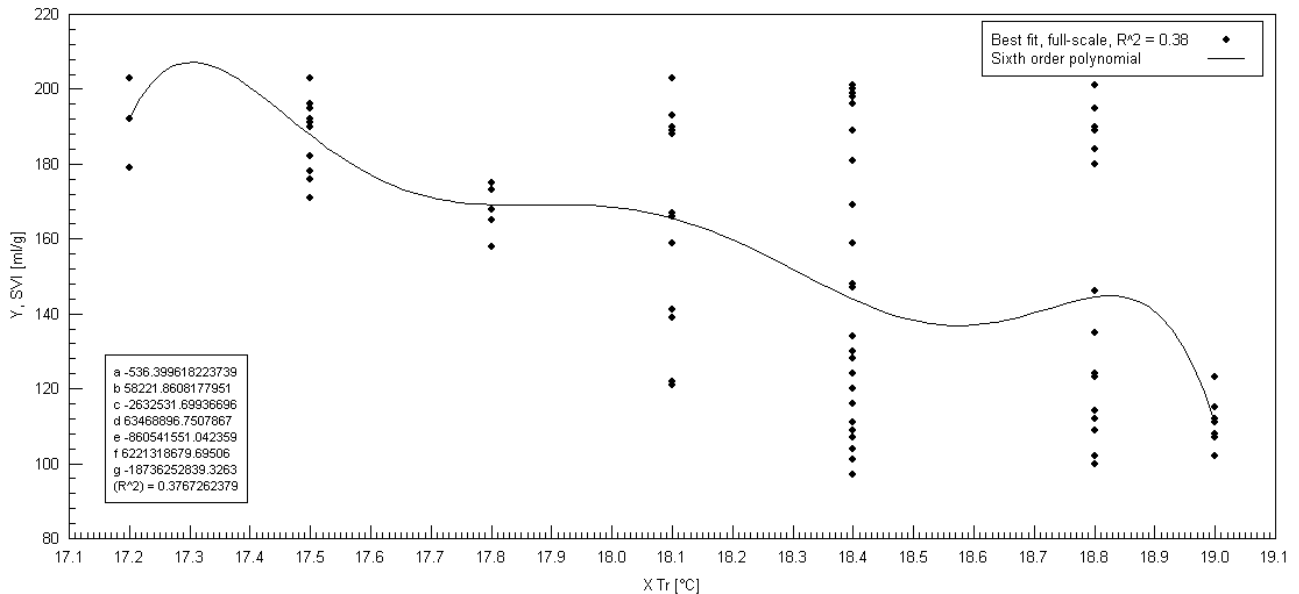
Figure 6-7 SVI data scatter according to T_r variation

A basic inverse relationship between SVI as the response variable and T_r as the dependent variable is visible in Figure 6-7, as SVI decreases as T_r increases. The large experimental SVI data scatter was present throughout the fixed T_r range, since the T_r data logger only recorded in 0.3°C increments.

This large data scatter indicates that the SVI data cannot be correlated with only T_r as a single dependent variable. The MLSS concentration is required as a second dependent variable in a 3-D model to reduce the data scatter and to obtain a best-fit correlation for the experimental and calculated data.

6.3.4.3 SVI link to MLSS concentration and T_r

The recorded data points and fitted correlation for the on-line MLSS concentration, the T_r, and the calculated SVI are shown in Figure 6-8. The x_1-, x_2- and y-axis represent MLSS concentration, T_r, and SVI respectively. The best-fit curve for SVI related to MLSS concentration and T_r for full-scale plant data is represented on Figure 6-8 by a polynomial with a R^2 of 0.84.

Figure 6-8 SVI related to MLSS concentration and T_r

The temperature impact on settling is demonstrated by the improved curve fitting when T_r data is included in the full-scale plant SVI evaluation. Figure 6-8 illustrates the relationship between SVI as the response variable, with MLSS concentration and T_r as the dependent variables. The SVI response, after a variation in either or both the MLSS concentration and T_r, can be predicted from Figure 6-8.

SVI increases from 97 towards 203 mℓ/g as the MLSS concentration increases from 4489 to 4923 mg/ℓ and the T_r decreases from 19.0 to 17.2°C. The ideal settling condition of the lowest SVI of 97 mℓ/g is obtained at the lowest MLSS concentration and the highest T_r. The inclusion of T_r in SVI correlations improves the curve fitting by a R^2 value of 0.15, from 0.69 to 0.84.

6.3.5 Model fitting: u_max dependence on MLSS concentration and T_r

The u_max dependence on MLSS concentration and T_r is statistically evaluated with individual and combined correlations in 2- and 3-D models.

6.3.5.1 u_max link to MLSS concentration

The recorded data points and a fitted trend for the full-scale on-line MLSS concentration and calculated u_max are shown in Figure 6-9. The x_1-axis indicates MLSS concentration and the y-axis indicates u_max. The best-fit curve for u_max related to MLSS concentration from full-scale data is represented by a polynomial with a R^2 of 0.58, as shown in Figure 6-9.
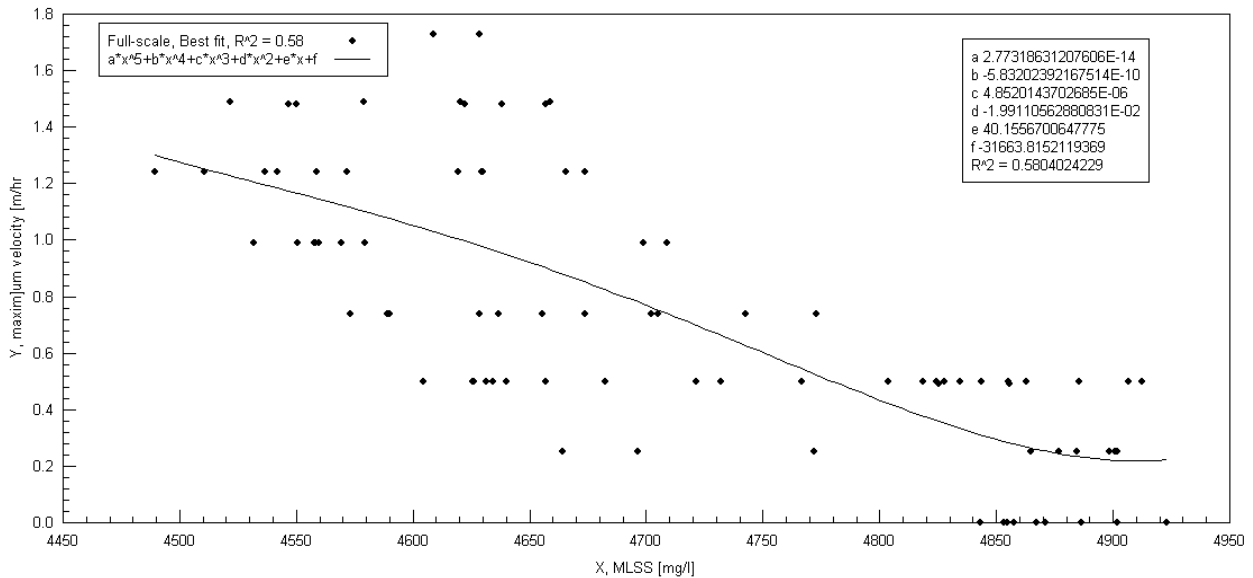
Figure 6-9 u_max related to MLSS concentration

The inverse relationship between u_max as the response variable and MLSS concentration as the dependent variable is confirmed, since u_max decreases according to the best-fit curve as MLSS concentration increases. The experimental u_max data scatter is visible from 0 to 1.73 m/hr throughout the MLSS range of 4489 to 4923 mg/ℓ.

6.3.5.2 u_max link to T_r

The recorded data points and a fitted trend for the on-line T_r and calculated u_max are shown in Figure 6-10. The x_1-axis indicates the T_r and the y-axis indicates the u_max. The best-fit curve for u_max related to T_r from the full-scale plant data is represented by a polynomial with a very low R^2 of only 0.26.
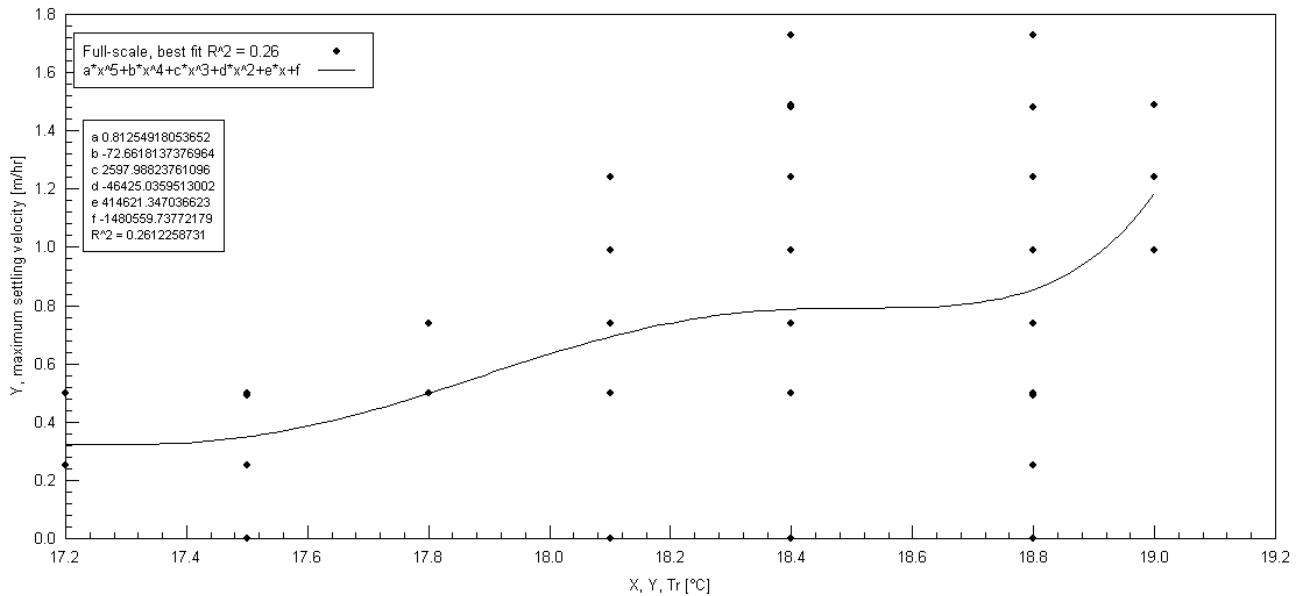
Figure 6-10 u_max data scatter according to T_r variation

A basic correlation between u_max as the response variable and T_r as the dependent variable is visible, as u_max increases according to the best-fit curve as T_r increases. The large field of experimental u_max data scatter is visible throughout the T_r range increments, since the T_r data logger only recorded in 0.3°C increments.

The large data scatter indicates that the u_max data cannot be correlated with only T_r as a single dependent variable. The MLSS concentration is required as a second dependent variable in a 3-D model to reduce the data scatter and to obtain a best-fit correlation for the experimental and calculated data.

6.3.5.3 u_max link to MLSS concentration and T_r

The recorded data points and fitted correlation for the on-line MLSS concentration, T_r, and calculated u_max are shown in Figure 6-11. The x_1-, x_2- and y-axis represent MLSS concentration, T_r, and u_max respectively. The best-fit curve for u_max related to MLSS concentration and T_r for full-scale plant data was represented on Figure 6-11 by a polynomial with a R^2 of 0.70.
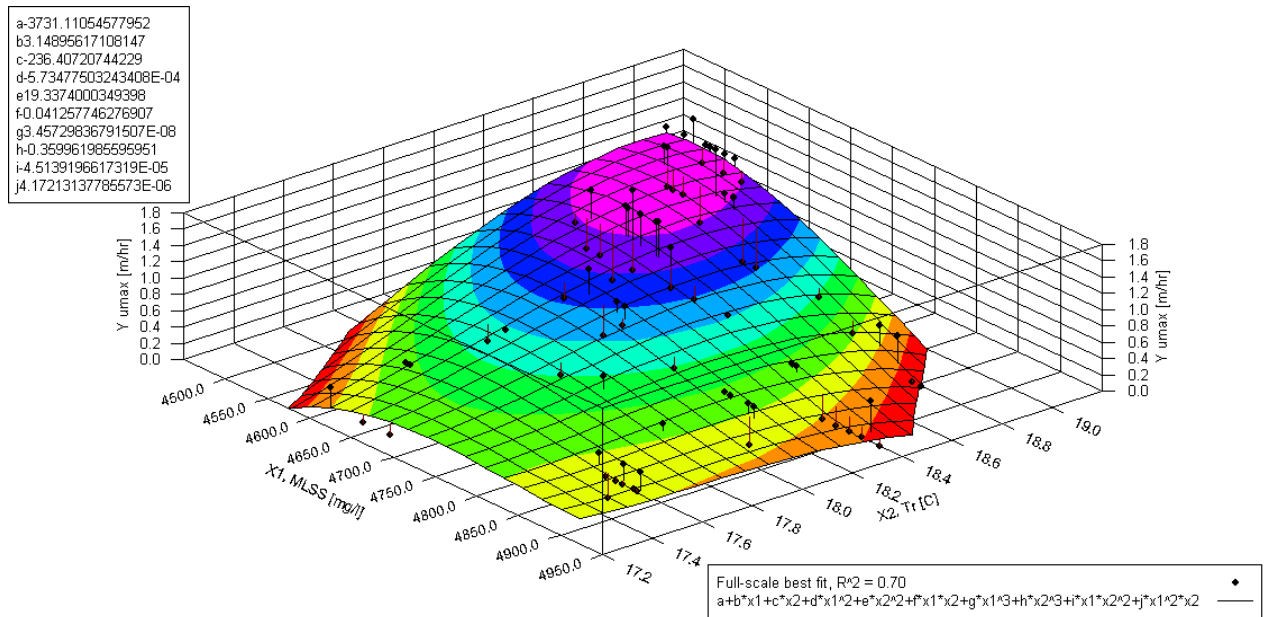
Figure 6-11 u_max related to MLSS concentration and T_r

The temperature impact on MLSS settling is demonstrated by the improved curve fitting when T_r data is included in the full-scale plant u_max evaluation. Figure 6-11 illustrates the relationship between u_max as the response variable, and MLSS concentration and T_r as the dependent variables. The u_max response, after a variation in either or both the MLSS concentration and T_r, can be predicted from Figure 6-11.

The u_max increases from 0 towards 1.7 m/hr, as the MLSS concentration decreases from 4923 to 4489 mg/ℓ, and the T_r increases from 17.2 to 19.0°C. The ideal settling condition of the highest u_max of 1.7 m/hr is obtained at the lowest MLSS concentration and the highest T_r. The inclusion of T_r in u_max correlations improved the curve fitting by a R^2 value of 0.12, from 0.58 to 0.70.

6.3.6 Model fitting: t_umax dependence on MLSS concentration and T_r

The t_umax dependence on MLSS concentration and T_r is statistically evaluated with individual and combined correlations in 2- and 3-D models.

6.3.6.1 t_umax link to MLSS concentration

The recorded data points and a fitted trend for the full-scale on-line MLSS concentration and calculated t_umax are shown in Figure 6-12. The x_1-axis indicates MLSS concentration and the y-axis indicates t_umax. The best-fit curve for t_umax related to MLSS concentration from full-scale data is represented by a polynomial with a R^2 of 0.70, as shown in Figure 6-12.
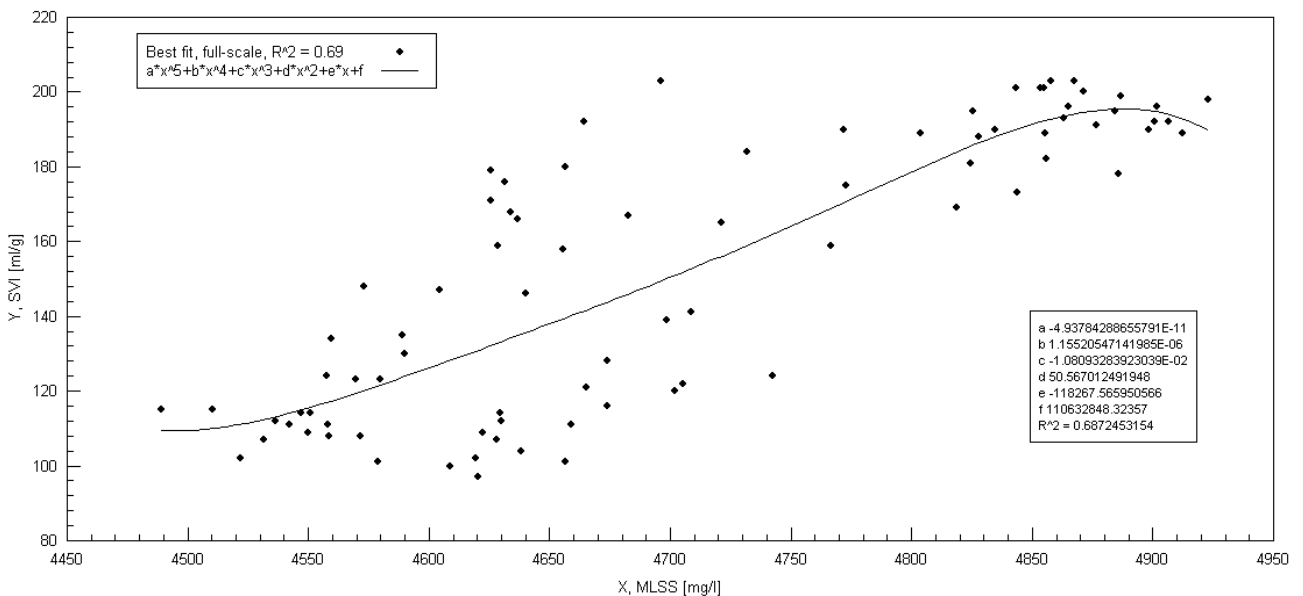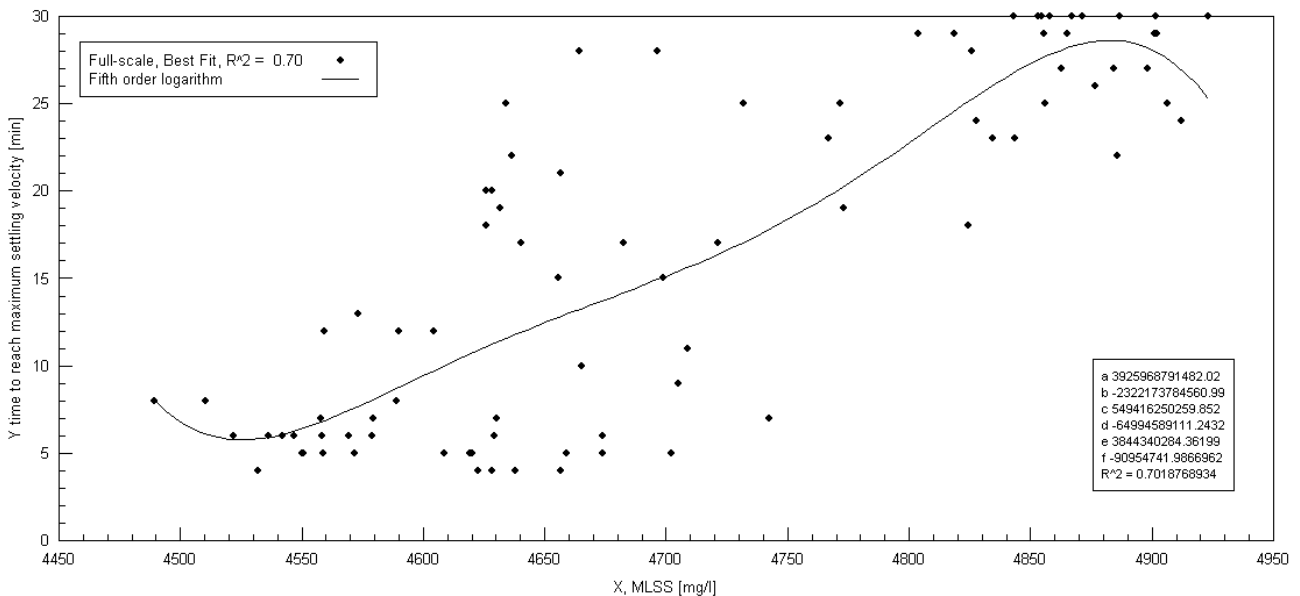

Figure 6-12 t_umax related to MLSS concentration

The direct relationship between t_umax as the response variable and MLSS concentration as the dependent variable is confirmed, since t_umax increases according to the best-fit curve as MLSS concentration increases. The experimental t_umax data scatter is visible from 4 to 30 minutes throughout the MLSS range of 4489 to 4923 mg/ℓ.

6.3.6.2 t_umax link to T_r

The recorded data points and a fitted trend for the on-line T_r and calculated t_umax are shown in Figure 6-13. The x_1-axis indicates T_r and the y-axis indicates t_umax. The best-fit curve for t_umax related to T_r from the full-scale plant data is represented by a polynomial with a very low R^2 of only 0.32.
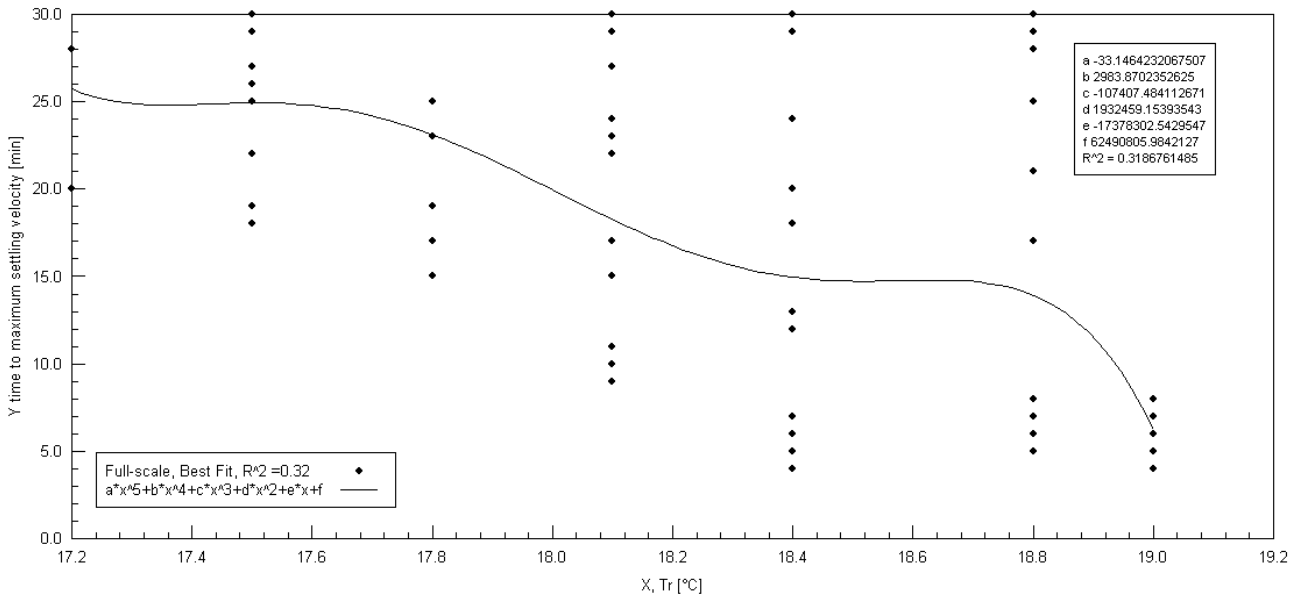
Figure 6-13 t_umax data scatter according to T_r variation

There is a poor correlation visible between t_umax as the response variable and T_r as the dependent variable, as t_umax decreases according to the best-fit curve as T_r increases. The large field of experimental t_umax data scatter was visible throughout the T_r range increments, since the T_r data logger only recorded in 0.3°C increments.

The large data scatter indicates that t_umax data cannot be correlated with only T_r as a single dependent variable. The MLSS concentration is required as a second dependent variable in a 3-D model to reduce the data scatter and to obtain a best-fit correlation for the experimental and calculated data.

6.3.6.3   t_umax link to MLSS concentration and T_r

The recorded data points and fitted correlation for the on-line MLSS concentration, T_r, and calculated t_umax are shown in Figure 6-14. The x_1-, x_2- and y-axis represent MLSS concentration, T_r, and t_umax respectively. The best-fit curve for t_umax related to MLSS concentration and T_r for full-scale plant data was represented on Figure 6-14 by a polynomial with a R^2 of 0.83.
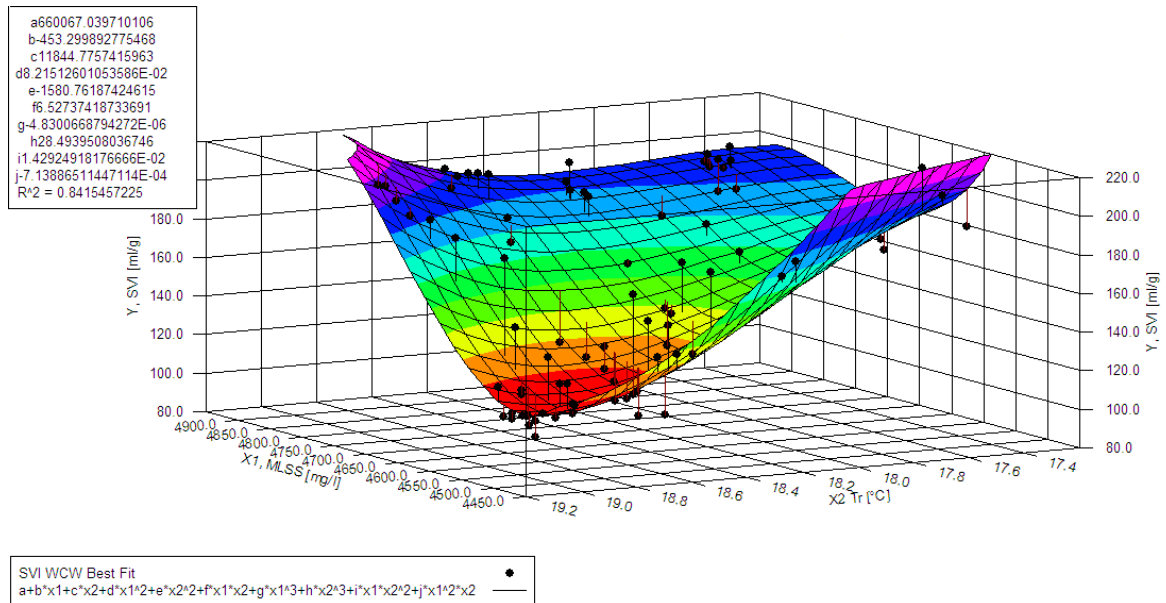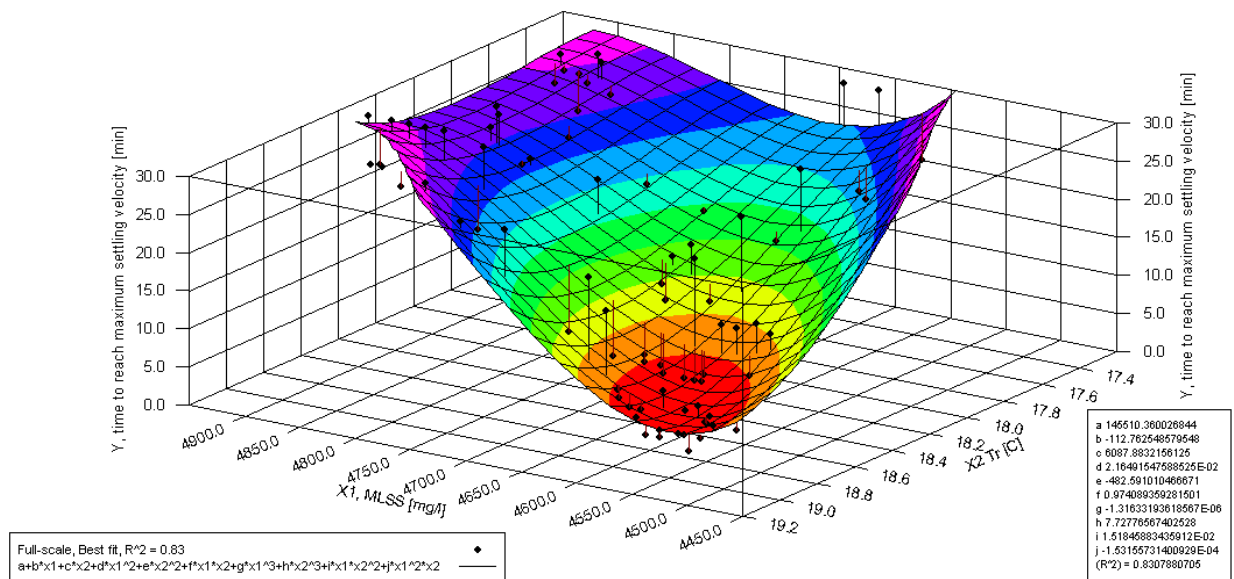

Figure 6-14 t_umax related to MLSS concentration and T_r

The temperature impact on MLSS settling is demonstrated by the improved curve fitting when T_r data is included in the full-scale plant t_umax evaluation. Figure 6-14 illustrates the relationship between t_umax as the response variable, and MLSS concentration and T_r as the dependent variables. The t_umax response, after a variation in either or both the MLSS concentration and T_r, can be predicted from Figure 6-14.

The t_umax increases from 4 towards 30 minutes, as the MLSS concentration increases from 4489 to 4923 mg/ℓ, and the T_r decreases from 19.0 to 17.2°C. The ideal settling condition of the lowest t_umax is obtained at the lowest MLSS concentration and the highest T_r. The inclusion of T_r in t_umax correlations improved the curve fitting by a R^2-value of 0.13, from 0.70 to 0.83.

6.3.7 Model fitting: Summary of curve-fitting correlations

The inclusion of T_r improves the MLSS settling correlations, which is measured according to R^2 increases, as listed in Table 6-2. The average R^2-value for the three MLSS settling parameters (SVI, u_max, t_umax) correlations with MLSS concentration was 0.66 without considering T_r. The inclusion of T_r in the MLSS concentration-based settling correlations improved the average R^2 value by 0.13 to a more acceptable 0.79.

Table 6-2 Best-fit MLSS settling correlations R^2 containing MLSS concentration and T_r

Settling parameter	MLSS concentration R^2	T_r R^2	MLSS concentration and T_r R^2
SVI [mℓ/g]	0.69	0.38	0.84
u_max [m/hr]	0.58	0.26	0.70
t_umax [min]	0.70	0.32	0.83
Average	**0.66**	**0.32**	**0.79**

6.3.8 SVI and settling parameter correlation procedure

SVI-based settling parameter correlations are developed experimentally with the on-line settling meter. These temperature dependent SVI correlations can then be used to predict u_max and t_umax responses over the operational SVI range, as required for plant design or process control purposes.

6.3.8.1 SVI and u_max correlation

The recorded data points and a fitted trend for the full-scale plant calculated SVI and calculated u_max are shown in Figure 6-15. The x_1-axis indicates SVI and the y-axis indicates u_max. The best-fit curve for u_max related to SVI is represented by a polynomial with a R^2 of 0.90.
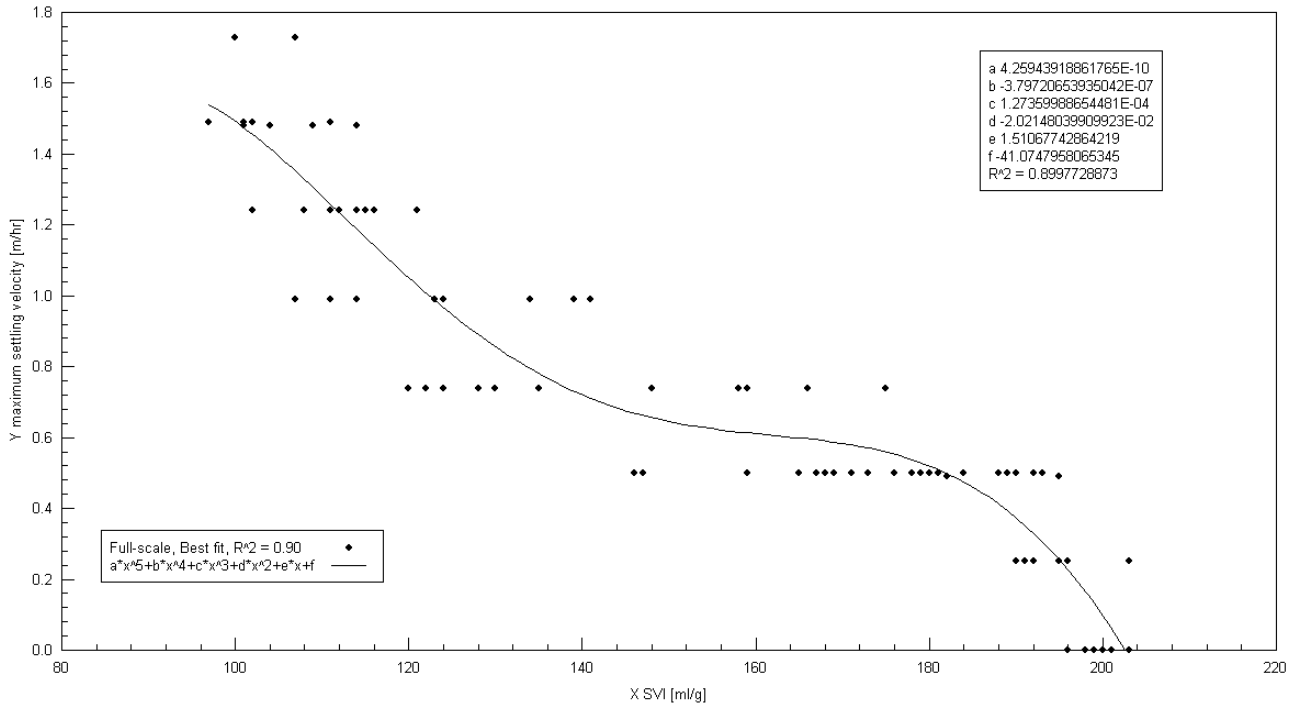
Figure 6-15 u_max related to SVI

The inclusion of T_r in the batch settling tests results in a calculated SVI range from 97 to 203 mℓ/g that correlates in an inverse relationship with u_max from 1.73 to 0 m/hr. The u_max response can now be predicted for a SVI variation, as shown in Figure 6-15. The good correlation between SVI and u_max confirms the results obtained by Sezgin (1982).

6.3.8.2 SVI and t_umax correlation

The recorded data points and a fitted trend for the full-scale plant calculated SVI and calculated t_umax are shown in Figure 6-16. The x_1-axis indicates SVI and the y-axis indicates t_umax. The best-fit curve for t_umax related to SVI is represented by a polynomial with a R^2 of 0.95.
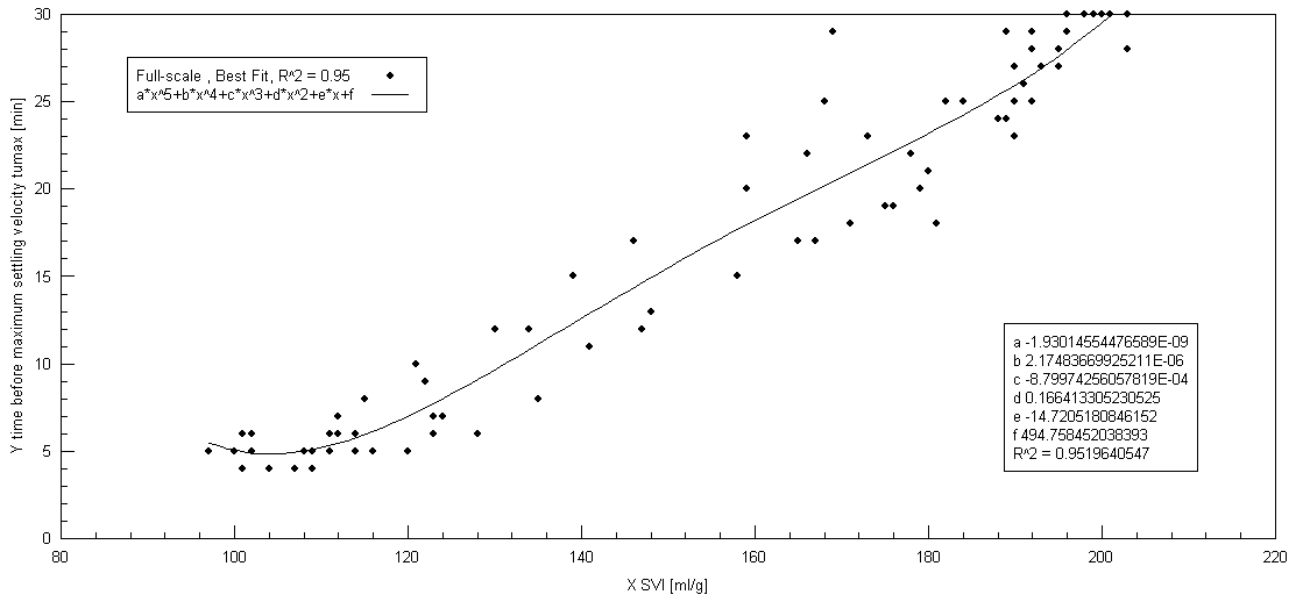
Figure 6-16 t_umax related to SVI

The inclusion of T_r in the batch settling tests results in a calculated SVI range from 97 to 203 mℓ/g that correlates in a direct relationship with t_umax from 4 to 30 minutes. The t_umax response can now be predicted for a SVI variation, as shown in Figure 6-16. Temperature-based settling correlations containing t_umax have not been reported in the available literature.

6.3.9 SVI correlations with u_max and t_umax: Summary of curve-fitting results

SVI data is obtained from on-line automated settling tests that include T_r variation recordings. The calculated SVI correlation with u_max and t_umax is summarised in Table 6-3.

Table 6-3 Summary of SVI correlations with u_max and t_umax

parameter	R^2
u_max	0.90
t_umax	0.95
average	0.93

The high R^2 of 0.90 and 0.95 illustrate the effect of T_r during MLSS settling. The temperature-based u_max and t_umax correlations with SVI, together with the coefficients, are summarised in Table 6-4.

Table 6-4 Coefficients for polynomial: u_max and t_umax correlations with SVI

coefficient	$y = a * x^5 + b * x^4 + c * x^3 + d * x^2 + e * x + f,$ $x = SVI [m\ell/g]$	
	$y = u\_max[m/hr]$	$y = t\_umax[minute]$
a	4.259E-10	-1.930E-9
b	-3.797E-7	2.175E-6
c	1.274E-4	-8.800E-4
d	-2.021E-2	0.1664
e	1.511	-14.7205
f	-41.075	494.758
R^2	0.90	0.95

These on-line-based settling parameter correlations with SVI illustrate the benefits of using automatic on-line settling meters. A settling meter detects the MLSS settling profile at T_r. MLSS settling characteristics are plant specific (Wilén, 2006), and on-line-based correlations will therefore reflect the responses of individual plant settling parameters over operational MLSS concentration and T_r ranges.

An on-line MLSS settling meter can be used to predict the settling characteristics of a BNR plant for design and operational purposes:

- a SVI correlation is developed with on-line reactor MLSS concentration and T_r (Figure 6-8),
- the complete SVI range can now be predicted from the known or assumed operational MLSS concentration and T_r ranges (Figure 6-8),
- u_max and t_umax correlations are developed with predicted SVI range (Figure 6-15 and Figure 6-16), and
- the u_max and t_umax range could now be predicted from the calculated SVI range (Figure 6-15 and Figure 6-16).

6.3.10 Simplified settling models: MLSS concentration and T_r

The statistical significance of a model, to account for the fraction of the variation among the data points represented by the model, is illustrated by R^2. Researchers have used R^2 as a general indicator of the statistical significance of settleability models (Daigger, 1995; Ekama *et al*., 1997), based on batch MLSS settling tests. The following 3-parameter 1st order polynomial function is chosen as the fitted regression model for the 11 settling parameters, based on R^2 and formula simplicity:

$$y = a + \frac{b}{x_1} + \frac{c}{x_2} + \varepsilon, \left(\varepsilon \approx \left(0, \sigma^2 \right) \right)$$

where y is the settling parameter, x_1 is the MLSS concentration [mg/ℓ], x_2 is the T_r [°C], a, b, c are regression constants, ε is the random error and σ^2 is the error variance.

This basic model format is easy to use, as summarised in Table 6-5. The 11 equations are a general representation of the experimental data. The data and models are only valid within the experimental MLSS concentration and T_r boundary conditions provided in Table 6-5. Refer also to Table 11-13 in Appendix H for a summary of additional regression variable results. The large t-ratios confirm that all parameters are significant. The low p values indicate that none of the parameters can be removed from the model.

Table 6-5 Summary of regression model constants for settling parameters

Parameter	4489 mg/ℓ < MLSS concentration < 4923 mg/ℓ, n = 85, ave. = 4705, st. dev. 127 17.2°C < T_r < 19.0°C, n = 85, ave. = 18.3, st. dev. = 0.5				
	a	b	c	R^2 Simplified	R^2 Best-fit
SVI	872.4200	-4624176.0614	4823.4021	0.71	0.84
t_umax	239.5623	-1290679.9382	939.9347	0.70	0.83
u_max	-9.2997	57454.2585	-39.8603	0.59	0.70
u_ave	-2.8943	18433.8191	-15.1792	0.76	0.87
h	1793.9619	-9200670.3014	7744.0213	0.76	0.87
u1	-1.1851	14418.7348	-31.9946	0.32	0.45
u2	-2.6708	33145.3653	-74.7660	0.59	0.71
u3	-3.6732	25152.0675	-26.7192	0.62	0.79
u4	-4.1828	19564.9547	3.4218	0.60	0.79
u5	-3.3897	11822.7573	18.7500	0.34	0.56
u6	-2.6835	8411.5793	18.8984	0.30	0.50

6.3.10.1 SVI correlation with MLSS concentration and T_r

The response relationship of SVI to MLSS concentration and T_r variations, obtained from the full-scale plant data, is presented by the following regression model, with $R^2 = 0.71$:

$$\text{SVI} = 872.4 - \frac{4624176.1}{\text{MLSS}} + \frac{4823.4}{T_r} \quad [\text{m}\ell/\text{g}] \qquad\qquad \text{Equation 6-1}$$

The plot of this model is shown in Figure 6-17. The x_1-axis represents the MLSS concentration range of 4489 to 4923 mg/ℓ, the x_2-axis represents the T_r range from 17.2 to 19.0°C, and the y_1-axis represents the SVI from 96 mℓ/g to 214 mℓ/g. The model is represented by a best-fit polynomial with a $R^2 = 0.84$.

Figure 6-17 SVI dependency on MLSS concentration and T_r

The SVI dependence on the full-scale T_r can be illustrated with a simulation. At an average constant MLSS concentration of 4500 mg/ℓ, the SVI change due to a T_r reduction from 19.0 to 17.2°C can be determined according to the SVI-model (Equation 6.1). The SVI increases by 26.5 mℓ/g, from 98.7 to 125.2 mℓ/g, with a corresponding relative SVI increase of 14.8 mℓ/g SVI per 1°C T_r reduction, or -14.8 mℓ/g SVI/1°C T_r.

This SVI correlation illustrates the extent of batch MLSS settling test result variations. The relatively small temperature reduction of 1.8°C contributes to a SVI increase of 26.5 mℓ/g. MLSS samples are taken from a reactor at T_r, and they are usually transported, stored, and tested at a different T_s, which could change by much more than 1.8°C.

6.3.10.2 u_max correlation with MLSS concentration and T_r

The response relationship of u_max to MLSS concentration and T_r variations is presented by the following regression model, with $R^2 = 0.59$:

$$u\_max = -2.2 + \frac{14785.4}{MLSS} - \frac{8.3}{T_r} \ [m/hr]$$
Equation 6-2

The plot of this model is shown in Figure 6-18. The x_1-axis represents the MLSS concentration range of 4489 to 4923 mg/ℓ, the x_2-axis represents the T_r range from 17.2 to 19.0°C, and the y-axis represents the u_max from 0.1 to 1.4 m/hr. The model is represented by a best-fit polynomial with $R^2 = 0.70$.
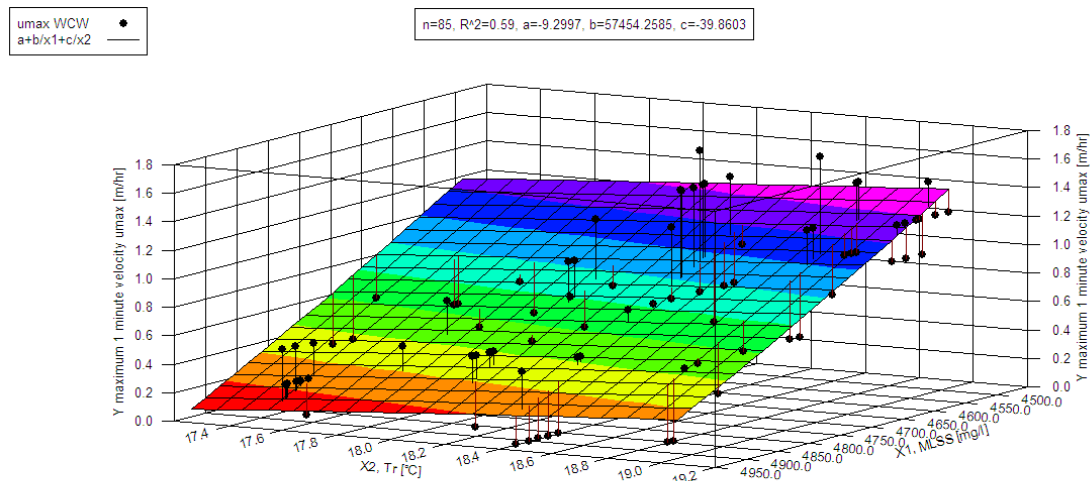
Figure 6-18 u_max dependency on MLSS concentration and T_r

A simulation can illustrate the dependence of u_max on the operational T_r. At an average constant MLSS concentration of 4500 mg/ℓ, the u_max change due to a T_r reduction from 19.0 to 17.2°C can be determined according to the u_max-model (Equation 6.2). The u_max decreases by 0.2 m/hr, from 1.4 to 1.2 m/hr, with a corresponding relative u_max decrease of 0.1 m/hr per 1°C T_r reduction, or 0.1m/hr u_max/1°C T_r.

These correlations have implications for full-scale MLSS settling control. The typical diurnal T_r variation of 1.8°C at a constant MLSS concentration, contributes to an u_max change of more than 0.1 m/hr. From the relatively low T_r dependence of u_max, it might

be argued that the 1-minute interval in the MLSS settling meter is not sensitive enough to reflect the true zone settling velocity. An improved u_max recording process is required for the on-line settling meter. It is recommended that the MLSS settling meter recording time interval be changed in future applications from 1 to at least 0.5 minutes.

These u_max settling velocity correlations have implications for clarifier design. Secondary tank clarifier design is usually conservative and based on bad MLSS settling characteristics (Van Haandel, 1992). The lower u_max will require a larger secondary settling tank capacity to ensure the solids load can be accommodated at the higher MLSS concentration and the lower T_r.

6.3.10.3 t_umax correlation with MLSS concentration and T_r

The response relationship of t_umax to MLSS concentration and T_r variations is presented by the following regression model, with $R^2 = 0.70$:

$$t\_u\max = 239.6 - \frac{1290679.9}{MLSS} + \frac{939.9}{T_r} \quad [minute]$$

Equation 6-3

The plot of this model is shown in Figure 6-19. The x_1-axis represents the MLSS concentration range of 4489 to 4923 mg/ℓ, the x_2-axis represents the T_r range from 17.2 to 19.0°C, and the y-axis represents the t_umax from 2 to 30 minutes. This model is represented by a best-fit polynomial with a $R^2 = 0.83$.
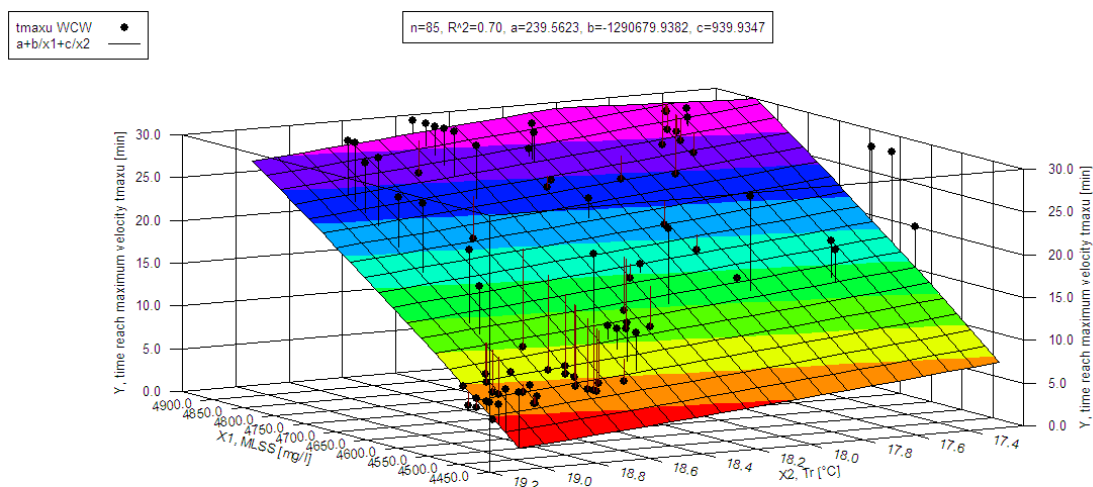
Figure 6-19 t_umax dependency on MLSS concentration and T_r

A simulation can illustrate the dependence of t_umax on T_r. At an average constant MLSS concentration of 4500 mg/ℓ, the t_umax change due to a T_r reduction from 19.0 to 17.2°C can be determined according to the t_umax-model (Equation 6.3). The t_umax increases by 4.2 minutes, from 2.2 to 6.5 minutes, with a corresponding relative t_umax increase of 2.4 minutes per 1°C T_r reduction, or 2.4 minute t_umax/1°C T_r.

These correlations have implications for MLSS settling control and design. The typical diurnal reactor temperature variation of 1.8°C, at a constant MLSS concentration, contributes to a reflocculation time increasing from 2.2 to 6.5 minutes (when u_max commences). The reflocculation lag time delay will require a larger stilling chamber to ensure reflocculation will take place at higher MLSS concentrations and T_r.

The correlations also have implications for MLSS sample handling. The dilution of the MLSS concentration of a sample for a DSVI calculation reduces the t_umax, as the bioflocs can start settling immediately as discrete particles. Sample handling, transport, storage, and tests at different room temperatures can lead to large temperature variations, as well as a corresponding change in reflocculation time.

6.3.10.4 u_ave correlation with MLSS concentration and T_r variation

The response relationship of u_ave to MLSS concentration and T_r variations is presented by the following regression model, with $R^2 = 0.76$:

$$u\_ave = -2.9 + \frac{18433.8}{MLSS} - \frac{15.2}{T_r} \ [m/hr] \hspace{3cm} \text{Equation 6-4}$$

The plot of this model is presented in Figure 6-20. The x_1-axis represents the MLSS concentration range of 4489 to 4923 mg/ℓ, the x_2-axis represents the T_r range from 17.2 to 19.0°C, and the y-axis represents u_ave from 0 to 0.4 m/hr. This model is represented by a best-fit polynomial with a $R^2 = 0.87$.
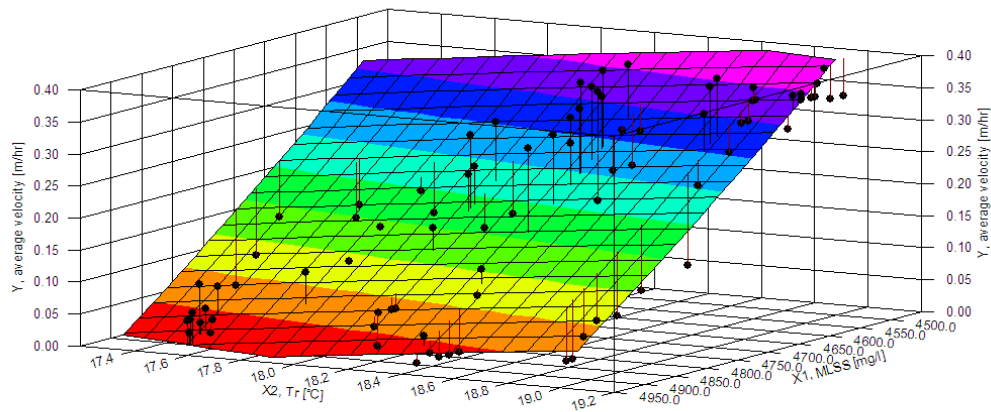
Figure 6-20 u_ave dependency on MLSS concentration and T_r

A simulation can illustrate the dependence of u_ave on the T_r. At an average constant MLSS concentration of 4500 mg/ℓ, the u_ave change due to a T_r reduction from 19.0 to 17.2°C can be determined according to the u_ave-model (Equation 6.4). The u_ave decreases by 0.1 m/hr, from 0.4 to 0.3 m/hr, with a corresponding relative u_ave decrease of 0.04 m/hr per 1°C T_r reduction, or 0.04 m/hr u_ave/ 1°C T_r.

The u_ave over 30 minutes is a rapid indicator of MLSS settling velocity, with the advantage that it can be directly calculated from the SV_{30} (according to MLSS height h settled over 30 minutes). The u_ave, as a general settling index, has similar shortcomings to the SVI, specifically regarding the height of the test cylinder or column used. It does not give any indications of MLSS settling changes occurring during the settling period. The parameter u_ave should be used with caution as a general settling indicator. For this study, the principle aim was to demonstrate the T_r dependence of u_ave, as shown in Figure 6-20.

6.3.10.5 h correlation with MLSS concentration and T_r variation

The response relationship of h to MLSS concentration and T_r variations obtained from the full-scale plant data is presented by the following regression model, with $R^2 = 0.76$:

$$h = 1794.0 - \frac{9200670.3}{\text{MLSS}} - \frac{7744.0}{T_r} \text{ [mm]}$$

Equation 6-5

The plot of this model is presented in Figure 6-21. The x_1-axis represents the MLSS concentration range of 4489 to 4923 mg/ℓ, the x_2-axis represents the T_r range from 17.2 to 19.0°C, and the y-axis represents h from 152 to 355.9 mm. This model is represented by a best-fit polynomial with a $R^2 = 0.87$.
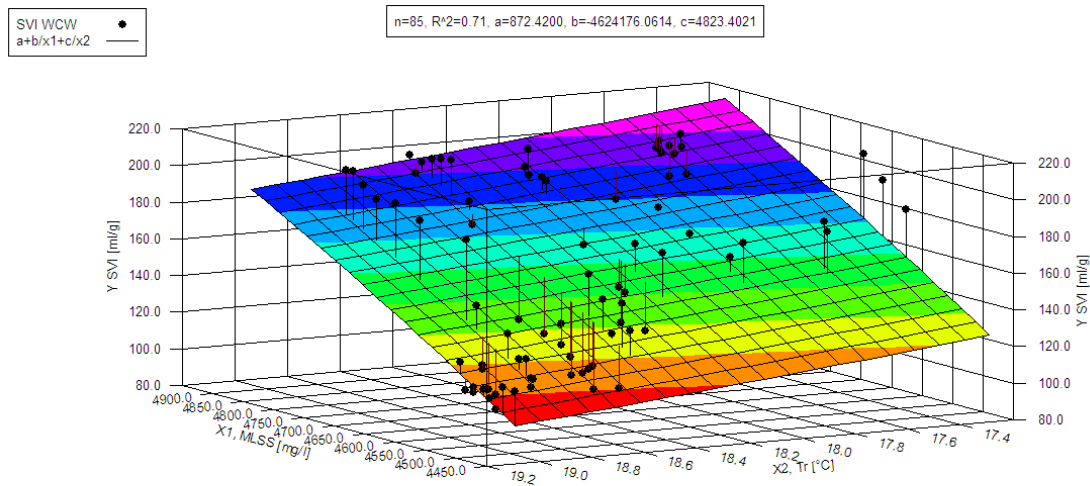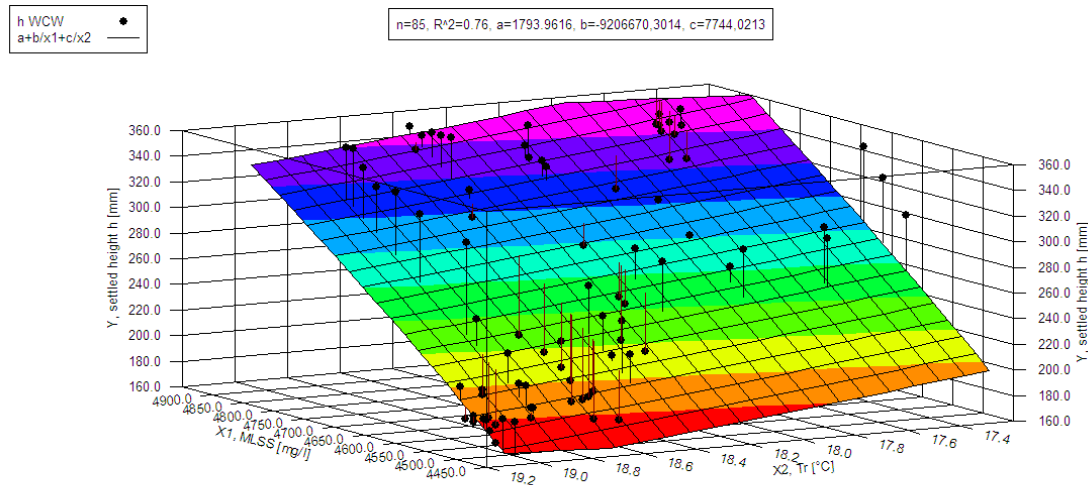

Figure 6-21 h dependency on MLSS concentration and T_r

A simulation can illustrate the dependence of h on T_r. At an average constant MLSS concentration of 4500 mg/ℓ, the h change due to a T_r reduction from 19.0 to 17.2°C can be determined according to the h-model (Equation 6.5). The h increases by 35 mm, from 157 to 192 mm, with a corresponding relative h increase of 19 mm per 1°C T_r reduction, or -19 mm h /1°C T_r.

6.3.10.6 Incremental velocity u1 to u6 simulation over 30 minutes

The 30-minute settling period is divided in 6 settling periods of 5 minutes each. The average settling velocity over these 5-minute periods is calculated as u1, u2, u3, u4, u5, u6. It was previously demonstrated that MLSS samples will settle faster and sooner (u_max higher and t_umax lower) at lower MLSS concentrations and at higher T_r.

For MLSS samples at a low MLSS concentration and a high T_r, the t_umax will be low and u1, u2, and u3 will therefore be higher. For MLSS samples at a high MLSS concentration and a low T_r, the t_umax will be higher. These MLSS samples will only

settle later in the 30-minute cycle, and u4, u5, and u6 will be subsequently higher for these unfavourable MLSS settling conditions (high MLSS concentration and low T_r).

To illustrate the incremental settling velocity changes according to MLSS concentration and T_r, the following 6 sections provide simplified models and regression graphs for u1 to u6.

6.3.10.7 u1 correlation with MLSS concentration and T_r variation

The response relationship of u1 (0 to 5 minutes) to MLSS concentration and T_r variations is presented by the following equation:

$$u1 = -1.2 + \frac{14418.7}{MLSS} - \frac{32.0}{T_r} \ [m/hr] \hspace{3cm} \text{Equation 6-6}$$

The model plot is shown in Figure 6-22, and u1 varies on the y-axis from 0 to 0.34 m/hr.

Figure 6-22 u1 dependency on MLSS concentration and T_r

A simulation can illustrate the dependence of the u1 on T_r. At an average constant MLSS concentration of 4500 mg/ℓ, the u1 change due to a T_r reduction from 19.0 to 17.2°C can be determined according to the u1-model (Equation 6.6). The u1 reduces from 0.34 to 0.19 m/hr, with a corresponding relative u1 decrease of 0.08 m/hr per 1°C T_r reduction, or 0.08 m/hr u1/1°C T_r.

The correlation between u1 and MLSS concentration is not represented in traditional models. The direct correlation between u1 and T_r is now illustrated with on-line evaluations, at an average of 0.08 m/hr per 1°C change. The correlations can be used as an indication of the reflocculation time. An u1 settling velocity of 0 m/hr indicates that the MLSS is still in suspension after 5 minutes and stage 2 zone settling has not started. The inverse correlation between t_umax and T_r is now illustrated for on-line evaluations according to the MLSS settling velocity.

These correlations can be used together with the reflocculation time to aid in the design of stilling chamber capacity, to ensure bioflocculation will take place at higher MLSS concentrations and lower T_r. The ISV will determine the loading capacity of the secondary settling tank (Wilén *et al.*, 2006).

6.3.10.8 u2 correlation with MLSS concentration and T_r variation

The response relationship of u2 (5 to 10 minutes) to MLSS concentration and T_r variations is presented by the following equation:

$$u2 = -2.7 + \frac{33145}{MLSS} - \frac{74.8}{T_r} \quad [m/hr]$$ Equation 6-7

The model plot is shown in Figure 6-23 , and u2 varies on the y-axis from 0 to 0.78 m/hr.
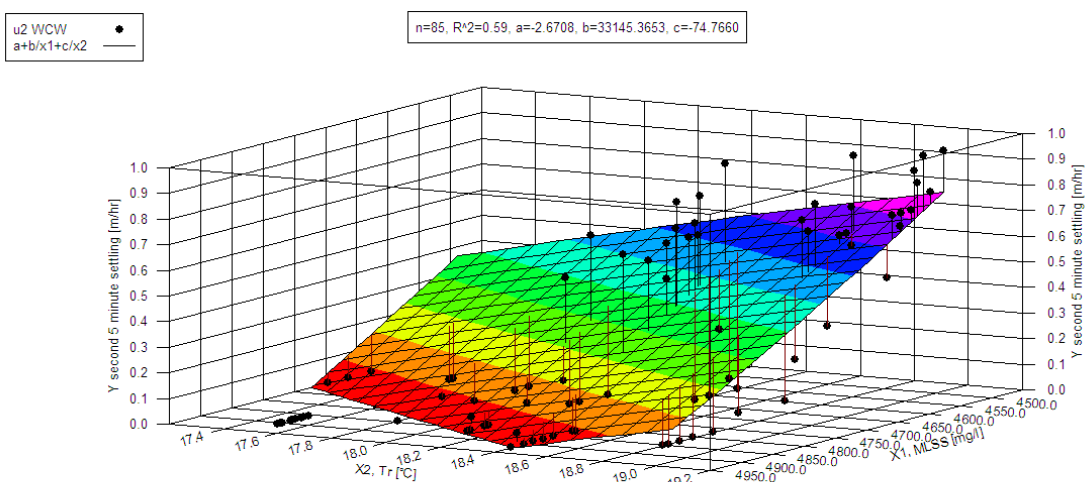
Figure 6-23 u2 dependency on MLSS concentration and T_r

A simulation can illustrate the dependence of the u2 on T_r. At an average constant MLSS concentration of 4500 mg/ℓ, the u2 change due to a T_r reduction from 19.0 to 17.2°C can be determined according to the u2-model (Equation 6.7). The u2 reduces from 0.76 to 0.42 m/hr, with a corresponding relative u2 decrease of 0.19 m/hr per 1°C T_r reduction, or 0.19 m/hr u1/1°C T_r.

The correlation between u2 and MLSS concentration is not represented in traditional models. The direct correlation between u2 and T_r is illustrated with on-line evaluations, at an average of 0.19 m/hr per 1°C change. The correlation can be used, together with u1, as an indication of the reflocculation time. An u2 settling velocity of 0 m/hr indicates that the MLSS is in suspension after 10 minutes and zone settling has not started. The inverse correlation between time to reach maximum settling velocity and T_r is now illustrated with on-line evaluations. These correlations can be used together with the reflocculation time to aid with design of stilling chamber capacity, to ensure bio-flocculation will take place in stilling chambers at higher MLSS concentrations and lower T_r.

6.3.10.9 u3 correlation with MLSS concentration and T_r variation

The response relationship of u3 (10 to 15 minutes) to MLSS concentration and T_r variations is presented by the following equation:

$$u3 = -3.7 + \frac{25152.1}{MLSS} - \frac{26.7}{T_r} \ [m/hr] \qquad\qquad \text{Equation 6-8}$$
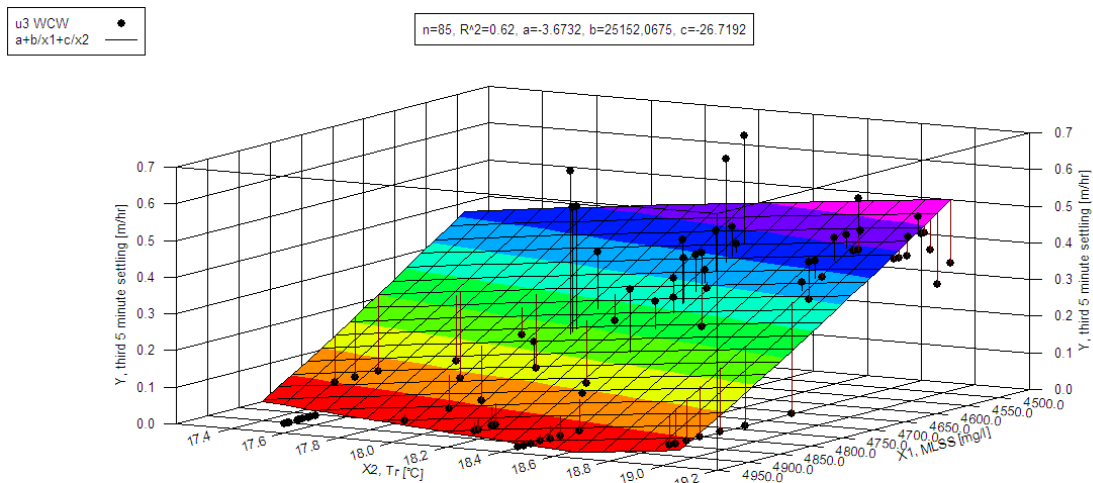
Figure 6-24 u3 dependency on MLSS concentration and T_r

The model plot is shown in Figure 6-24, and u3 varies on the y-axis from 0 to 0.52 m/hr.

A simulation can illustrate the dependence of the u3 on T_r. At an average constant MLSS concentration of 4500 mg/ℓ, the u3 change due to a T_r reduction from 19.0 to 17.2°C can be determined according to the u3-model (Equation 6.8). The u3 reduces from 0.51 to 0.39 m/hr, with a corresponding relative u3 decrease of 0.07 m/hr per 1°C T_r reduction, or 0.07 m/hr u3/1°C T_r.

The correlation between u3 and MLSS concentration is not represented in traditional models. The direct correlation between u3 and T_r is now illustrated for on-line evaluations, at an average of 0.07 m/hr per 1°C change. The colder MLSS samples at higher MLSS concentrations only start to settle after 10 minutes, and the u3 incremental settling velocity is therefore higher at the high MLSS concentration and the low T_r range.

6.3.10.10 u4 correlation with MLSS concentration and T_r variation

The response relationship of u4 (15 to 20 minutes) to MLSS concentration and T_r variations is presented by the following equation:

$$u4 = -4.2 + \frac{19565.0}{\text{MLSS}} + \frac{3.4}{T_r} \quad [\text{m/hr}]$$

Equation 6-9
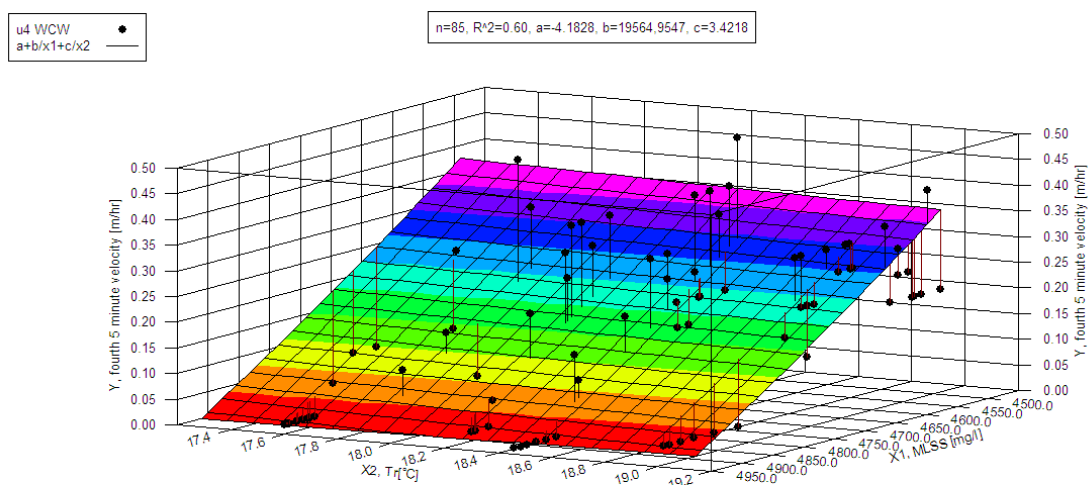
Figure 6-25 u4 dependency on MLSS concentration and T_r

The model plot is shown in Figure 6-25, and u4 varies on the y-axis from 0 to 0.37 m/hr.

A simulation can illustrate the dependence of the u4 on T_r. At an average constant MLSS concentration of 4500 mg/ℓ, the u4 change due to a T_r reduction from 19.0 to 17.2°C can be determined according to the u4-model (Equation 6.9). The u4 increases from 0.35 to 0.36 m/hr, with a corresponding relative u4 increase of 0.01 m/hr per 1°C T_r reduction, or - 0.01 m/hr u4/1°C T_r.

The correlation between u4 and MLSS concentration is not represented in traditional models. The u4 (settling velocity over the fourth 5-minute settling period) follows now a different pattern from previous incremental velocities up to 15 minutes. All the easily flocculating MLSS at the high temperature has flocculated and settled over these first 15 minutes. The MLSS at the colder temperature only starts to settle after 15 minutes, and u4 is therefore higher in the low temperature range. The inverse correlation between u4 and T_r is illustrated from the on-line evaluations at an average of -0.01 m/hr per 1°C change.

6.3.10.11 u5 correlation with MLSS concentration and T_r variation
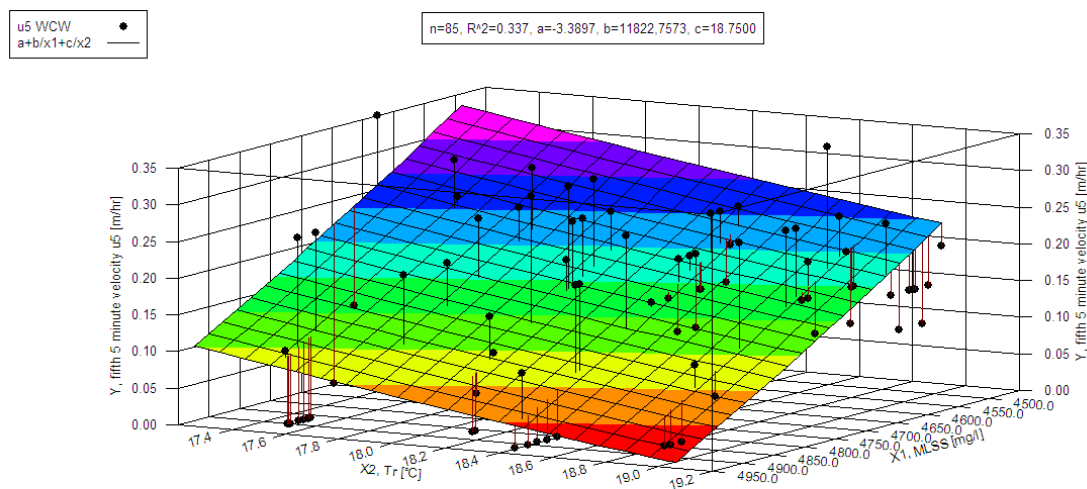
Figure 6-26 u5 dependency on MLSS concentration and T_r

The response relationship of u5 (20 to 25 minutes) to MLSS concentration and T_r variations is presented by the following equation:

$$u5 = -3.4 + \frac{11822.8}{MLSS} + \frac{18.8}{T_r} \ [m/hr] \hspace{4cm} \text{Equation 6-10}$$

The model plot is shown in Figure 6-26, and u5 varies on the y-axis from 0 to 0.33 m/hr.

A simulation can illustrate the dependence of the u5 on T_r. At an average constant MLSS concentration of 4500 mg/ℓ, the u5 change due to a T_r reduction from 19.0 to 17.2°C can be determined according to the u5-model (Equation 6.10). The u5 increases from 0.22 to 0.31 m/hr, with a corresponding relative u5 increase of 0.05 m/hr per 1°C T_r reduction, or - 0.05 m/hr u5/1°C T_r.

The correlation between u5 and MLSS concentration is not represented in traditional models. The settling velocity over the fifth 5-minute settling period now follows the same inverse pattern as identified previously in u4. All the easily flocculating MLSS at the high temperature has flocculated and settled over the first 15 minutes. Some MLSS sample at the colder temperature only start to settle after 20 to 25 minutes, and the settling velocity is therefore higher in the lower temperature range. The inverse correlation between u5 and T_r is illustrated for on-line evaluations at an average of -0.05 m/hr per 1°C change.

6.3.10.12   u6 correlation with MLSS concentration and T_r variation
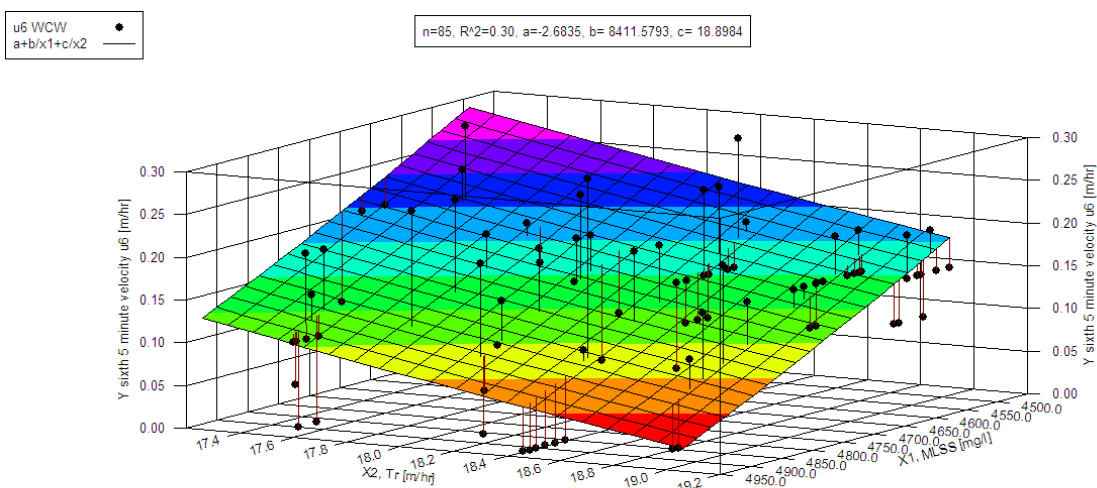
Figure 6-27 u6 dependency on MLSS concentration and T_r

The response relationship of u6 (25 to 30 minutes) to MLSS concentration and T_r variations is presented by the following equation:

$$u6 = -2.7 + \frac{8411.6}{MLSS} + \frac{18.9}{T_r} \quad [m/hr] \qquad \text{Equation 6-11}$$

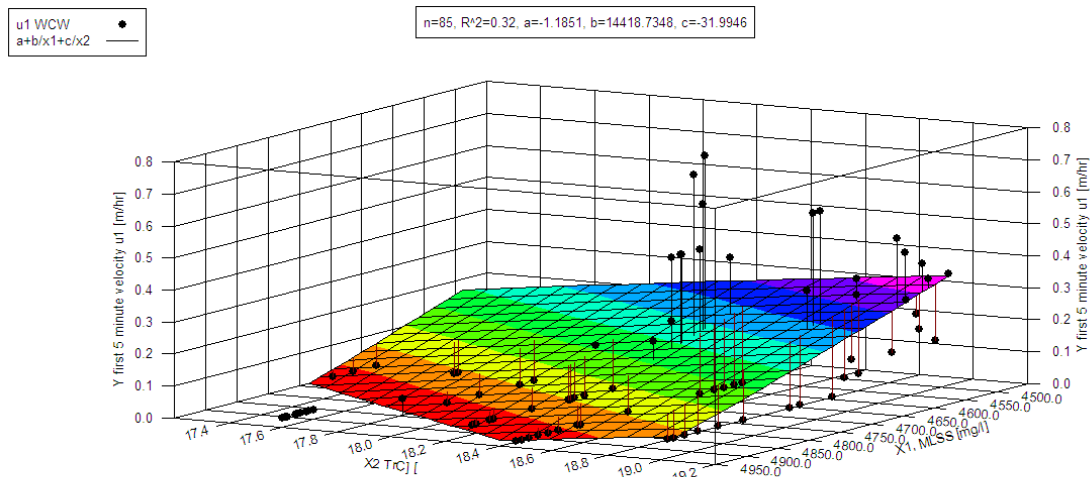The model plot is shown in Figure 6-27, and u6 varies on the y-axis from 0.02 to 0.29 m/hr.

A simulation can illustrate the dependence of u6 on T_r. At an average constant MLSS concentration of 4500 mg/ℓ, the u6 change due to a T_r reduction from 19.0 to 17.2°C can be determined according to the u6-model (Equation 6.11). The u6 increases from 0.18 to 0.27 m/hr, with a corresponding relative u6 increase of 0.05 m/hr per 1°C T_r reduction, or - 0.05 m/hr u6/1°C T_r.

The settling velocity over the sixth 5-minute period now follows the same pattern as identified in u4 and u5. All the easily flocculating MLSS at higher temperatures has flocculated and settled over the first 15 minutes. The MLSS at the colder temperature only starts to settle after 15 to 25 minutes, and the u6 settling velocity is therefore higher in the lower T_r range. The inverse correlation between u6 and T_r is illustrated for the on-line evaluation, at an average of -0.05 m/hr per 1°C change.

6.3.11 Settling models results summary

The experimental range for settling parameters is provided in Table 6-6. Modelled values differ slightly from experimental values due to regression curve-fitting calculations.

Table 6-6 Settling parameters model prediction over experimental range

Parameter	Unit	Minimum experimental parameter value	Minimum modelled parameter value	Maximum experimental parameter value	Maximum modelled parameter value
SVI	[mℓ/g]	97	96.2	203	213.5
t_umax	[min.]	4.0	1.5	30.0	32.0
u_max	[m/hr]	0.00	0.05	1.73	1.40
u_ave	[m/hr]	0.01	-0.03	0.39	0.41
h	[mm]	162.0	151.9	355.9	375.3
u1	[m/hr]	0.00	-0.12	0.74	0.34
u2	[m/hr]	0.00	-0.28	0.94	0.78
u3	[m/hr]	0.00	-0.12	0.69	0.52
u4	[m/hr]	0.00	-0.03	0.49	0.37
u5	[m/hr]	0.00	0.00	0.35	0.33
u6	[m/hr]	0.00	0.02	0.30	0.29

The experimental parameter list is compared to the modelled range for the same parameters, with the minimum and maximum values indicating the comparative predicted values. The model equation can be recalculated with a new parameter range, if the predicted values fall outside the experimental range.

Model equations were not recalculated, as the principle aim of the modelling was to illustrate T_r-based MLSS settling correlations for a full-scale plant-specific experimental condition. The development of more representative parameter models will require additional experimental data over a wider operational range.

6.3.12 Settling models simulation results

An average MLSS concentration of 4500 mg/ℓ is used with the boundary temperature range from 19.0 to 17.2°C to calculate settling parameters. The results are summarised in Table 6-7. The relative change to settling parameters is based on a 1°C T_r reduction. Direct and inverse relationships are quantified respectively by positive and negative parameter changes.

Table 6-7 Modelled settling parameters simulation based on T_r variation

Parameter	MLSS concentration constant [mg/ℓ]	Tr High [°C]	calculated parameter	Tr Low [°C]	Tr change [°C]	calculated parameter	parameter change	parameter relative change	unit
SVI	4500	19.0	99	17.2	1.8	125	-26.5	-14.8	mℓ/g/1°C
t_umax	4500	19.0	2.2	17.2	1.8	6.5	-4.2	-2.4	min/1°C
u_max	4500	19.0	1.4	17.2	1.8	1.2	0.2	0.1	m/hr/1°C
u_ave	4500	19.0	0.4	17.2	1.8	0.3	0.1	0.04	m/hr/1°C
h	4500	19.0	157	17.2	1.8	192	-35	-19	mm/1°C
U1	4500	19.0	0.34	17.2	1.8	0.19	0.14	0.08	m/hr/1°C
U2	4500	19.0	0.76	17.2	1.8	0.42	0.34	0.19	m/hr/1°C
U3	4500	19.0	0.51	17.2	1.8	0.39	0.12	0.07	m/hr/1°C
U4	4500	19.0	0.35	17.2	1.8	0.36	-0.02	-0.01	m/hr/1°C
U5	4500	19.0	0.22	17.2	1.8	0.31	-0.08	-0.05	m/hr/1°C
U6	4500	19.0	0.18	17.2	1.8	0.27	-0.09	-0.05	m/hr/1°C

6.4 Summary

A custom-made automated MLSS settling meter provides semi-continuous MLSS settling profiles for use in settling parameter modelling. The experimental work consists of four main aspects at a full-scale plant reactor:

1. diurnal variations in h, T_r, MLSS concentration, and SVI,

2. best-fit modelling of three settling parameters (SVI, u_max and t_umax) with MLSS concentration and T_r,

3. model fitting of SVI with u_max and t_umax, and

4. basic modelling and simulation of 11 settling parameters with MLSS concentration and T_r.

The on-line MLSS settling evaluation at a full-scale plant reactor provides the following results:

- The diurnal trends follow sinusoidal wave profiles, with an inverse relationship between T_r and settling meter h, MLSS concentration, and SVI,

- The SVI, u_max, and t_umax were unsatisfactorily correlated to MLSS concentration alone, with R^2-values of 0.69, 0.58, and 0.70 respectively due to visible data scatter. The inclusion of T_r improved the corresponding best-fit correlations to R^2-values of 0.84, 0.70, and 0.83, with large t-ratios and low p values indicating the importance of T_r,

- The temperature-based SVI was correlated to u_max and t_umax at R^2-values of 0.90 and 0.95 respectively,

- The basic 3-parameter settling model provided significant changes for the 11 settling parameter, based on simulated operational T_r variations at constant MLSS concentrations, as summarised in Table 6-7.

6.5   Conclusions

- The governing role of MLSS concentration during MLSS settling might hide the effects of other factors affecting MLSS settling, such as temperature. The settling parameters, such as SVI, mirror the diurnal MLSS concentration profile, but the diurnal temperature fluctuation changes inversely with the corresponding MLSS concentration. The on-line MLSS settling meter collects enough data points based on operational conditions to generate temperature dependent MLSS settling profiles that identify and represent the effects of temperature.

• The small, but significant effect of short-term temperature variation on MLSS settling is proved statistically with improved settling models. Settling parameters are unsatisfactorily correlated with MLSS concentration alone. The inclusion of T_r improved the corresponding best-fit correlations, with R^2-values increases larger than 0.1 obtained for the full-scale plant data.

• The temperature effect on settling parameters is illustrated with simplified settling models. Simulations illustrate the changes to settling parameters, based on temperature changes at constant MLSS concentrations. The SVI increase of 14.8 mℓ/g per 1°C T_r reduction is coincidentally identical to the batch settling SVI test results (-14.8 mℓ/g per 1°C T_s). The time to reach u_max increases by 2.4 minutes per 1°C T_r reduction, while the u_max increases by 0.1 m/hr per 1°C T_r increase.

• The incremental 5-minute settling velocity models produce distinctive trends over the 30-minute settling period:

1. A direct relationship exists over the first 15 minutes between u1, u2, u3, and T_r, similar to the u_ave and u_max relationships with T_r,
2. After 15 minutes, the settling trend changes, and for the next 15 minutes u4, u5, and u6 change inversely with T_r variations, and
3. MLSS samples at higher MLSS concentration and lower T_r did not settle over the first 15 minutes, and the colder MLSS samples only started to settle between 15 and 30 minutes, creating inverse MLSS settling velocity to T_r relationships.

• The modelled settling parameter values are only valid for the experimental boundary conditions, as indicated on the individual graphs. Predictions based on the settling parameter models are invalid outside these tested MLSS concentration and T_r ranges.

• With the above conclusions, a suitable approach is provided to improve the reliability of MLSS settling tests. The effects of short-term temperature variations before and during MLSS settling tests can be significantly reduced with the use of an on-line MLSS settling meter.

7   SUMMARY OF RESULTS

The results of this project are summarised according to the project aims, with a summary of the experimental results provided in Table 7-1:

• The literature review confirms the lack of basic temperature compensation procedures and equipment, and the recording of temperature data, required in the determination of MLSS settling parameters. Limited research information is available on operational temperature conditions during MLSS settleability evaluations, and it appears that temperature-based MLSS settleability models are not readily available.

• Large settling velocity increases are calculated for a simplified single biofloc settling over an extended temperature range. Basic theoretical principles simulate the effect of changes in temperature related water and biofloc characteristics.

• A preliminary temperature survey at pilot- and full-scale plant reactors identifies short- and long-term T_r fluctuations that follow T_a profiles. Meteorological factors and unidentified plant specific factors influence T_{raw}.

• A batch MLSS settling evaluation indicates that container size and reactor zone sampling points have a limited influence on the SVI and ISV of a well-settling MLSS. Supernatant turbidity improves from the anaerobic zone throughout the reactor up to the end region of the aerobic zone. The immediate environment of the MLSS sample has a direct influence on MLSS settling test results. A 4.3°C temperature increase over 30 minutes, by MLSS sample placement in direct sunshine instead of shade, results in a 63 mℓ/g SVI decrease. This relationship illustrates the essential need for temperature compensation and environmental conditions recordings during MLSS settling tests.

• The diurnal variations in MLSS settling meter data show distinct sinusoidal wave profiles. Best-fit models of settling parameters illustrate statistically with improved data fitting the positive impact of T_r inclusion in MLSS concentration-based models. The SVI relationships with the two settling parameters u_max and t_umax reflect the ease of development of on-line-based parameter correlations. Simulations of settling parameters with MLSS concentration and T_r illustrate the extent of parameter change during a

temperature variation. A 1.8°C diurnal T_r fluctuation results in a 26.5 mℓ/g SVI change. This SVI increase of 14.8 mℓ/g per 1°C T_r decrease illustrates the close inverse relationship between MLSS settleability and temperature. Additional parameter relationships that are identified in the project are listed in Table 7-1.

- Incremental settling data indicates that MLSS concentration and T_r determine the t_umax, which in turn indicates during which 5-minute period the settling velocity will be the highest. There is a direct relationship between the settling velocity and T_r. The only exception occurs during the last three stages of the incremental 5-minute settling periods over 30 minutes. The on-line-based diurnal settling profiles indicate that settling velocity increases later in the 30-minute settling period during high MLSS concentration and low T_r conditions. The colder MLSS sample only starts settling after a longer reflocculation period (e.g. 15 to 30 minutes).

- The significant effects of short-term temperature variations on MLSS settling parameters have been determined theoretically and experimentally, thereby achieving the main project aim.

Table 7-1 MLSS settling parameter variation summary

Index / Parameter	Batch MLSS settling tests T_s increase Constant MLSS concentration	On-line full-scale plant T_r increase Constant MLSS concentration	On-line full-scale plant Constant T_r MLSS concentration increase	Relationship with BNR reactor zones
SVI	Inverse, -14.8 mℓ/g/1°C	Inverse, -14.8 mℓ/g/1°C	Direct correlation	Relatively constant
t_umax	-	Inverse, -2.4 min./1°C	Direct correlation	-
u_max	-	Direct, 0.1 m/hr/1°C	Inverse correlation	-
u_ave	-	Direct, 0.04 m/hr/1°C	Inverse correlation	-
ISV	Direct, 0.12 m/hr/1°C	-	-	Relatively constant
h	-	Inverse, -19 mm/1°C	Direct correlation	-
u1	-	Direct 0.08 m/hr/1°C	Inverse correlation	-
u2	-	Direct 0.19 m/hr/1°C	Inverse correlation	-
u3	-	Direct 0.07 m/hr/1°C	Inverse correlation	-
u4	-	Inverse -0.01 m/hr/1°C	Inverse correlation	-
u5	-	Inverse -0.05m/hr/1°C	Inverse correlation	-
u6	-	Inverse -0.05 m/hr/1°C	Inverse correlation	-
Turbidity	Direct 1.42 FNU/1°C	-	-	Reduction through reactor

8   CONCLUSIONS

- The impact of MLSS concentration dominates other MLSS settling factors, according to the format of existing settling models. The effect of diurnal T_r fluctuations is not easily detected with conventional batch settling tests due to rapid changes in T_s. An on-line MLSS settling meter combines both diurnal MLSS concentrations and T_r fluctuations, to generate improved temperature dependent MLSS settling models.

- The batch MLSS settling test in a graduated cylinder is the most widely used method to determine settling parameters such as SVI, but temperature compensation or recording procedures are rarely implemented. The significant effect of short-term temperature variations on MLSS sample settling is illustrated with two evaluations (batch and on-line), at an average 14.8 mℓ/g SVI increase per 1°C decrease.

- There is a direct relationship between MLSS settling velocity and T_r. The only exception occurs during some of the incremental settling velocity stages. The incremental settling velocities increase in the second half of the 30-minute settling period in the lower T_r range, because the colder MLSS sample only starts settling after a longer reflocculation period. Incremental settling data indicates that MLSS concentration and T_r determine t_umax, and it also specifies the highest settling velocity during the six 5-minute settling stages in the 30-minute period.

- Existing MLSS settling parameter models are based on MLSS concentration, without incorporating temperature. The effect that temperature inclusion has on settling models is illustrated with three settling parameter models, where the statistical improvement is illustrated by an average R^2 increase of 0.13.

- Conventional batch settling equipment and basic procedures are not suitable to effortlessly identify temperature dependent MLSS settling changes over small operational T_r ranges. The settleability impact of diurnal T_r fluctuations and T_s change during sample handling are not easily detected from routine batch MLSS settling tests performed on a daily basis.

- Automated MLSS settling meters are ideally suited to perform semi-continuous MLSS settling tests. These MLSS settling profiles were not linked before to diurnal T_r fluctuations. The effect of diurnal T_r variations on settling parameters is illustrated on a full-scale plant with on-line based correlations between SVI and two settling velocity parameters at an average R^2 of 0.93.

- SVI test results are used for operational settleability control and design purposes, but do usually not include information about MLSS concentration, environmental test conditions or container dimensions. Temperature variations of about 4.3°C during 30-minute settling test periods result in an average SVI change exceeding 60 mℓ/g. These rapid T_s variations illustrate the need to include reference temperature conditions in MLSS settling reports and experimental methods.

- Temperature is not a process parameter observed at most operational plants. Preliminary temperature recordings indicated significant short- and long-term temperature changes of a few degrees Celsius in full-scale and pilot plant reactors and at different aeration systems.

- Basic MLSS settling models that are based on fundamental theories are not readily available to simulate dynamic plant temperature conditions. Preliminary calculations illustrate large settling velocity changes of about 2 to 11 m/hr, created by water and biofloc property changes, over an extended temperature range of 20°C.

9   RESEARCH CONTRIBUTION

This study quantifies the significant effects of short-term temperature variations on batch and on-line MLSS settling parameters. An automated MLSS settling method is introduced to reduce the effects of sample temperature variations observed before and during settling tests. This method is suitable to determine MLSS settling parameters on-line during dynamic operational conditions. Effects of short-term temperature fluctuations are thus included in settling parameters, together with the long-established MLSS concentration.

A future research need would be to use such an automated MLSS settling meter at a wider selection of plant reactors to develop plant specific settling models. The effects of different reactor temperatures, based on surface or bubble aeration systems, will be represented by distinctive MLSS settling profiles and associated settling parameter correlations. Specific temperature sensitive processes such as nitrification and MLSS settling influences reactor and clarifier design and operation, which will be enhanced with the availability of the improved parameter correlations.

A second research need would be to use an on-line settling meter to measure alternative settling indexes, such as SSVI and DSVI, during diurnal temperature fluctuations. The principle aim of the current study is to illustrate the effects of short-term temperature variations on MLSS settling. Basic settling parameters are modelled to illustrate the temperature effect, without considering the limitations of certain settling parameters and test methods, such as the SVI. Future temperature-based SSVI and DSVI models will be beneficial for the management and design of wastewater treatment plants.

The established BNR reactor design procedures, which are used in countries with extreme weather patterns such as South Africa, consider long-term T_r fluctuations to ensure nutrient removal is guaranteed at a low T_r. In future, this lowest operational T_r should be included in secondary settling tank design. Specific reactor design to limit the effect of meteorological factors, as well as the use of bubble aeration applications, are two design steps that can be promoted to reduce the lowest operational T_r. The future inclusion of modelled and plant specific T_r-based plant performance data, obtained from on-line MLSS settling meters, establishes opportunities to optimise not only BNR, but also improve secondary settling tank design.

10 REFERENCES

Agridiotis V, Forster CF, Balavoine C, Wolter C and Carliell-Marquet C (2006) An examination of the surface characteristics of activated sludge in relation to bulking during the treatment of paper mill wastewater. *Water and Environmental Journal*, 20 (3) 141-149.

Akça L, Kinaci C and Karpuzcu M (1993) A model for optimum design of activated sludge plants. *Wat. Res.* 27 (9) 1461-1468.

Al-Yousfi AB, Mason SH, Romagnoli RJ and Williams JB (2000) Viscous sludge bulking due to *zoogloea* proliferation at an industrial wastewater treatment plant: background, causes and remedies. *Proc. of the 1st World Water Congress of the International Water Association (IWA)*. July 3-7, Paris, France.

Andreadakis AD (1993) Physical and chemical properties of activated sludge floc. *Wat. Res.* 27 (12) 1707-1714.

APHA (1998) *Standard Methods for the Examination of Water and Wastewater*. 20th edn., American Public Health Association (APHA), Washington, D.C., USA.

Archibald F and Young F (2004) Common stresses affecting activated sludge health and performance – what the four-assay set can tell us. *Wat. Sci. Tech*. 50 (3) 49-55.

ATI (2007) *Instrument data sheet* [http://analyticaltechnology.com/cms/; accessed 29/10/07].

Azimi AA and Horan NJ (1991) The influence of reactor mixing characteristics on the rate of nitrification in the activated sludge process. *Wat. Res*. 25 (4) 419-423.

Baetens D, Vanrolleghem PA, van Loosdrecht MCM and Hosten LH (1999) Temperature effects in Bio-P removal. *Wat. Sci. Tech*. 39 (1) 215-225.

Banadda EN, Smets IY, Jenne R and Van Impe JF (2005) Predicting the onset of filamentous bulking in biological wastewater treatment systems by exploiting image analysis information. *Bioprocess Biosyst. Eng.* (27) 339-348.

Banks CJ, Koloskov GB, Lock AC and Heaven S (2003) A computer simulation of the oxygen balance in a cold climate winter storage WSP during the critical spring warm-up period. *Wat. Sci. Tech*. 48 (2) 189-196.

Barbusiński K and Kościelniak H (1995) Influence off substrate loading intensity on floc size in activated sludge process. *Wat. Res*. 29 (7) 1703-1710.

Barnard JL (1974) Nutrient removal in biological systems. *Proc. of the biennial conference and exhibition, Institute of Water Pollution Control (IWPC)*, April 7-11, Salisbury (Harare), Zimbabwe.

Bergh SG (1996) *Diagnosis Problems in Wastewater Settling*. PhD Thesis, Lund Institute of Technology, Sweden.

Berktay A (1998) Properties of Sludge Produced From the Pressurized Wastewater Treatment Process. *Tr. J. of Engineering and Environmental Science* 22 377-385.

Bhargava DS and Rajagopal K (1993) Differentiation between transition zone and compression in zone settling. *Wat. Res.* 27 (3) 457-463.

Bień J, Kamizela T, Wolny L and Stępniak L (2005) Settleability and compressibility of activated sludge prepared with ultrasounds. *Proc. of the 9th IWA Conference on Diffuse Pollution: Technical Programme and Abstracts of the Conference on Management of Residues Emanating from the Water and Wastewater Treatment*, 9-12 August, Johannesburg, South Africa.

Biggs C, Lant P and Hounslow M (2003) Modelling the effect of shear history on activated sludge flocculation. *Wat. Sci. Tech.* 47 (11) 251-257.

Biggs CA, Ford AM and Lant PA (2001) Activated sludge flocculation: direct determination of the effect of calcium ions. *Wat. Sci. Tech*. 43 (11) 75-82.

Blackbeard JR, Ekama GA and Marais GvR (1986) A Survey of Filamentous Bulking and Foaming in Activated-Sludge Plants in South Africa. *Wat. Pollut. Control* 85 (1) 90-100.

Bruus JH, Nielsen PH and Keiding K (1992) On the stability of activated sludge flocs with implications to dewatering. *Wat. Res*. 26 (12) 1597-1604.

Bux F and Kasan HC (1994a) A microbiological survey of ten activated sludge plants. *Water SA* 20 (1) 61-72.

Bux F and Kasan HC (1994b) Comparison of selected methods for relative assessment of surface charge on waste sludge biomass. *Water SA* 20 (1) 73-76.

Bye CM and Dold PL (1999) Evaluation of Correlations for Zone Settling Velocity Parameters Based on Sludge Volume Index-Type Measures and Consequences in Settling Tank Design. *Water Environ. Res.* 71 (7) 1333-1344.

Bye CM and Dold PL (1998) Sludge volume index settleability measures: effect of solids characteristics and test parameters. *Water Environ. Res.* 70 (1) 87-93.

Casey T and Alexander WV (2001) *Design and operating strategies to minimize bulking by anoxic-aerobic filamentous organisms in nutrient removal activated sludge plants.* WRC report no 775/1/01, Pretoria, South Africa.

Casey TG, Ekama GA, Wentzel MC and Marais GvR (1995) Filamentous organism bulking in nutrient removal activated sludge systems. Paper 1: A historical overview of causes and control. *Water SA* 21 (3) 231-238.

Catunda PFC and Van Haandel AC (1992) Activated sludge settling Part I: Experimental determination of activated sludge settleability. *Water SA* 18 (3) 165-172.

Cenens C, Smets IY, Ryckaert VG and Van Impe JF (2000) Modelling the competition between flocforming and filamentous bacteria in activated sludge waste water treatment systems – I. Evaluation of mathematical models based on kinetic selection theory. *Wat. Res.* 34 (9) 2525-2534.

Çetin FD and Sürücü G (1990) Effects of Temperature and pH on the settleability of activated sludge flocs. *Wat. Sci. Tech.* 22 (9) 249-254.

Chaignon V, Lartiges BS, El Samrani A and Mustin C (2002) Evolution of size distribution and transfer of mineral particles between flocs in activated sludges: an insight into floc exchange dynamics. *Wat. Res.* 36 (3) 676-684.

Cho SH, Colin F, Sardin M and Prost C (1993) Settling velocity model of activated sludge. *Wat. Res.* 27 (7) 1237-1242.

Clements MS (1976) The Application of Static Column Tests to Sedimentation Tank Design. *Wat. Pollut. Control* 75 (3) 360-376.

Cloete TE and Muyima NYO (1997) *Microbial community analysis: the key to the design of biological wastewater treatment systems*. IAWQ Scientific and Technical Report no. 5, Cambridge, England.

Cooper P, Upton JE, Smith M and Churchley J (1995) Biological Nutrient removal: Design Snags, Operational Problems and Costs. *J.IWEM.* 9 (2) 7-18.

Daigger GT (1995) Development of refined clarifier operating diagrams using an updated settling characteristic database. *Wat. Environ. Res.* 67 (1) 95-100.

Daigger GT and Roper (jr.) RE (1985) The relationship between SVI and activated sludge settling characteristics. *J. Wat. Pollut. Cont. Fed.,* 57 (8) 859-866.

Dangcong P, Bernet N, Delgenes JP and Moletta R (1999) Aerobic granular sludge – a case report. Rapid Communication. *Wat. Res*. 33 (3) 890-893.

DataFit (2005) *Statistical software package*, version 8.1.69, Oakdale Engineering, evaluation copy, US. [http://www.curvefitting.com; accessed 15/01/2005].

De Clercq J, Nopens I, Defrancq J and Vanrolleghem PA (2007) Extending and calibrating a mechanistic hindered and compression settling model for activated sludge using in-depth batch experiments. *Wat. Res. (in press)*.

De Clercq J, Devissher M, Boonen I, Vanrolleghem PA and Defrancq J (2003) A new one-dimensional clarifier model – verification using full-scale experimental data. *Wat. Sci. Tech.* 47 (12) 105-112.

De Clercq B (2003) *Computational Fluid dynamics of settling tanks: Development of experiments and rheological, settling and scraper submodels*. PhD Thesis. Ghent University, Faculty of Agricultural and Applied Biological Science, Belgium.

Dick RI and Vesilind PA (1969) The sludge volume index - what is it? *J. Wat. Pollut. Cont. Fed.* 41 (7) 1285-1291.

Dochain D and Vanrolleghem PA (2001) *Dynamical Modelling and Estimation in Wastewater Treatment Processes*. IWA Publishing, Cornwall, UK.

Droste RL (1997) *Theory and practice of water and wastewater treatment*. 1st edn., John Wiley & Sons, Inc., USA.

Drysdale GD, Atkinson BW, Mudaly DD, Kasan HC and Bux F (2000) *Investigation of the microbial contribution to nutrient removal in an activated sludge wastewater treatment process*. WRC report 822/1/00, Pretoria, South Africa.

Dupont R and Dahl C (1995) A one-dimensional model for a secondary settling tank including density current and short-circuiting. *Wat. Sci. Tech.* 31 (2) 215-224.

Durmaz B and Sanin FD (2001) Effect of carbon to nitrogen ratio on the composition of microbial extracellular polymers in activated sludge. *Wat. Sci. Tech.* 44 (10) 221-229.

Ekama GA, Barnard JL, Günthert FW, Krebs P, McCorquodale JA, Parker DS and Wahlberg EJ (1997) *Secondary Settling Tanks: Theory, modelling, design and operation*. IAWQ

Scientific and Technical Report No. 6, IWA Publishing, Simpson Drewett and Co. Ltd., Richmond, Surrey, England.

Ekama GA (1988) *Sludge settleability and filamentous organisms*. Association of Water Treatment Personnel Seminar and Mini Trade Fair '88, Athlone Wastewater Treatment Works, 24 November, Cape Town, South Africa.

Ekama GA and Marais GvR (1986) Sludge Settleability and Secondary Settling Tank Design Procedures. *Wat. Pollut. Control* 85 (2) 101-113.

Ekama GA, Marais GvR and Blackbeard JR (1985) *Final report to the Water Research Commission on a two year exploratory study on activated sludge bulking and foaming problems in Southern Africa (1983-1984)*. University of Cape Town Research Report no W 54, WRC report 114/1/85, Pretoria, South Africa.

Ekama GA and Marais GvR (1984) Two improved activated sludge settleability parameters. *IMESA* 6 (9) 20-26.

Erdal UG (2002) *The effects of temperature on system performance and bacterial community structure in a biological phosphorus removal system*. PhD Thesis, Virginia Polytechnic Institute and State University, Blacksber, Virginia, USA [http://scholar.lib.vt.edu/theses/available/etd-03082002-154444/; accessed 23/08/2004].

Ericsson B and Eriksson L (1988) Activated sludge characteristics in a phosphorus depleted environment. *Wat. Res.* 22 (2) 151-162.

Etterer T and Wilderer PA (2001) Generation and properties of aerobic granular sludge. *Wat. Sci. Tech.* 43 (3) 19-26.

Excel (2007) *Software program* [http://office.microsoft.com/; accessed 27/10/2007].

Forster CF and Dallas-Newton J (1980) Activated Sludge Settlement – Some Suppositions and Suggestions. *Wat. Pollut. Control* 79 (3) 338-351.

Forster CF (1976) Bioflocculation in the Activated Sludge Process. *Water SA* 2 (3) 119-125.

Fourier (2007) *Instrument data sheet* [http://www.fouriersystems.com/; accessed 27/10/2007]

Gerardi MH (2002) *Settleability Problems and Loss of Solids in the Activated Sludge Process*. John Wiley & Sons, Hoboken, New Jersey, United States of America.

Gernaey K, Vanderhasselt A, Bogaert H, Vanrolleghem P and Verstraete W (1998) Sensors to monitor biological nitrogen removal and activated sludge settling. *Journal of Microbiological Methods* 32 193-204.

Gillot S and Vanrolleghem PA (2003) Equilibrium temperature in aerated basins-comparison of two prediction models. *Wat. Res*. 37 3742-3748.

Grady (jr.) CPL and Filipe CDM (2000) Ecological engineering of bioreactors for wastewater treatment. *Water, Air, and Soil Pollution* 123 117-132.

Gregory R and Zabel TF (1990) *Water Quality and Treatment*. 4th ed., Chap. 7, American Water Works Association, McGraw-Hill, USA.

Grijspeerdt K and Verstraete W (1997) Image analysis to estimate the settleability and concentration of activated sludge. *Wat. Res*. 31 (5) 1126-1134.

Grijspeerdt K, Vanrolleghem P and Verstraete W (1995) Selection of one-dimensional sedimentation: models for on-line use. *Wat. Sci. Tech.* 31 (2) 193-204.

Härtel L and Pöpel HJ (1992) A dynamic secondary clarifier model including processes of sludge thickening. *Wat. Sci. Tech.* 25 (6) 267-284.

Hasar H, Kinaci C, Ünlü A, Torul H and Ipek U (2004) Rheological properties of activated sludge in a sMBR. *Biochemical Engineering Journal*. 20 (1) 1-6.

Hasselblad S and Xu S (1996) On-line estimations of settling capacity in secondary clarifier. *Wat. Sci. Tech.* 34 (3-4) 323-328.

Hercules S, Tsai M-W, Lakay MT, Wentzel MC and Ekama GA (2002) *Full–scale demonstration of filamentous bulking control at a biological nutrient removal activated sludge plant.* WRC report 823/1/02, Pretoria, South Africa.

Ho KM, Gerges H and Lau TK (2006) Development of final sedimentation tank maximum operating capacity curves using Vesilind settling parameters and mathematical modelling. *Proc. of Weftec 2006*, October 21-25, Dallas, Texas, USA.

Ingildsen P (2002) *Realising full-scale control in wastewater treatment systems using in situ nutrient sensors*. Ph.D. Thesis, Lund Institute of Technology, Sweden.

IWPC (1977) *Handleiding vir rioolwerke-operateurs: Die suiwering van rioolwater*. 2nd edn. Institute of Water Pollution Control (IWPC), Johannesburg, South Africa.

Janczukowicz W, Szewczyk M, Krzemieniewski M and Pesta J (2001) Settling Properties of Activated Sludge from a Sequencing Batch Reactor (SBR) *Polish Journal of Environmental Studies* 10 (1) 15-20.

Jang H and Schuler AJ (2006) The case for variable density: a new perspective on activated sludge settling. *Proc. of Weftec 2006*, October 21-25, Dallas, Texas, USA.

Janssen PMJ, Meinema K and Van der Roets (2002) Biological Phosphorus removal: Manual for design and operation, STOWA report, IWA Publishing, London, UK.

Jenkins D, Richard MG and Daigger GT (1986) *Manual on the causes and control of activated sludge bulking and foaming.* Water Research Commission, Pretoria, South Africa.

Jenkins D, Richard MG and Neethling JB (1984) Causes and Control of Activated-Sludge Bulking. *Wat. Pollut. Control* 83 (4) 455-472.

Jeyanayagam S, Venner I and Hammett CE (2006) A site-specific tool for optimising final clarifier design and operation. *Proc. of Weftec 2006*, October 21-25, Dallas, Texas, USA.

Jin B, Wilén BM and Lant P (2003) A comprehensive insight into floc characteristics and their impact on compressibility and settleability of activated sludge. *Chem. Eng. J.* 95 (1-3) 221-235.

Jokela P and Immonen J (2002) Dissolved air flotation clarification of activated sludge and wastewaters from chemical industry. *Wat. Sci. Tech.* 47 (1) 205-210.

Jones GA and Franklin BC (1985) The Prevention of Filamentous Bulking of Activated Sludge by Operation Means at Halifax Sewage-Treatment Works. *Wat. Pollut. Control* 84 (3) 329-346.

Kabouris JC and Georgakakos AP (1990) Optimal control of the activated sludge process. *Wat. Res.* 24 (10) 1197-1208.

Kaewpipat K and Grady (jr.) CPL (2002) Microbial population dynamics in laboratory-scale activated sludge reactors. *Wat. Sci. Tech.* 46 (1-2) 19-27.

Kazami AA and Furumai H (2000) A simple settling model for batch activated sludge process. *Wat. Sci. Tech.* 42 (3-4) 9-16.

Keller J, Yuan Z and Blackall LL (2002) Integrating process engineering and microbiology tools to advance activated sludge wastewater treatment research and development. *Reviews in Env. Science and Biotech*. 1 83-97.

Kim HS, Shin MS, Jang DS and Jung SH (2006) Indepth diagnosis of a secondary clarifier by the application of radiotracer technique and numerical modeling. *Wat. Sci. Tech*. 54 (8) 83-92.

Kim J, Kim S and Yoon J (2003) The evaluation of a density current experiment as a verification tool of a secondary settling model. *Wat. Sci. Tech*. 47 (12) 113-118.

Kim Y, Pipes WO and Chung P-G (1998) Control of activated sludge bulking by operating clarifiers in a series. *Wat. Sci. Tech*. 38 (8-9) 1-8.

Kim Y, Pipes WO and Chung P-G (1997) Estimation of suspended solids concentrations in activated sludge settling tanks. *Wat. Sci. Tech*. 35 (8) 127-135.

Kjellerup BV, Keiding K and Nielsen PH (2001) Monitoring and troubleshooting of non-filamentous settling and dewatering problems in an industrial activated sludge treatment plant. *Wat. Sci. Tech*. 44 (2-3) 155-162.

Kolmetz K, Dunn AS, Som AMd, Sim CP and Mustaffa Z (2003) Benchmarking Waste Water Treatment Systems. *Proc. of International Conference on Chemical and Bioprocess Engineering,* School of Engineering and Information, Technology University Malaysia Sabah, 27-29 August, Malaysia.

Krebs P (1995) Success and shortcomings of clarifier modelling. *Wat Sci. Tech*. 31 (2) 181-191.

Krishna C and Van Loosdrecht MCM (1999) Effect of temperature on storage polymers and settleability of activated sludge. *Wat. Res*. 33 (10) 2374-2382.

Kristensen GH, Jørgensen PE and Nielsen PH (1994) Settling characteristics of activated sludge in Danish treatment plants with biological nutrient removal. *Wat. Sci. Tech*. 29 (7) 157-165.

Kruit J, Hulsbeek J and Visser A (2002) Bulking sludge solved?! *Wat. Sci. Tech*. 46 (1-2) 457-464.

Liao BQ, Allen DG, Droppo IG, Leppard GG and Liss SN (2001) Surface properties of sludge and their role in bioflocculation and settleability. *Wat. Res*. 35 (2) 339–350.

Liss SN, Liao BQ, Droppo IG, Allen DG and Leppard GG (2002) Effect of solids retention time on floc structure. *Wat. Sci. Tech.* 46 (1-2) 431-438.

Lilley ID, Pybus PJ and Power SPB (1997) *Operating Manual for Biological Nutrient Removal Wastewater Treatment Works*. WRC Report No TT 83/97, Water Research Commission, Pretoria, South Africa.

Lynggaard-Jensen A and Lading A (2006) On-line determination of sludge settling velocity for flux-based real-time control of secondary clarifiers. *Wat. Sci. Tech.* 54 (11-12) 249-256.

Madoni P, Davoli D and Gibin G (2000) Survey of filamentous microorganisms from bulking and foaming activated-sludge plants in Italy. *Wat. Res.* 34 (6) 1767-1772.

Makinia J, Wells SA and Zima P (2005) Temperature Modeling in Activated Sludge Systems: A Case Study. *Wat. Environ. Res.* 77 (5) 197-204.

Mamais D, Nikitopoulos G, Andronikou E, Gavalakis E, Andreadakis A, Noutsopoulos C, Giotakis C and Tsimarakis G (2006) Influence of the presence of long chain fatty acids (LCFAs) in the sewage on the growth of *M. Parvicella* in activated sludge wastewater treatment plants. *Global NEST Journal* 8 (1) 82-88.

Maqueda MAM, Martinez SA, Narváez D, Rodriguez MG, Aguilar R and Herrero VM (2006) Dynamic modelling of an activated sludge system of a petrochemical plant operating at high temperatures. *Wat. Sci. Tech.* 53 (11) 135-142.

Martínez M, Sànchez-Marrè M, Comas J and Rodríguez-Roda I (2006) Case-based reasoning, a promising tool to face solids separation problems in the activated sludge process. *Wat. Sci. Tech.* 53 (1) 209-216.

Martins AMP, Heijnen JJ and Van Loosdrecht MCM (2003) Effect of dissolved oxygen concentration on sludge settling. *Appl. Microbiol. Biotechnol.* 62 (5-6) 586-593.

Mazzolani G, Pirozzi F and d'Antoni G (1998) A generalised settling approach in the numerical modeling of sedimentation tanks. *Wat. Sci. Tech.* 38 (3) 95-102.

MC Systems (2007) *Instrument data sheet* [http://www.mcsystems.co.za/; accessed 27/10/2007].

Merck (2007) *Instrument data sheet* [http://www.merck.de/servlet/PB/menu/1001723/index.html; accessed 27/10/2007].

Mines (jr.) RO and Horn CR (2004) Misconceptions about Unstirred SVI. *Proc. of the 2004 World Water and Environmental Resources Congress*, 27 June - 1 July, Salt Lake City, USA.

Moghadam MA, Soheili M and Esfahani MM (2005) Effect of Ionic Strength on Settling of Activated Sludge. *Iranian J. Env. Health Sci. Eng.* 2 (1) 1-5.

Morgan-Sagastume F and Allen DG (2003) Effects of temperature transient conditions on aerobic biological treatment of wastewater. *Wat. Res.* 37 (15) 3590-3601.

Murthy (1998) *Bioflocculation: implications for activated sludge properties and wastewater treatment.* PhD Thesis, Virginia Polytechnic Institute and State University, Blacksburg, USA.

Nakhla G and Lugowski A (2003) Control of filamentous organisms in food-processing wastewater treatment by intermittent aeration and selectors. *J. Chem. Technol. Biotechnol.* 78 420-430.

Námer J and Ganczarczyk JJ (1993) Settling properties of digested sludge particle aggregates. *Wat. Res.* 27 (8) 1285-1294.

Nell JH (1980) A review of the causes and control of filamentous sludge bulking. *Proc. of the Institute of Water Pollution Control (IWPC) conference,* June 2-5, Pretoria, South Africa.

Novak JT, Muller CD and Murthy SN (2001) Floc structure and the role of cations. *Wat. Sci. Tech.* 44 (10) 209-213.

Novák L, Larrea L, Wanner J and Garcia-Heras JL (1993) Non-filamentous activated sludge bulking in a laboratory scale system. *Wat. Res.* 27 (8) 1339-1346.

Ødegaard H (2000) Advanced compact wastewater treatment based on coagulation and moving bed biofilm processes. *Wat. Sci. Tech.* 42 (12) 33-48.

Oldham WK and Rabinowitz B (2002) Development of biological nutrient removal technology in western Canada. *J. Environ. Eng. Sci.* 1 33-43.

Örmeci B and Vesilind PA (2001) Response to comments on "Development of an improved synthetic sludge: a possible surrogate for studying activated sludge dewatering characteristics". Authors' Reply, *Wat. Res.* 35 (5) 1365-1366.

Örmeci B and Vesilind PA (2000) Development of an improved synthetic sludge: a possible surrogate for studying activated sludge dewatering characteristics. *Wat. Res.* 34 (4) 1069-1078.

Osborn DW, Lötter LH, Pitman AR and Nicholls AH (1986) Report to the Water Research Commission on a three year study on the enhancement of biological phosphate removal by altering process feed composition, WRC report no 137/1/86, Pretoria, South Africa.

Otterpohl R and Freund M (1992) Dynamic models for clarifiers of activated sludge plants with dry and wet weather flows. *Wat. Sci. Tech.* 26 (5-6) 1391-1400.

Ozinsky AE and Ekama GA (1995) Secondary settling tank modelling and design Part 2: Linking sludge settleability measures. *Water SA* 21 (4) 333-349.

Parker D, Appleton R, Bratby J and Melcer H (2004) North American performance experience with anoxic and anaerobic selectors for activated sludge bulking. *Wat. Sci. Tech.* 50 (7) 221-228.

Parker DS, Wahlberg EJ and Gerges HZ (2000) Improving secondary clarifier performance and capacity using a structured diagnostic approach. *Wat. Sci. Tech.* 41 (9) 201-208.

Parker D, Butler R, Finger R, Fisher R, Fox W, Kido W, Merrill S, Newman G, Pope R, Slapper J and Wahlberg E (1996) Design and operations experience with flocculator-clarifiers in large plants. *Wat. Sci. Tech.* 33 (12) 163-170.

Patoczka J, Lauria JF, Scheri JJ, Sheehan JF (1998) Stress testing of final clarifier and polymer use for flow maximization. *Proc. of the 71st Annual Conference & Exposition, Water Environment Federation (WEFTEC)*, Orlando, Florida, USA.

Pitman AR (1996) Bulking and foaming in BNR plants in Johannesburg: problems and solutions. *Wat. Sci. Tech.* 34 (3-4) 291-298.

Pitman AR (1991) Design considerations for nutrient removal activated sludge plants. *Wat. Sci. Tech.* 23 (5) 781-790.

Pitman AR (1975) Bioflocculation as Means of Improving the Dewatering Characteristics of Activated Sludges. *Wat. Pollut. Control* 74 (6) 688-700.

Pöpel HJ and Fischer A (1998) Combined influence of temperature and process loading on the effluent concentration of biological treatment. *Wat. Sci. Tech.* 38 (8-9) 129-136.

Pretorius WA (1987) A conceptual basis for microbial selection in biological wastewater treatment. *Wat. Res*. 21 (8) 891-894.

Randall CW, Barnard JL and Stensel HD (1992) *Design and Retrofit of Wastewater Treatment Plants for Biological Nutrient Removal.* In: Eckenfelder WW, Malina JF and Patterson JW (Library Editors), 1st edn., Water Quality Management Library, Vol. 5, Technomic Publishing Company, Lancaster, Pennsylvania, USA.

Rasmussen MR and Larsen T (1997) On-line measurement of settling characteristics in activated sludge. *Wat. Sci. Tech.* 36 (4) 307-312.

Rasmussen H, Bruus JH, Keiding K and Nielsen PH (1993) Observations on dewaterability and physical, chemical and microbiological changes in anaerobically stored activated sludge from a nutrient removal plant. *Wat. Res.* 28 (2) 417-425.

Reardon RD (2005) Clarification concepts for treating peak wet weather wastewater flows. *Proc. of the Annual Conference & Exposition, Water Environment Federation (WEFTEC)*, 4431-4443 http://www.cdm.com/ NR/rdonlyres/ 961C910A-77A0-4B71-A845-B0068B878C55/0Tertiary Clarifier Design Concepts and Considerations.pdf [accessed 21/12/06].

Renko EK (1996) A model for batch settling curve. *Water SA* 22 (4) 339-344.

Royce (1999) *Suspended Solids Analysers and Sensors*. Data Sheet 10/99 TS. Royce Instrument Corporation, New Orleans, USA [http://www.roycetechnologies.com/; accessed 27/10/2007].

Sanin FD (2002) Effect of solution chemistry on the rheological properties of activated sludge. *Water SA* 28 (2) 207-211.

Sarioglu M and Horan N (1996) An equation for the empirical design of anoxic zones used to eliminate rising sludges at nitrifying activated sludge plants. *Wat. Sci. Tech*. 33 (3) 185-194.

Scherfig J, Schleisner L, Brønd S and Kilde N (1996) Dynamic temperature changes in wastewater treatment plants. *Wat. Environ. Res*. 68 (2) 143-151.

Schuler AJ and Jang H (2007a) Density effects on activated sludge zone settling velocities. *Wat. Res*. 41 1814-1822.

Schuler AJ and Jang H (2007b) Microsphere addition for the study of biomass properties and density effects on settleability in biological wastewater treatment systems. *Wat. Res*. 41 2163-2170.

Schutte F (2006) *Handbook for the operation of water treatment works*. Water Research Commission, Research Report TT265/06, Pretoria, South Africa.

Schwartz-Mittelmann A and Galil NI (2000) Biological mechanisms involved in bioflocculation disturbances caused by phenol. *Wat. Sci. Tech*. 42 (1-2) 105-110.

Scuras S, Daigger GT and Grady (jr.) CPL (1998) Modeling the activated sludge floc microenvironment. *Wat. Sci. Tech.* 37 (3) 243-250.

Seka AM, Van de Wiele T and Verstraete W (2001) Feasibility of a multi-component additive for efficient control of activated sludge filamentous bulking. *Wat. Res*. 35 (12) 2995-3003.

Sekine T, Tsugura H, Urushibara S, Furuya N, Fujimoto E and Matsui S (1989) Evaluation of settleability of activated sludge using a sludge settling analyser. *Wat. Res*. 23 (3) 361-367.

Sezgin M (1982) Variation of sludge volume index with activated sludge characteristics. *Wat. Res*. 16 83-88.

Simon J, Wiese J and Steinmetz H (2005) Results of field tests and possible applications for in-situ sludge volume probes. *Proc. 2nd IWA-ICA,* Busan, South Korea.

Smollen M and Ekama GA (1984) Comparison of empirical settling-velocity equations in flux theory for secondary settling tanks. *Water SA* 10 (4) 175-184.

Sötemann SW, Vermande SM, Wentzel MC and Ekama GA (2002) Comparison of the performance of an external nitrification biological nutrient removal activated sludge system with a UCT biological nutrient removal activated sludge system. *Water SA Special Edition: WISA Biennial conference proceedings 2002*. 105-113.

South African Weather Service (2007) *Climate data* [http://www.weathersa. co.za/ Climat /Climstats/; Accessed 25/06/07].

Spicer PT and Pratsinis SE (1996) Shear-induced flocculation: the evolution of floc structure and the shape of the size distribution at steady state. *Wat. Res*. 30 (5) 1049-1056.

Sponza DT (2004) Properties of Four Biological Flocs as Related to Settling. *J. Environ. Eng.* 130 (11) 1289-1300.

Stypka A (1998) *Factors influencing sludge settling parameters and solids flux in the activated sludge process: A literature review. Report No 4*, Royal Institute of Technology, Kungl Teknisa Högskolan, Stockholm, Sweden ISBN 91-7170-363-2. [http://www.lwr.kth.se/Forskningsprojekt/Polishproject/ JPS4.pdf, accessed 20/3/2006].

Sürücü G and Çetin FD (1989) Effect of temperature, pH and DO concentration on the filterability and compressibility of activated sludge. *Wat. Res*. 23 (11) 1389-1395.

Tadesse I, Green FB and Puhakka JA (2004) Seasonal and diurnal variations of temperature, pH and dissolved oxygen in advanced integrated wastewater pond system[®] treating tannery effluent. *Wat. Res*. 38 (3) 645-654.

Taebi-Harandy A and Schroeder ED (2000) Formation of density currents in secondary clarifier. *Wat. Res*. 34 (4) 1225-1232.

Takács I, Patry GG and Nolasco D (1991) A dynamic model of the clarification – thickening process. *Wat. Res*. 25 (10) 1263-1271.

Tandoi V, Jenkins D and Wanner J (2006) *Activated Sludge Separation Problems: Theory, control measures, practical experience*. IWA Scientific and Technical Report No. 16, IWA Publishing, London, England.

Tchobanoglous G, Burton FL and Stensel HD (2003) *Wastewater Engineering: Treatment and Reuse*. 4th edn., Metcalf and Eddy Inc., McGraw-Hill, New York, USA.

Testo (2007) *Instrument data sheet* [http://www.testo.co.uk; accessed 27/10/2007].

Urbain V, Block JC and Manem J (1993) Bioflocculation in activated sludge: an analytical approach. *Wat. Res*. 27 (5) 829-838.

Vanderhasselt A and Vanrolleghem (2000) Estimation of sludge sedimentation parameters from single batch settling curves. *Wat. Res*. 34 (2) 395-406.

Vanderhasselt A and Verstraete W (1999) Short-term effects of additives on sludge sedimentation characteristics. *Wat. Res*. 33 (2) 381-390.

Vanderhasselt A, De Clercq B, Vanderhaegen B, Vanrolleghem P and Verstraete W (1999a) On-line control of polymer addition to prevent massive sludge washout. *J. Envir. Engrg.* 125 1014-1021.

Vanderhasselt A, Aspegren H, Vanrolleghem P and Verstraete W (1999b) Settling characterisation using on-line sensors at a full-scale wastewater treatment plant. *Water SA* 25 (4) 453-458.

Van Der Walt JJ (1998) Is a sedimentation tank really that simple? *Proc. of the Water Institute of South Africa (WISA) Biennial Conference & Exhibition*, May 4-7, Cape Town, South Africa.

Van Haandel (1992) Activated sludge settling Part II: Settling theory and application to design and optimisation. *Water SA* 18 (3) 173-180.

Van Huyssteen JA, Barnard JL and Hendriksz J (1990) The Olifantsfontein nutrient removal plant. *Wat. Sci. Tech.* 22 (7/8) 1-8.

Van Leeuwen J and Pretorius WA (1988) Sludge Bulking Control with Ozone. *J. Inst. Wat. and Env. Mngmnt.* 2 (2) 223-227.

Van Niekerk AM, Jenkins D and Richard MG (1987) The competitive growth of zoogloea ramigera and type 021N in activated sludge and pure culture – a model for low F/M bulking. *Proc. of the biennial conference and exhibition, Institute of Water Pollution Control (IWPC)*, May 12-15, Port Elizabeth, South Africa.

Vanrolleghem PA, Clercq BD, Clercq JD, Devisscher M, Kinnear DJ and Nopens I (2006) New measurement techniques for secondary settlers: a review. *Wat. Sci. Tech.* 53 (4-5) 419-429.

Vanrolleghem PA, Insel G, Petersen B, Sin G, De Pauw D, Nopens I, Dovermann H, Weijers S and Gernaey K (2003) A comprehensive model calibration procedure for activated sludge models. *Proc. Weftec 2003*.

Vanrolleghem PA and Lee DS (2003) On-line monitoring equipment for wastewater treatment processes: state of the art. *Wat. Sci. Tech.* 47 (2) 1-34.

Vanrolleghem PA, Van der Schueren D, Krikilion G, Grijspeerdt K, Willems P and Verstraete W (1996) On-line quantification of settling properties with in-sensor experiments in an automated settlometer. *Wat. Sci. Tech.* 33 (1) 37-51.

Wahlberg EJ (2004) *Activated sludge process optimisation*. United States Patent 6811706. [http://www.freepatentsonline.com/6811706.html, accessed 18/12/06].

Wahlberg EJ, Crowley JP, Bower J, Bittner M and Margolis Z (1996) Why the Activated Sludge Process Is So Hard to Operate: Modeling Brings New Light to Operations. *Proc. of the 69th Annual Conference & Exposition, Water Environment Federation (WEFTEC)*, October 5-9, Dallas, Texas, USA.

Wanner J, Kucman K and Grau P (1988) Activated sludge process combined with biofilm cultivation. *Wat. Res.* 22 (2) 207-215.

Weast RC (1985) *CRC Handbook of Physics and Chemistry*, 65th edn., CRC Press. Inc., Florida, USA.

Wells SA, Bashkatov D and Makinia J (2005) Modeling and evaluating temperature dynamics in wastewater treatment plants. *Proc. of the ASCE EWRI World Water and Environmental Resource congress*. May 15-19, Anchorage, Alaska.

Wentzel MC, Ekama GA, Dold PL, Loewenthal RE and Marais GvR (1988) *Final report to the Water Research Commission on a four year contract on research into biological excess phosphorus removal (1984-1987),* UCT report W60, Cape Town, South Africa.

Werker AG (2006) An evaluation of full-scale activated sludge dynamics using microbial fatty acid analysis. *Wat. Sci. Tech.* 54 (1) 11-19.

White MJD (1976) Design and Control of Secondary Settlement Tanks. *Wat. Pollut. Control* 75 (4) 459-467.

Wilén BM, Onuki M, Hermansson M, Lumley D and Mino T (2006) Influence of flocculation and settling properties of activated sludge in relation to secondary settler performance. *Wat. Sci. Tech.* 54 (1) 147-155.

Wilén BM, Keiding K and Nielsen PH (2000) Anaerobic deflocculation and aerobic reflocculation of activated sludge. *Wat. Res.* 34 (16) 3933-3942.

Wilén BM (1999) *Properties of Activated Sludge Flocs*. PhD Thesis, Dissertation No 15, Department of Sanitary Engineering, Chalmers University of Technology, Göteborg, Sweden.

Wilén BM and Balmér P (1999) The effect of dissolved oxygen concentration on the structure, size and size distribution of activated sludge flocs. *Wat. Res.* 33 (2) 391-400.

Wünsch B, Heine W and Neis U (2002) *Combating bulking sludge with ultrasound.* 1st edn., Neis U (ed.), Ultrasound in Environmental Engineering II, TU Hamburg, Germany.

WRC (1984) *Theory, design and operation of nutrient removal activated sludge processes.* Water Research Commission, Pretoria, South Africa.

YSI (2007) *Instrument data sheet* [https://www.ysi.com/; accessed 27/10/2007].

Yuan Y (2001) *Hydrodynamic Behaviour of Biological Aggregates: Settling and Coagulation with Small Particles.* MPhil Thesis, Publication no. 75244, Hong Kong University, Hong Kong. [www.hku.hk/rss/rs2001 /rpg_14100_gen; accessed 26/6/2003].

Zhang D, Li Z, Lu P, Zhang T and Xu D (2006a) A method for characterizing the complete settling process of activated sludge. *Wat. Res.* 40 (14) 2637-2644.

Zhang S, Yang F, Liu Y, Zhang X, Yamada Y and Furukawa K (2006b) Performance of a metallic membrane bioreactor treating simulated distillery wastewater at temperatures of 30 to 45°C. *Desalination* 194 146-155.

11 APPENDICES

The following list is a summary of information provided in Appendix A to Appendix H:

11.1 Appendix A: T_r measurements: surface and bubble aeration plant data

Table 11-1 Long-term T_r variation data

WCW 1

Module 1: surface turbine aeration			
05 July 2006	Temp @ 08h30	Temp @ 09h45	Temp @ 13h00
Stage 1 North	12.5	12.9	13.4
Stage 1 South	12.6	12.9	13.4
Stage 2 North	11.5	11.6	12.1
Stage 2 South	11.9	11.8	12
average	12.1	12.3	12.7

Module 2: submerged diffuser bubble aeration			
05 July 2006	Temp @ 08h30	Temp @ 09h45	Temp @ 13h00
North DO 1	17.7	17.8	18
South DO 2	17.7	17.8	18
North DO 3	17.6	17.7	17.9
South DO 4	17.8	18.0	18.3
North DO 5	17.6	17.7	18
South DO 6	17.7	17.7	17.9
average	17.7	17.8	18.0

Module 3: submerged diffuser bubble aeration			
05 July 2006	Temp @ 08h30	Temp @ 09h45	Temp @ 13h00
North DO 1	17.5	17.6	17.8
South DO 2	17.9	18.0	18.2
North DO 3	17.8	17.8	18
South DO 4	17.6	17.7	17.9
North DO 5	17.8	17.9	18.2
South DO 6	17.6	17.7	17.9
average	17.7	17.8	18.0

Module 1: surface turbine aeration			
28 October 2006	Temp @ 08h30		Temp @ 12h00
Stage 1 North			
Stage 1 South			
Stage 2 North	20.6		20.5
Stage 2 South	20.5		20.5
average	20.6		20.5

Module 2: submerged diffuser bubble aeration			
28 October 2006	Temp @ 08h30		Temp @ 12h00
North DO 1	22.8		23
South DO 2	22.6		22.8
North DO 3	22.8		23
South DO 4	23.1		23.4
North DO 5	23.4		23.6
South DO 6	23		23.1
average	23.0		23.2

Module 3: submerged diffuser bubble aeration			
28 October 2006	Temp @ 08h30		Temp @ 12h00
North DO 1	22.3		22.5
South DO 2	22.5		22.7
North DO 3	22.6		22.9
South DO 4	23		23.3
North DO 5	22.5		22.8
South DO 6	22.5		22.7
average	22.6		22.8

WCW 2

Module 1: surface turbine aeration		
26 June 2006	Temp @ 08h00	Temp @ 17:20
leg 1 DO1	14.4	15.2
leg 2 DO2	14.2	
Aerator out	14.1	
RAS return	14.2	
Clarifier 1 out	14.2	
Clarifier 2 out	14.1	
average leg 12	14.3	15.2

Module 2: surface turbine aeration		
26 June 2006	Temp @ 08h00	Temp @ 17:20
leg 1 DO1	14.2	14.7
leg 2 DO2	13.8	
Aerator out	13.9	
RAS return	13.9	
Clarifier 1 out	13.8	
Clarifier 2 out	13.8	
average leg 12	14	14.7

Pilot Plant: submerged diffuser aeration		
26 June 2006	Temp @ 08:00	Temp @ 17:20
Aerobic 6	9.7	16.6
Ambient	0.3	14.3

Module 1: surface turbine aeration		
27 October 2006	Temp @ 09h00	Temp @ 13:15
leg 1 DO1	21.7	22
leg 2 DO2	21.4	21.8
Aerator out		
RAS return		
Clarifier 1 out		
Clarifier 2 out		
average leg 12	21.6	21.9

Module 2: surface turbine aeration		
27 October 2006	Temp @ 09h00	Temp @ 13:15
leg 1 DO1	21.8	22.2
leg 2 DO2	21.5	21.9
Aerator out		
RAS return		
Clarifier 1 out		
Clarifier 2 out		
average leg 12	21.7	22.1

Remark:

WCW1 = plant 2

WCW2 = plant 1

WCW1a = plant 2 module 1

WCW1b = plant 2 module 2 and 3

WCW2a = plant 1 module 1 and 2

WCW2b = only on-line T_r data

WCW2c = plant 1 pilot

11.2 Appendix B: Raw sewage plant inflow diurnal temperature variation
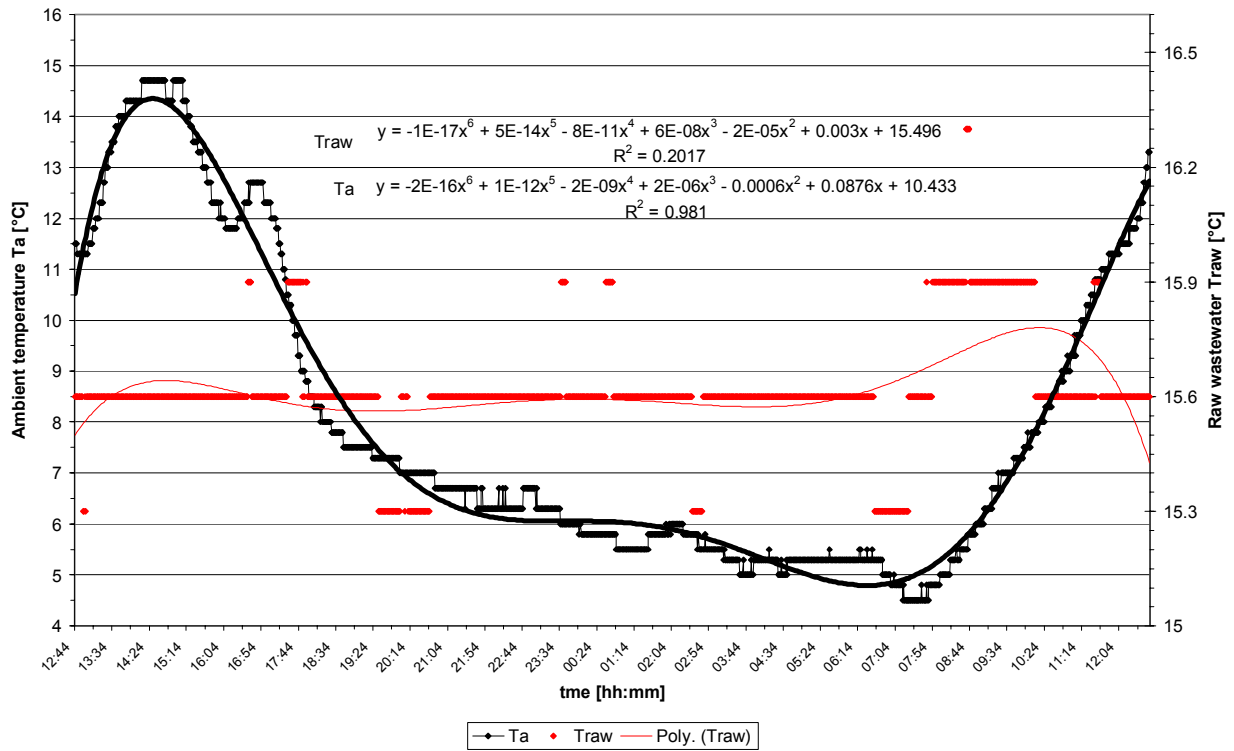
Figure 11-1 T_{raw} and T_a data points and diurnal profiles

11.3 Appendix C: MLSS concentration meter reading T_s-based variations

Table 11-2 Test data: MLSS concentration meter reading variation with T_s

exp15-1-7a	time	T	MLSS	T Ambient
	13:53	23.5	6.17	22.1
	14:10	28.2	6.10	
	14:17	30.1	6.13	
	14:20	31.00	6.14	
	14:25	32.00	6.05	
	14:40	30.4	6.23	
	14:54	27.5	6.22	

exp15-1-7b	time	T	MLSS
	13:53	23.8	4.66
	14:10	27.5	4.66
	14:17	27.4	4.58
	14:20	27.6	4.59
	14:25	27.7	4.60
	14:40	25.3	4.61
	14:54	23.1	4.70

$y = -0.0082x + 6.3867$
$R^2 = 0.1351$

$y = -0.0109x + 5.0682$
$R^2 = 0.5506$
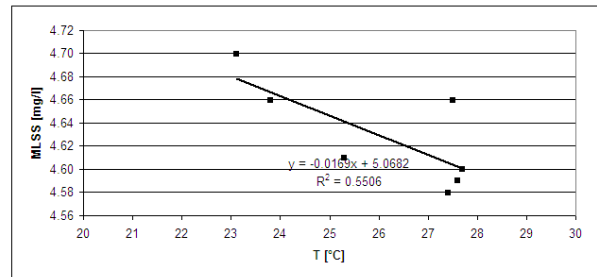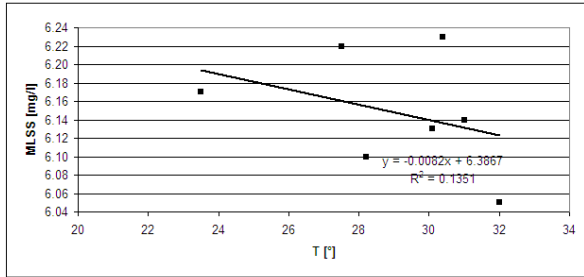
exp4-1-7	time	T	MLSS
	13:53	19.8	4.66
	14:13	30.5	4.62
	14:13	16.5	4.69
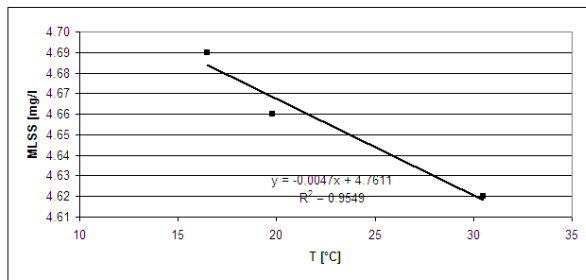
exp8-1-7a	time	T	MLSS
	14:00	23.1	7.33
		18.1	7.42
		33.8	7.20
		23.4	7.35

$y = -0.0047x + 4.7611$
$R^2 = 0.9549$

$y = -0.0138x + 7.665$
$R^2 = 0.9862$
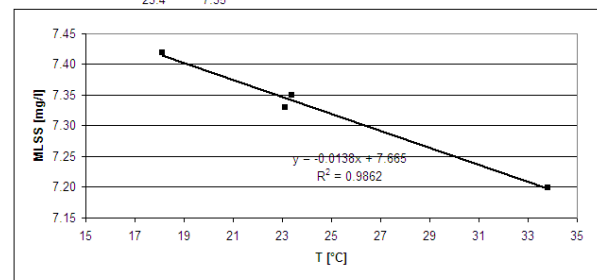
exp11-1-7	time	T	MLSS	T Ambient
	15:05	23.8	6.80	25.2
		24.3	6.62	
		19.1	6.81	
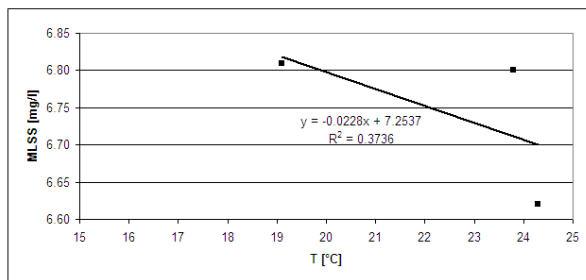
exp8-1-7b	time	T	MLSS
	14:00	23.2	4.97
		17.2	5.04
		33.5	4.80
		23.5	4.9

$y = -0.0228x + 7.2537$
$R^2 = 0.3736$

$y = -0.0146x + 5.2826$
$R^2 = 0.9251$
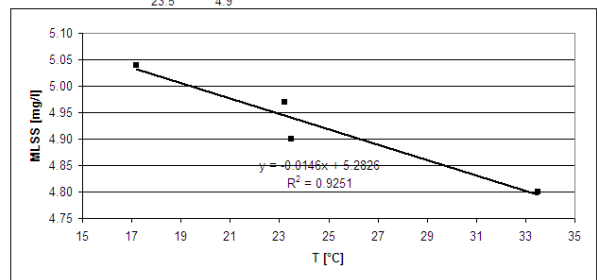
	temperature 1	temperature 2	MLSS 1	MLSS 2	change in MLSS
exp15-1-7a	15	25	6.26	6.18	-0.08 g/l
exp15-1-7b	15	25	4.81	4.65	-0.17 g/l
exp4-1-7	15	25	4.69	4.64	-0.05 g/l
exp8-1-7a	15	25	7.46	7.32	-0.14 g/l
exp11-1-7	15	25	6.91	6.68	-0.23 g/l
exp8-1-7b	15	25	5.06	4.92	-0.15 g/l
					-0.14 g/l over 10°C
					-0.014 g/l over 1°C
					-14 mg/l over 1°C

11.4 Appendix D: Batch MLSS settling data

Table 11-3 Summary of experimental batch settling test reactor zone conditions and results

Parameter	Statistics	Anaerobic	Anoxic	Aerobic 1	Aerobic 2	Aerobic 3	Aerobic 4
DO [mg/ℓ]	Average	0.09	0.07	2.34	2.90	1.91	2.94
	St. dev.	002	0.01	0.54	0.51	0.48	0.31
	n	29	29	29	29	29	29
T [℃]	Average	17.9	17.9	18.9	18.8	18.1	17.8
	St. dev.	1.2	1.3	1.3	1.2	1.3	1.3
	n	29	29	29	29	29	29
MLSS [mg/ℓ]	Average	3536	3531	3440	3415	3399	3382
	St. dev.	300	263	285	262	258	273
	n	35	35	35	35	35	35
SVI [mℓ/g]	Average	121	123	105	98	104	101
	St. dev.	31	30	12	9	12	11
	n	34	34	34	34	34	34
ISV [m/hr]	Average	2.1	1.9	1.8	2.1	2.0	2.1
	St. dev.	0.6	0.5	0.5	0.6	0.6	0.5
	n	34	34	34	34	34	34
Turb [FNU]	Average	140	98	60	44	31	30
	St. dev.	24	21	15	11	11	9
	n	34	34	34	34	34	34

Table 11-4 Batch MLSS settling sample extended cooling and heating

Temperature change	Position	T [°C] at 0 minutes	T [°C] at 30 minutes	SVI [mℓ/g]	SVI increase [mℓ/g/1°C]	ISV [m/hr]	ISV decrease [m/hr/1°C]	Turbidity [FNU]	Turbidity increase [FNU/1°C]
Cooled	Sun	8.6	16.1	131	-	0.53	-	15	-
Cooled	Shade	6.4	10.8	164	-6.2	0.04	0.09	7	1.5
Heated	Sun	29.0	27.3	106	-	1.76	-	33	-
Heated	Shade	25.5	25.3	106	0	1.76	0	21	6.0

Table 11-5 Batch settling test results data, with temperature and container size variation

Container	Condition & Temperature	SVI 19/6	SVI 21/6	SVI 19/7	SVI Ave	u 19/6	u 21/6	u 19/7	u Ave	Tur 19/6	Tur 21/6	Tur 19/7	Tur Ave
	MLSS [mg/ℓ]	4210	3930	4470	4203	4210	3930	4470	4203	4210	3930	4470	4203
1ℓ	Shade	181	170	172	174	0.00	0.09	0.04	0.04	14	19	9	14
	T30 [°C]	17.0	19.5	20.9	19.1	17.0	19.5	20.9	19.1	17.0	19.5	20.9	19.1
1ℓ	Sun	105	104	116	108	0.92	1.06	0.11	0.70	20	23	14	19
	T 30 [°C]	21.5	23.8	25.2	23.5	21.5	23.8	25.2	23.5	21.5	23.8	25.2	23.5
2ℓ	Shade	195	137	181	171	0.31	0.88	0.13	0.44	14	-	14	14
	T 30 [°C]	17.0	19.5	20.7	19.1	17.0	19.5	20.7	19.1	17.0	-	20.7	19.1
2ℓ	Cool, shade	-	164	-	164	-	0.04	-	0.04	-	7	-	7
	T 30 [°C]	-	10.8	-	10.8	-	10.8	-	10.8	-	10.8	-	10.8
2ℓ	Cool, sun	-	131	-	131	-	0.53	-	0.53	-	15	-	15
	T 30 [°C]	-	16.1	-	16.1	-	16.1	-	16.1	-	16.1	-	16.1
2ℓ	Heat, shade	-	106	-	106	-	1.76	-	1.76	-	21	-	21
	T 30 [°C]	-	25.3	-	25.3	-	25.3	-	25.3	-	25.3	-	25.3
2ℓ	Heat, sun	-	106	-	106	-	1.76	-	0.76	-	33	-	33
	T 30 [°C]	-	27.3	-	27.3	-	27.3	-	27.3	-	27.3	-	27.3
2ℓ	Dilute, shade	-	122	-	122	-	1.89	-	1.89	-	21	-	21
	T 30 [°C]	-	19.1	-	19.1	-	19.1	-	19.1	-	19.1	-	19.1
2ℓ	Dilute, sun	-	102	-	102	-	2.73	-	2.73	-	23	-	23
	T 30 [°C]	-	23.2	-	23.2	-	23.2	-	23.2	-	23.2	-	23.2
2ℓ	Sun	109	106	119	111	0.62	1.50	0.40	0.84	15	21	23	21
	T 30 [°C]	20.9	23.6	25.1	23.2	20.9	23.6	25.1	23.2	20.9	23.6	25.1	23.2
20ℓ	Sun	112	-	139	126	0.97	-	0.31	0.64	18	-	11	15
	T 30 [°C]	19.0	-	22.2	20.6	19.0	-	22.2	20.6	19.0	-	22.2	20.6

11.4.1 SVI variation
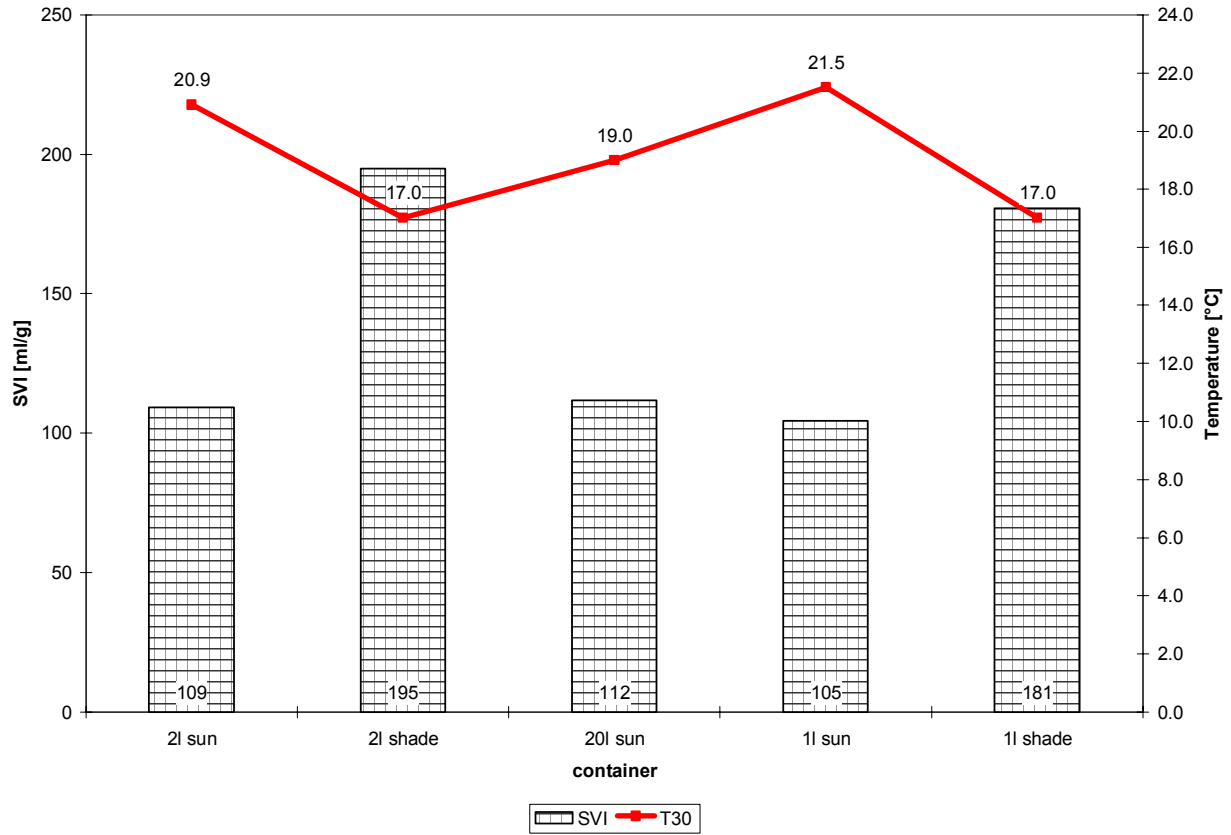
Figure 11-2 SVI, different containers, T_s after 30 min., MLSS 4210 mg/ℓ
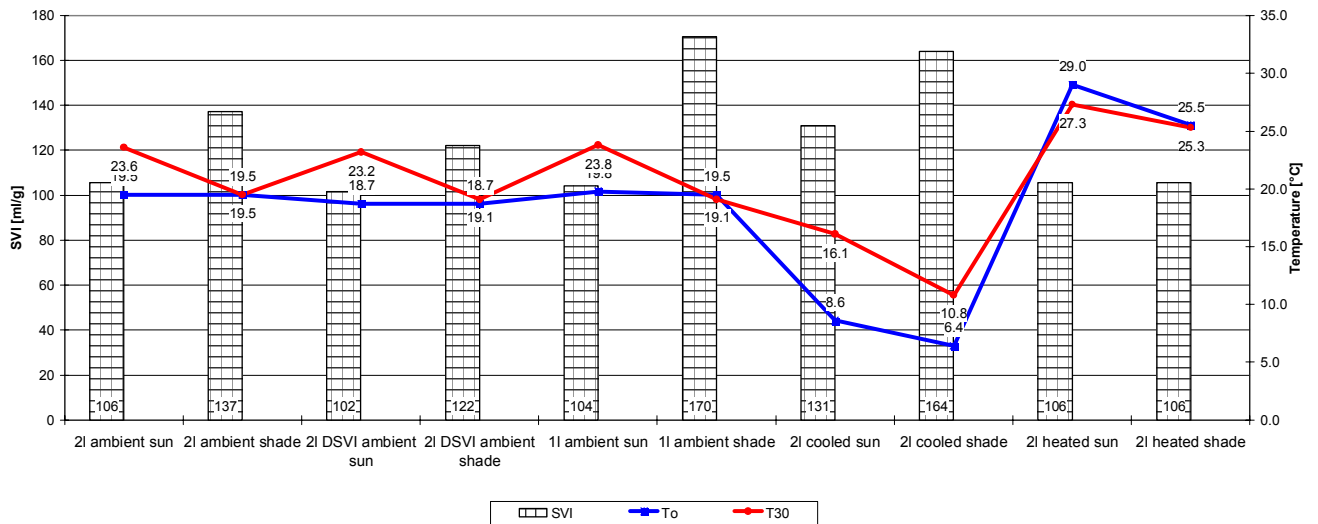
Figure 11-3 SVI, different containers, T_s after 0 and 30 min., MLSS 3930 mg/ℓ
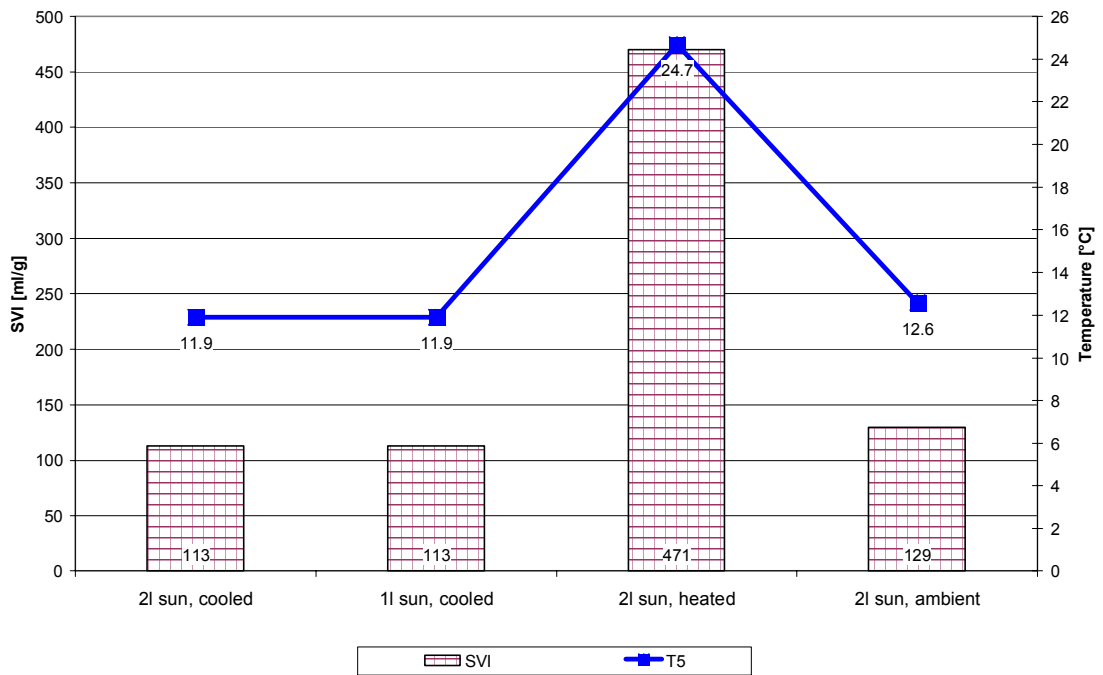
Figure 11-4 SVI, different containers, T_s after 5 min., MLSS 4250 mg/ℓ
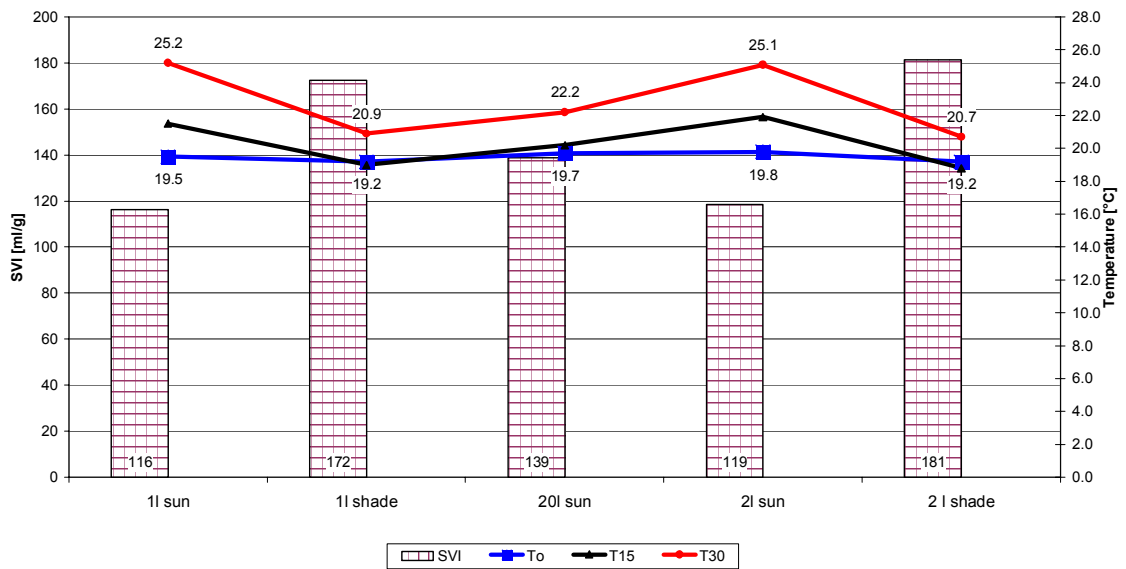
Figure 11-5 SVI, different containers, T_s after 0, 15 and 30 min., MLSS 4470 mg/ℓ

11.4.2 Zone settling velocity variation
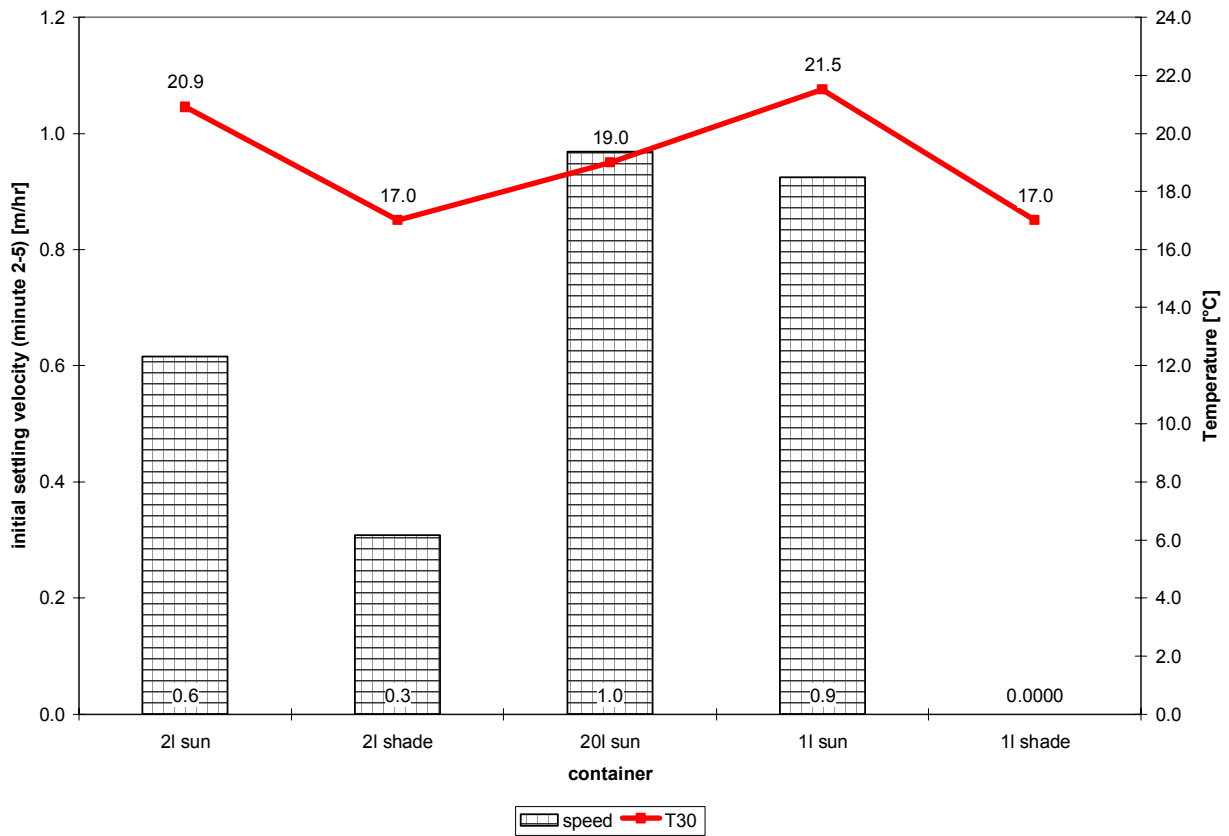
Figure 11-6 Initial settling velocity, T_s after 30 min., MLSS 4210 mg/ℓ
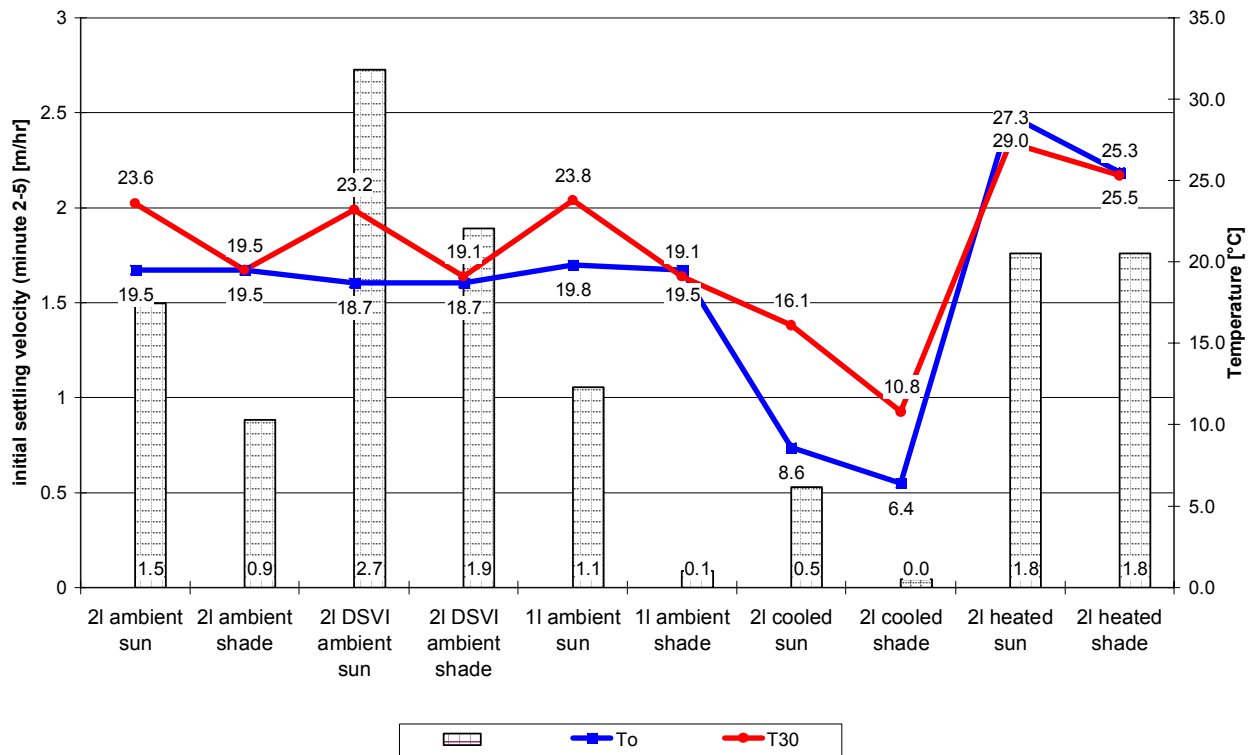
Figure 11-7 ISV, T_s after 0 and 30 min., MLSS 3930 mg/ℓ
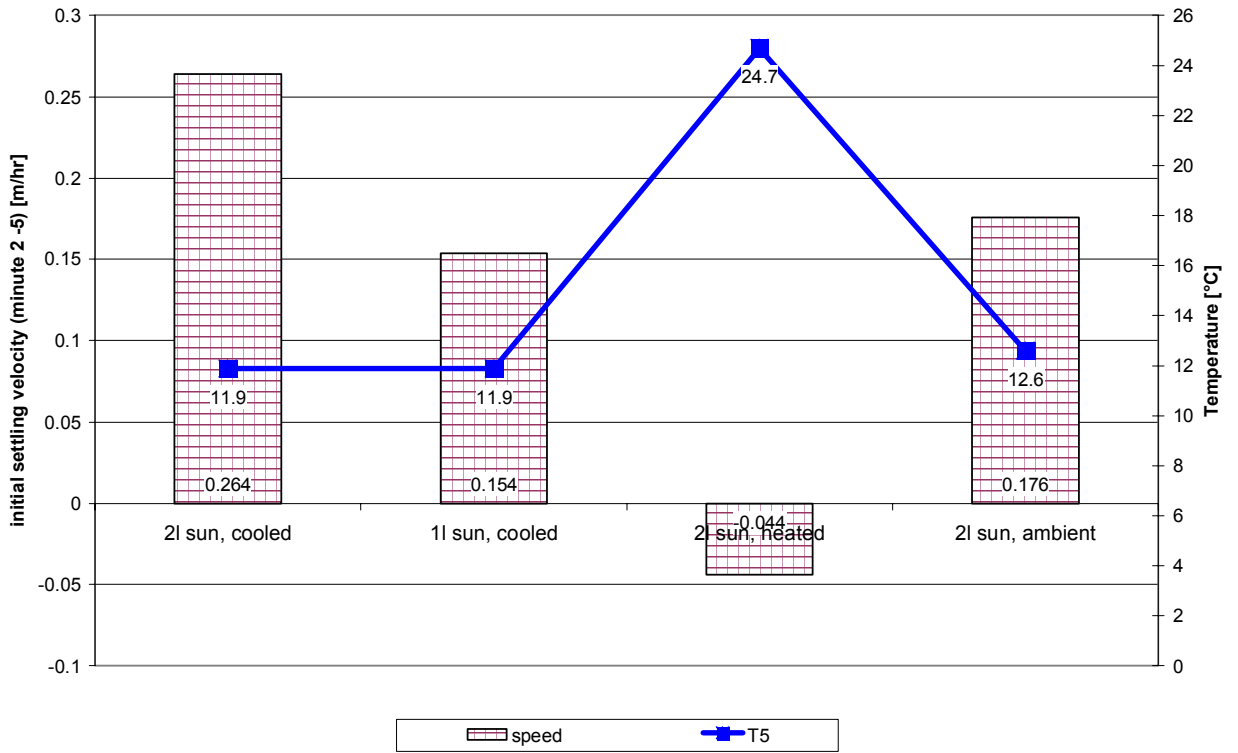
Figure 11-8 ISV, T_s after 5 min., MLSS 4250 mg/ℓ
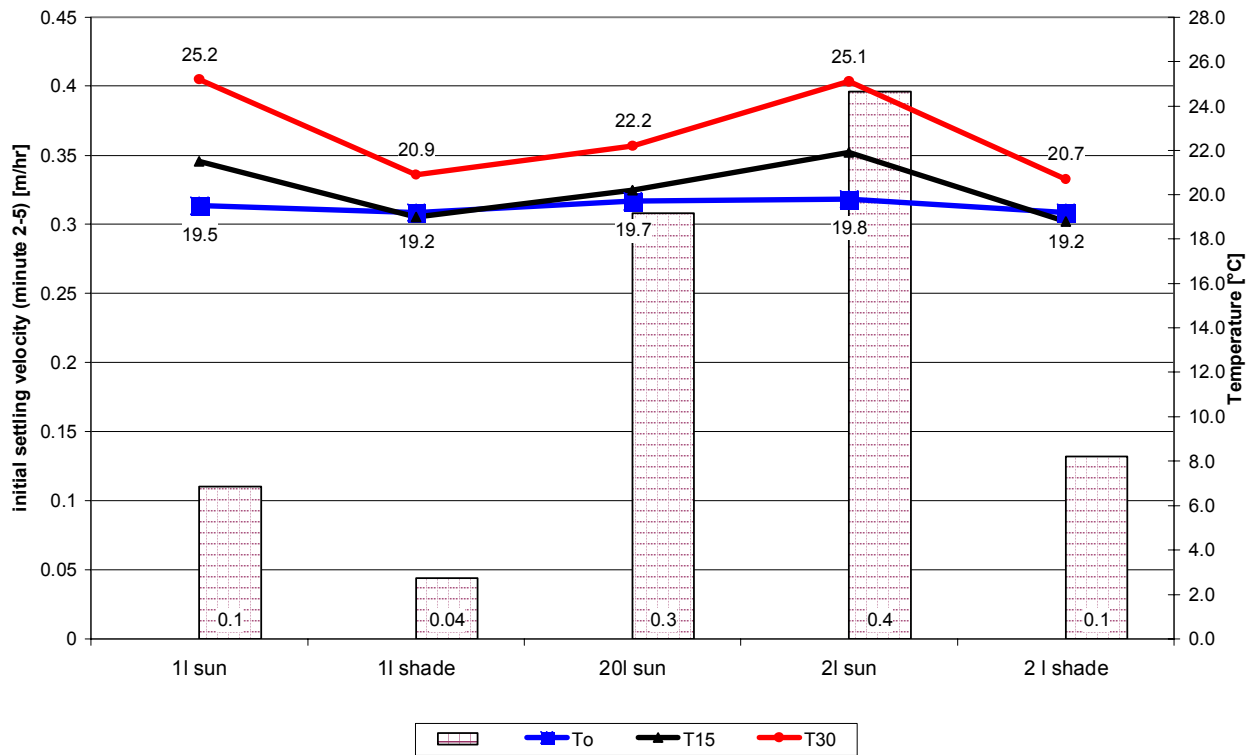
Figure 11-9 ISV, T_s after 0, 15 and 30 min., MLSS 4470 mg/ℓ

11.4.3 Turbidity variation
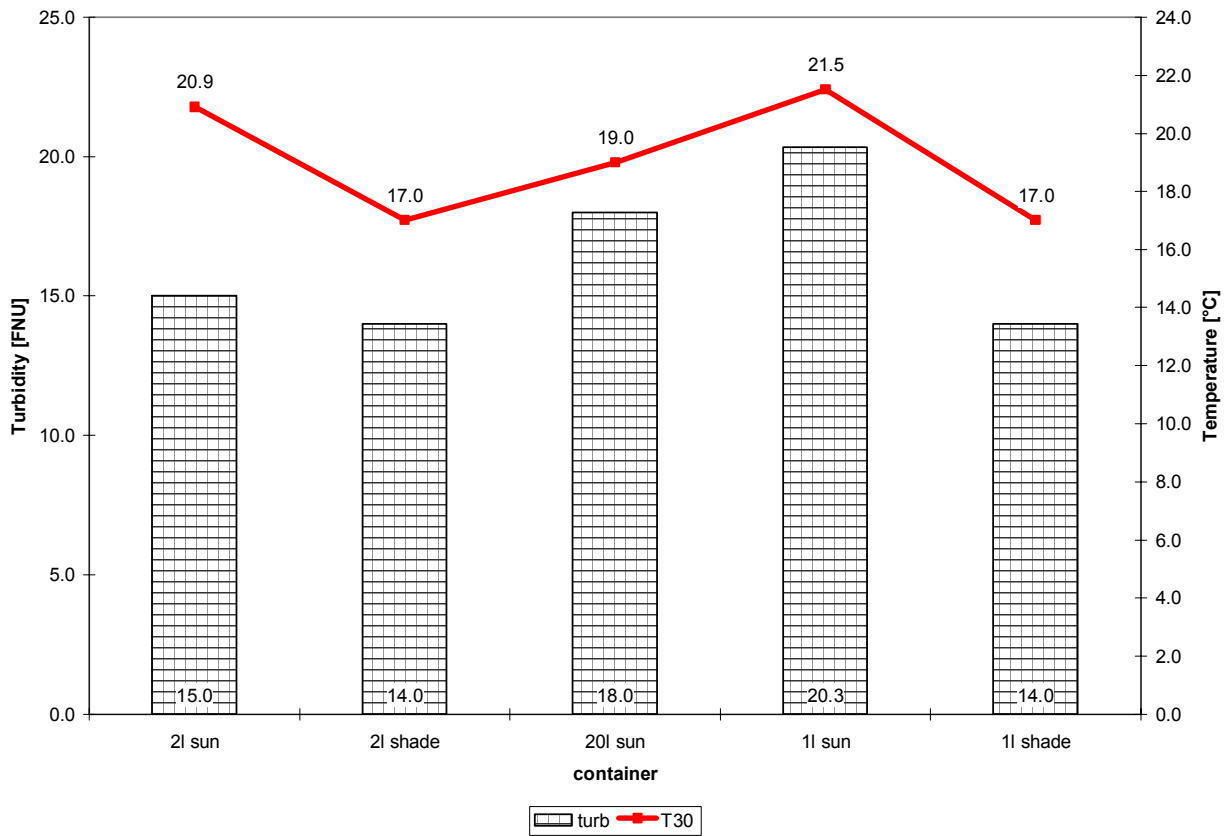
Figure 11-10 Turbidity, 30 min. settling, T_s after 30 min., MLSS 4210 mg/ℓ
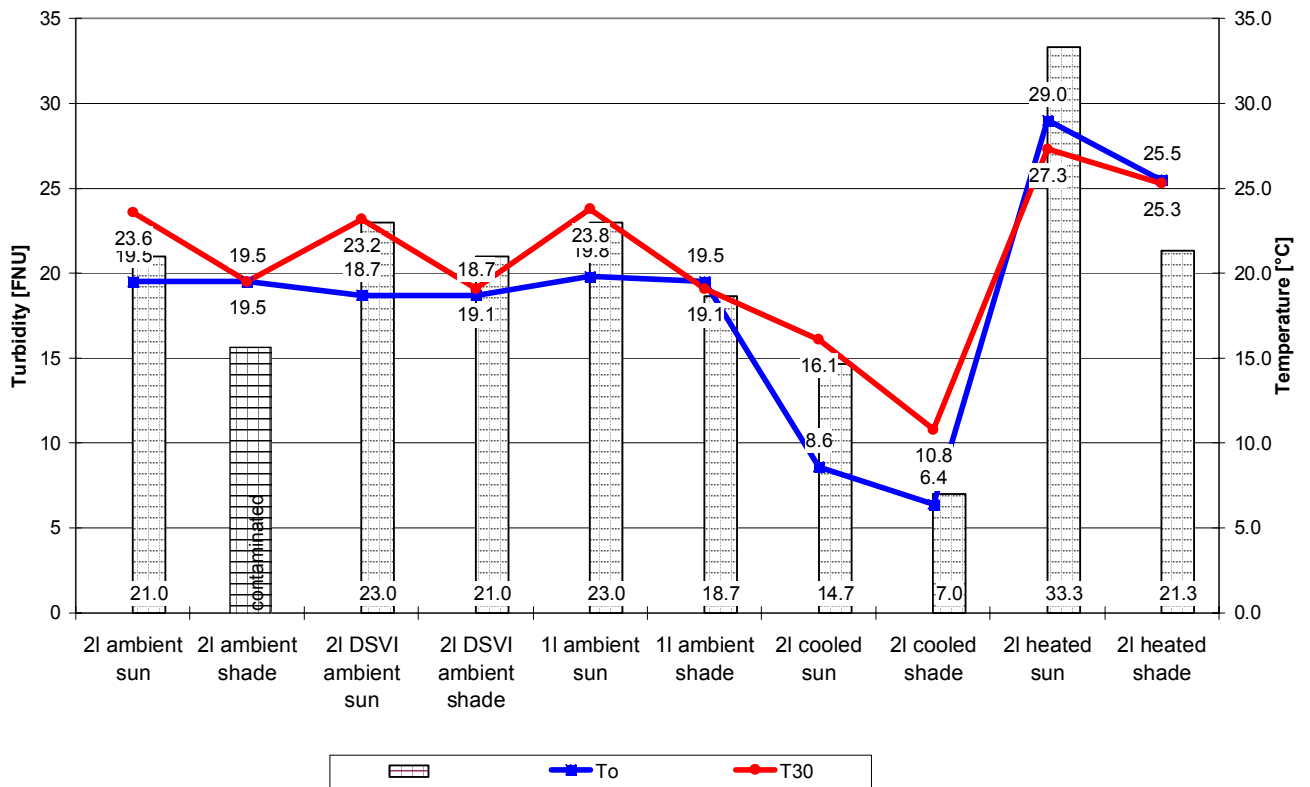
Figure 11-11 Turbidity, 30 min. settling, T_s after 0 and 30 min, MLSS 3930 mg/ℓ
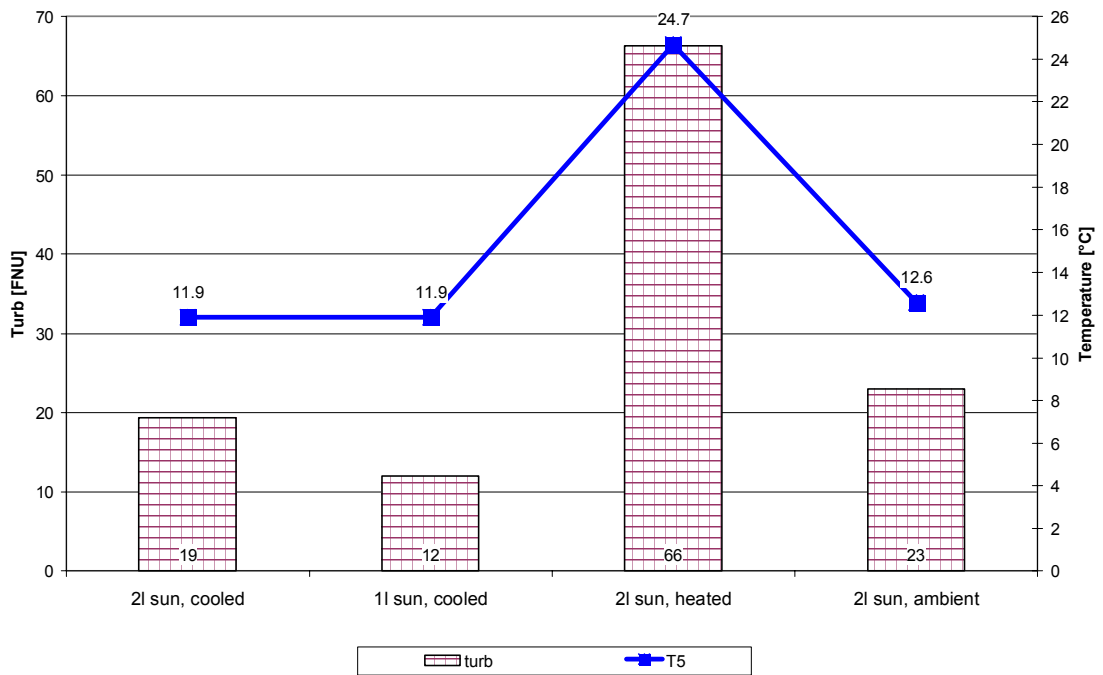
Figure 11-12 Turbidity, 30 min. settling, T_s after 5 min., MLSS 4250 mg/ℓ
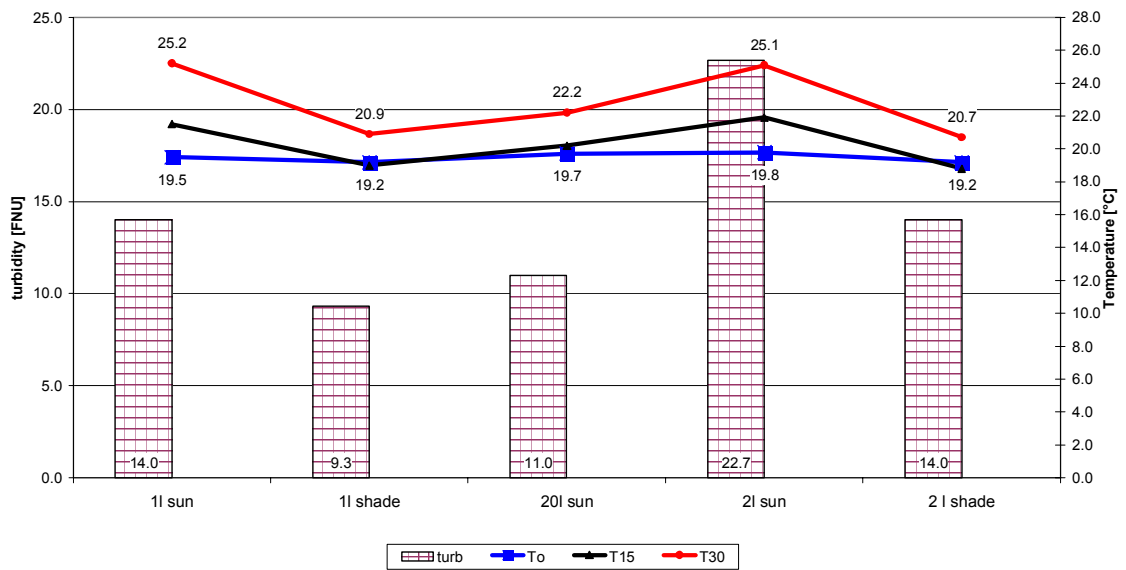
Figure 11-13 Turbidity, 30 min. settling, T_s after 0, 15 and 30 min., MLSS 4470 mg/ℓ

11.5 Appendix E: On-line meter data

An example of a typical Excel spreadsheet diagram with an original 12-hour profile of h and T_a logger data is provided in Figure 11-14. The T_a profile varies from about 5 to 25°C, whereas the 30-minute MLSS settling profiles final h value varies from about 359 mm to 210 mm. The period between each moving settling profile indicates the meter cleaning and standby cycle.

Figure 11-14 Consecutive 30-minute settling profiles from MLSS settling meter data, h and T_a readings over 12 hours

Table 11-6 Summary of on-line experimental data

Parameter	MLSS Concentration	u1	u2	u3	u4	u5	u6	T_r	T_a	h	SV_{30}	SVI	u_ave	u_max	t_umax
	[mg/ℓ]	[m/hr]	[m/hr]	[m/hr]	[m/hr]	[m/hr]	[m/hr]	[°C]	[°C]	[mm]	[mℓ/ℓ]	[mℓ/g]	[m/hr]	[m/hr]	[min.]
Average	4700	0.1	0.3	0.2	0.2	0.2	0.1	18.3	23.6	259	717	151	0.2	0.8	16.2
St. dev.	129	0.2	0.4	0.2	0.1	0.1	0.1	0.5	5.3	68	190	37	0.1	0.5	9.8
n	559	83	83	83	83	83	83	83	83	83	83	83	83	83	83

Figure 11-15 Two-day T_a and T_r profiles

Figure 11-16 Two-day T_r and MLSS concentration profiles
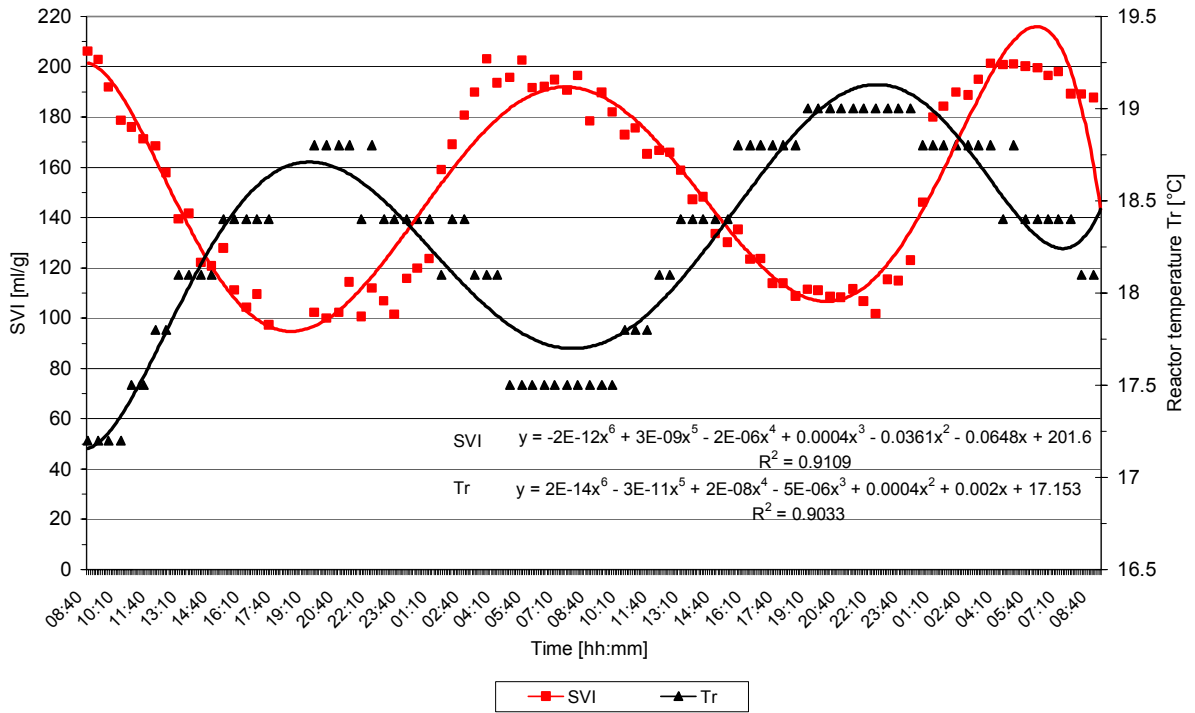
Figure 11-17 Two-day SVI and T_r profiles
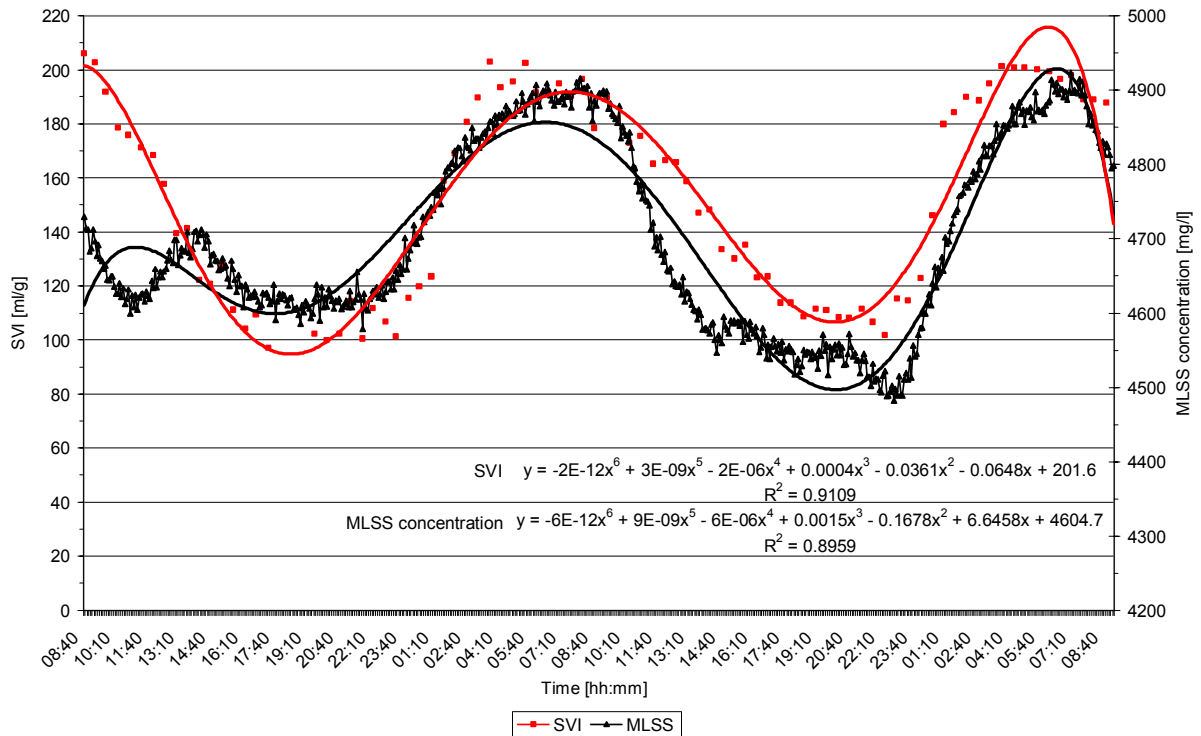
Figure 11-18 Two-day SVI and MLSS concentration profiles

11.6 Appendix F: Photograph of MLSS settling meter
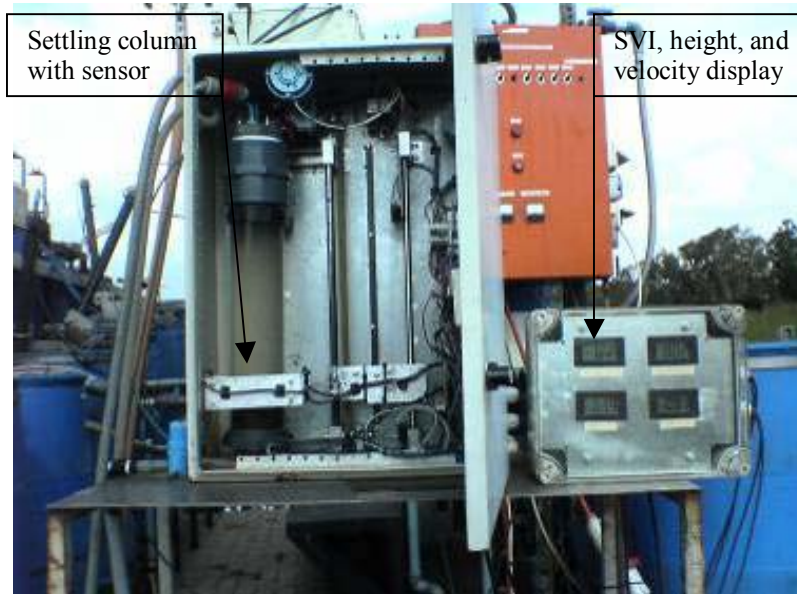
Photograph 1 MLSS settling meter and output display

11.7 Appendix G: Settleability factors summary

11.7.1 Biofloc composition and structure

Table 11-7 Biofloc composition and structural properties affecting settling aspects

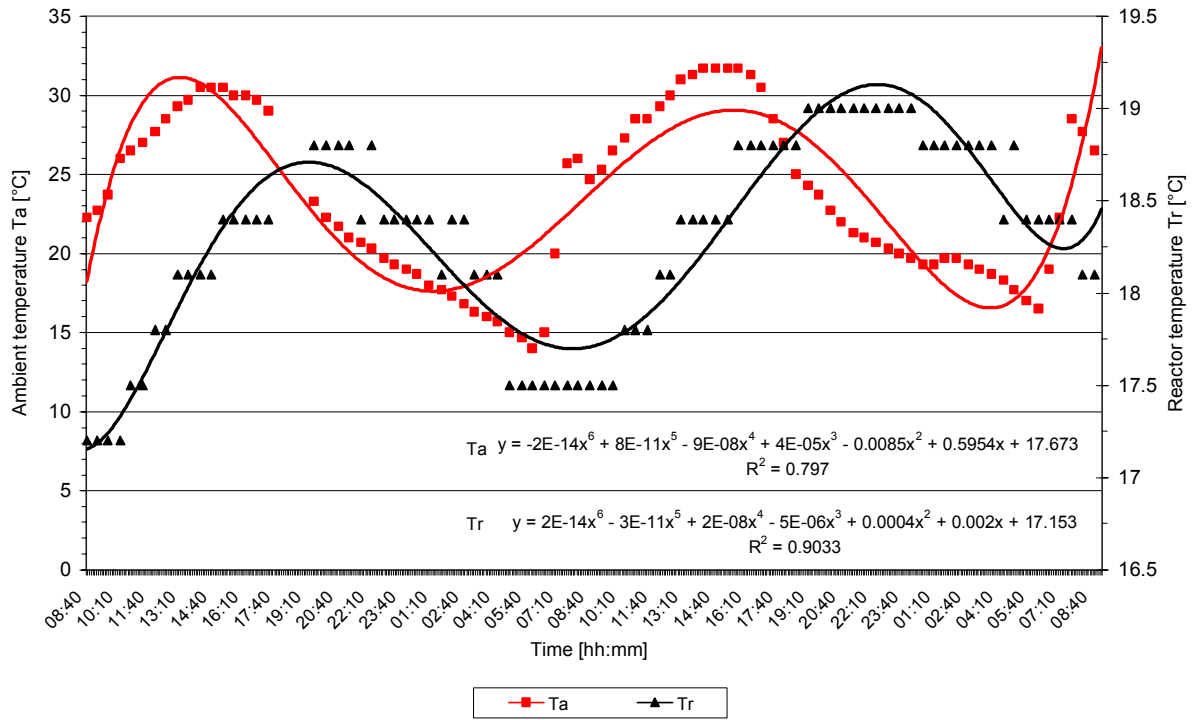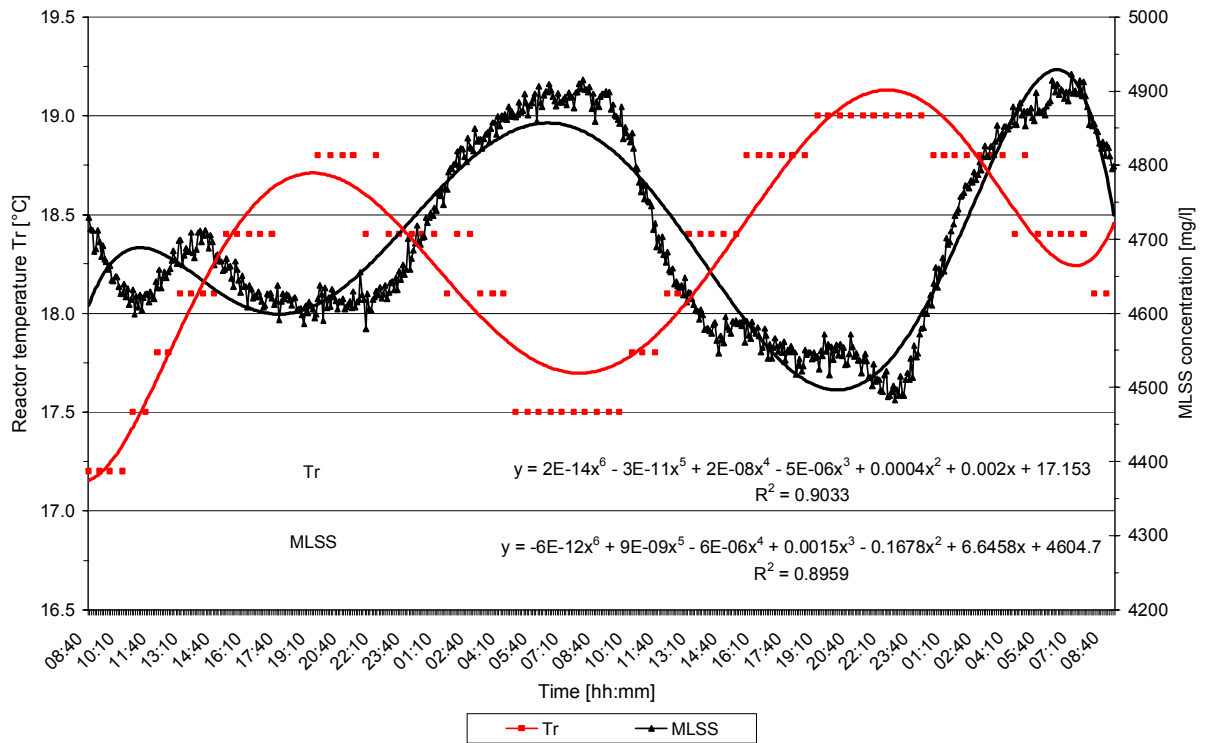| Parameter	Improve settling	Worsen settling	Impact description	Typical range	Reference
Density	Higher density with specific gravity (SG) of floc up to 1.06	Lower density with SG of floc up to 1.02	Heavier particles settle and compact faster	1.020	Bień *et al.*, 2005; Murthy 1998; Andreadakis, 1993;
ECP	More ECP (up to 15%) protects biofloc	Less ECP	ECP Layer decrease surface roughness, provides protective coat to flocs	N/A	Liss *et al.*, 2002; Frolund et al., 1996;
Growth stage	End of log growth phase, start endogenous	Log growth or end of endogenous	Non-settleable at start, dispersed at end	N/A	Kolmentz, 2003;
Organism type	Floc former: filament ratio balance; higher organisms: swimming or crawling, such as protozoans and rotifers	Microorganism imbalance: filaments dominate over floc formers	Filaments dominance prevent settling (leads to bulking), Bridging between flocs, Floc formers suppressed, Filaments prevent downward sludge and upward water movement Higher organisms feed on dispersed flocs and free bacteria	3-5 filaments per floc-former	Martins *et al.*, 2003; Forster and Dallas-Newton, 1980; Blackbeard *et al.*, 1986; Bux and Kasan (1994a);
Polyphosphate	Higher P increases settling velocity	N/A	Cells store polyphosphate, P increases biofloc density	N/A	De Clercq, 2003;
Porosity	Low porosity or high porosity	High porosity	Low porosity biofloc has higher density and is firm and compact and improves settling, but high porosity can also improve settling velocity of aggregate, as water can rise through settling blanket flocs Larger size more porous, and resulting lower density Low DO cause filaments and irregular shaped porous flocs	N/A	Martins *et al.*, 2003; Barbusiński and Kościelniak, 1995; Námer and Ganczarczyk, 1993;
Shape	Irregular shaped improve clarification efficiency and bridging Round, regularly shaped improves settling velocity and compression	Sphere (reduce clarification efficiency)	Shape away from sphere reduces settling velocity but improves sweep flocculation	N/A	Martins *et al.*, 2003;
Size	Medium size 200-500 μm	Too Small (no filtering effect) or too large (too porous and low density)	Balance between growth and fragmentation Settling velocity directly related to size (diameter) Anaerobic inside large flocs: break-up Surface shear increases with floc diameter	0.5 to 1000 μm	Spicer and Pratsinis, 1996; Kolmentz *et al.*, 2003 ; Randall *et al.*, 1992; Wilén, 1999;
Surface charge	Higher charge	Lower charge	Negative surface charge provides negative adsorption sites to bind to positive metal cations Surface charge influences filament length (coil or straight)	-20 to -50 mV; -15 to -30 mEq/gSS	Bux and Kasan, 1994b; Liss *et al.*, 2002; Forster, 1976; Örmeci and Vesilind, 2000;
Surface solvent interaction (hydrophobicity)	Hydrophobicity larger (hydrophobic surface)	Hydrophobicity smaller (hydrophilic surface)	Cells and flocs adhere easier to hydrophobic surface	N/A	Liss *et al.*, 2002; Agridiotis *et al.*, 2006;

11.7.2 Wastewater characteristics

Table 11-8 Wastewater characteristics affecting settling aspects

Parameter	Improve settling	Worsen settling	Impact description	Reference
Alkalinity	Normal alkalinity	Low alkalinity	Low alkalinity – no buffer for nitrification loss – defocculation High alkalinity increases settling rate (>500 mg/ℓ as $CaCO_3$)	Nell, 1980; Rasmussen *et al.*, 1993
Ammonia	Low ammonia concentration < 1.5mg/ℓ	Higher ammonia concentration	Nitrification bacteria attached to surface of compact flocs	Kruit *et al.*, 2002; Wanner *et al.*, 1988
Bacteria	Floc formers: filaments ratio balance	Filaments > floc-formers Floc formers > filaments	Filament growth leads to bulking and settling reduction	Tandoi *et al.*, 2006;
C: N: P or nutrient composition or trace elements	COD: N: P > 100:5:1 COD: NH_4 > 5 (nitrogen limited)	COD: N: P < 100:5:1 COD: NH_4 < 5 (carbon limited) Iron concentration low	Filaments favour N and P deficiency High C synthesis of cells and ECP production, but low C fungal growth, filaments Endogenous growth phase, filaments	Tandoi *et al.*, 2006; Nakhla and Lugowski (2003); Durmaz and Sanin (2001); Nell, 1980; Ekama *et al.*, 1997; Al-Yousfi *et al.*, 2000
Floc water	Bound floc water	Capillary water	Well formed flocs holds bound floc water, Deflocculated flocs hold capillary water, Bound water is released and decreased at low DO, Bound water is decreased at high salinity and conductivity.	Sürücü and Çetin, 1989; Forster, 1976; Sanin, 2002
FOG	No excessive quantities	Fats oils grease (FOG) from industrial sources	FOG coat flocs, and interfere with bacterial activity structure FOG covers porosity channels, and hinders water flow and entrap air bubbles	Gerardi, 2002
Metal cations	Divalent (Copper > Calcium > Magnesium selectivity to floc matrix) Divalent: Monovalent ratio > 0.5	Monovalent (sodium, potassium, ammonium)	Charge bridging and when by divalent ion, a larger surface area Biofloc is an ion exchange medium: monovalent ion exchange for divalent ion (Calcium instead of Magnesium or Sodium) Lower net negative surface charge and lower interparticle distance Increase floc size and density, stable structure, decrease porosity with divalent ions Binding ability of charged and uncharged groups on ECP	Murthy, 1998; Biggs *et al.*, 2001; Gerardi, 2002; Sürücü and Çetin, 1989; Tandoi *et al.*, 2006; Urbain *et al.*, 1993; Bruus *et al.*, 1992; Novak *et al.*, 2001;
MLVSS	Low active fraction	High active fraction	Settleability decreases at higher active fraction (or young sludge age)	Catunda and Van Haandel, 1992; Gerardi, 2002
Nitrate	Nitrate low < 1 mg/ℓ	Nitrate > 1 to 2 mg/ℓ (Anoxic to aerobic zone)	Filaments reduce NO_3 to NO_2 and will proliferate Floc formers reduce NO_2 to N_2 to proliferate Anoxic conditions in secondary settling tank release insoluble nitrogen gas bubbles which attach to flocs and float to surface	Hercules *et al.*, 2002; Sötemann *et al.*, 2002
Nitrogen gas	Denitrification that is completed improves compression	Denitrification not complete	Insoluble nitrogen gas adhere to bioflocs and specifically filaments, increase biofloc buoyancy	Madoni *et al.*, 2000; de Clercq, 2003
pH	Neutral pH near 7 (range 6.5 to 8.5)	Alkaline pH (pH > 8.5) or acidic pH (pH < 6.5)	No large variations in pH for stable MLSS settling, Alkaline conditions can improve settling, Filamentous fungi growth at low pH, filament proliferation when denitrification incomplete for alkalinity recovery Negative charge reduces at lower pH Deflocculation at low pH	Nell, 1980; Sürücü and Çetin, 1989; Pitman, 1975; Ekama *et al.*, 1997; Drysdale *et al.*, 2000; Gerardi, 2002;

Septicity	Increase septicity	Decreased septicity	Lower bacterial fibril charge	Gerardi, 2002
Sewage feed age	Fresh sewage (normal age) Low levels of sulphide no impact (0.5 – 2.0 mMol)	Long sewage feed age: septic sewage Acetate and sulphide: carbon sources for filaments, Sulphide from industrial sources	Filament dominance under septic conditions Deflocculation at S > 2.7 mMol	Kjellerup et al., 2001; Martinez et al., 2006; van Niekerk et al., 1987; Jenkins et al., 1984
Soaps, detergents, emulsifying agents	No excessive quantities	High concentrations industrial sources	Surface active compounds cause deflocculation of colloids, dispersed cells, small flocs, Decrease surface tension and attack perimeter of floc, Foam production and toxicity.	Kjellerup et al., 2001; Gerardi, 2002
Solids content	Normal MLSS concentration: 3000 to 6000 mg/ℓ (Extended aeration)	Low MLSS concentration High MLSS concentration	All aspects of settling related to solids content or MLSS concentration MLSS settling velocity and concentration modelled accordingly	Bhargava and Rajagopal, 1993; Catunda and Van Haandel, 1992
TDS	High TDS, specifically salinity (sodium and potassium ions) High strength: up to 0.06 M for monovalent and divalent cations	Low TDS Dilution of sample with water	High TDS: Larger floc area, elongated shape, decreased shape factor due to electrostatic and hydrophobic reactions Low TDS: Deflocculation, high turbidity Diluted sample has lower ionic strength, leads to deflocculation	Moghadam et al., 2005; Gerardi, 2002; Chaignon et al., 2002;
Temperature: long- term (seasonal variation)	Summer and early autumn (high temperature)	Winter and early spring (low temperature)	Filament growth at lower temperature ($T_r < 20°C$), M. parvicella growth only at $T_r < 20°$; Zoogloea growths more at lower T_r	Kristensen et al., 1994; Mamais et al., 2006; Al-Yousfi et al., 2000;
Temperature: short-term (diurnal variation)	Day (high Temperature)	Night (low temperature)	Physical changes to water and biofloc	Makinia et al., 2005;
Toxicants	Limited toxic concentrations	Toxic (industrial) discharges such as organic compounds e.g. phenol	Deflocculation from biofloc disintegration Large viscous clumpy bioflocs Instantaneous floc break-up	Morgan-Sagastume and Allen, 2003; Wilén, 1999; Schwartz-Mittelmann and Galil, 2000;
VFA and LCVFA	VFA and LCVFA low concentration	VFA and LCVFA concentration	Filaments use VFA to proliferate	Kruit et al., 2002;
Viscosity	Low	High	Improved MLSS settling at lower viscosity Viscosity is inversely related to T_s	Hasar et al., 2004;

11.7.3 Process and reactor configuration

Table 11-9 Process and reactor configuration affecting settling factors

Parameter	Improve settling	Worsen settling	Impact description on settling aspect	Reference
Aeration intensity	Low velocity surface aeration or bubble aeration	High velocity surface aeration or over - aeration causing turbulence	Physical floc break-up of shearing of sections High shear leads to irreversible floc size reductions	Ekama *et al.*, 1997; Biggs *et al.*, 2003; Parker *et al.*, 1996;
Aeration method	Fine bubble Surface aeration with draught tubes	Coarse bubble Point source surface aeration	No low DO tension in bubble aeration Turbulence for floc break-up	Van Huyssteen *et al.*, 1990; Ekama *et al.*, 1997
Aerobic reactor zone size	>55% to 60%	< 55 to 60%	Filament proliferate at low DO conditions and large anaerobic zones	Ekama *et al.*, 1997; Cooper *et al.*, 1995; Tandoi *et al.*, 2006; Pitman, 1991;
Anaerobic reactor zone size	Short anaerobic retention time Anaerobic reactor < 10%	Longer anaerobic retention time Anaerobic reactor > 10%	Deflocculation at long anaerobic time Filament growth at large anaerobic zone	Wilén, 1999; Cooper *et al.*, 1995;
Attached growth	Support material available for attached growth in reactor	No attached growth, only suspended growth in biofloc	Biofilm carrier material in reactor requires no RAS recycle Biofloc grow on inert particle or carrier such as foam or plastic discs, Maximum particle volume 40% to ensure complete mixing Reduce filamentous growth in biofilm due to anoxic zone	Wanner *et al.*, 1988; Ødegaard, 2000;
Combined sewers	Separate	Combined	Combined infiltration, high hydraulic loads due to storm water	Wilén, 1999;
Environmental	Quiescent conditions	Rainfall, wind	Rainfall dilute inflow through infiltration, hydraulic load Wind will enhance density currents and move surface scum	Ekama *et al.*, 1997; Van der Walt, 1998;
HRT in settling tank	As per design	Too short	Microorganism washout at low HRT over design capacity	Pretorius, 1987;
Inflow feed configuration	Discontinuous or intermittently fed Cyclic loading	Continuously fed	Substrate gradient favours floc-formers above filaments Larger stronger flocs with cyclic	Dangcong *et al.*, 1999; Wilén and Balmer, 1999;
Mixing intensity	Gentle mixing: for contact and suspension	Low intensity mixing: dead zones High intensity mixing: unwanted DO input	Bioflocs contact, induce flocculation Mixing reduce wall effects during settling tests in cylinders	Wilén, 1999; Grijspeerdt and Verstraete, 1997; Berktay, 1998;
Prefermentation	No prefermentation, (or Prefermentation depending on VFA)	Prefermented settled sewage reactor feed	*M. parvicella* store LCVFA under anaerobic conditions But 7.5 mg/ℓ VFA per 1 mg/ℓ P can minimise anaerobic zone size and improve settling	Mamais *et al.*, 2006; Cooper *et al.*, 1995;
Primary settling	Primary settling No primary settling	No primary settling Primary settling	Remove some RBCOD and VFA which simulates growth of filaments such as *Microthrix parvicella*	Mamais *et al.*, 2006; Tandoi *et al.*, 2006;

			Nutrient rations change	
Reactor configuration	Plug flow or SBR or oxidation ditch Declining growth phase	Completely mixed reactor Log growth phase	Spatial substrate gradient in plug flow favours floc-formers Temporal substrate gradient SBR favours floc-formers Completely mixed reactor has backmixing and mobile organisms proliferate	Droste, 1997; Janczukowicz *et al.*, 2001; Azimi and Horan, 1991; van Niekerk *et al.*, 1987; White, 1976; Pitman, 1975; Kruit *et al.*, 2002
Reactor surface flow	Free surface flowing Reactor zone surface organism removal Mechanical foam removal	Internal recirculation of foam/scum microorganisms Trapped foam	Remove scum/foam organisms out of system Surface layers with foam / floating matter retention age > sludge age of bulk activated sludge : due to trapping and recirculation, cause foam proliferation Surface aerators have surface pump-back action to return foam upstream	Tandoi *et al.*, 2006; Blackbeard *et al.*, 1986; Madoni *et al.*, 2000; Pitman, 1991; Pitman, 1996
Selectors	Sectionalised selector short HRT: 5 minutes in 3 sections Selectors loading: 100 mg COD. g MLSS .h^{-1}	HRT not suitable Too large or too small selector Selector loading too low or high	High VFA uptake by floc-formers, substrate gradient favours floc-formers Flocformers are fast-growers, filaments are slow-growers Too small selector: substrate into reactor, Too large selector: removal of substrate too large	Tandoi *et al.*, 2006; Kruit *et al.*, 2002; Cenens *et al.*, 2000; Van Niekerk *et al.*, 1987;
Settling tank design	Deep tank (>5m): sweep flocculation Large centre well: reflocculation Sloped floor: fast sludge removal Baffles: surface scum removal	Shallow tank (< 5m depth) Small centre well Flat floor: slow sludge removal No baffles	sweep flocculation reflocculation denitrification surface foam	Parker *et al.*, 1996;
Settling tanks configuration	Tanks in series	Tanks in parallel	Micro-organism selection occurring in tanks by removing filaments in 1st tank	Kim *et al.*, 1998;
Simultaneous precipitation	Precipitation	No precipitation	C and P nutrient deficiencies and filamentous growth from precipitation Stabilisation time required to restore settling	Ødegaard, 2000; Ericsson and Eriksson, 1988; Janssen *et al.*, 2002;
Turbulence: hydraulic jump or pumping	Low turbulence and gentle transfer (Can enhance settling if DO is increased)	High turbulence, high pump impeller velocity	Biofloc deflocculate during shear, Break-up more during aggregation	Wilén, 1999;
Ultrasound	Sonification time low (about 180s) at 22kHz and 16 μm,	Sonification time high (about 360s) at 22kHz and 16 μm	Ultrasonic cavitation bubbles can destroy filaments with Increased settling velocity, lower SVI, lower hydration, but at high intensity shear cause cell destruction, dispersed floc, and irreversible deflocculation	Bień *et al.* 2005; Wünsch *et al.*, 2002;

11.7.4 Operational factors

Table 11-10 Operational factors affecting settling factors

Parameter	Improve settling	Worsen settling aspect	Impact description on settling aspect	Reference
Additives: Synthetic polymers, inorganic coagulants, anti-foaming agents, weighing agents	Structure change to compact dense flocs; Hydrophobicity increase	Overdosing of these additives, and introduction of new constituents	Fast changes within 30 to 45 min., ideal as short-term standby or emergency use but temporary measure only (e.g. 4 hr) with relative high cost of chemicals Ballasting effect, floc restructuring, thin biofilm Initial lag period, SVI, ISV, SV_{30} improvement	Wilén, 1999; Agridiotis et al., 2006; Patoczka et al., 1998; Vanderhasselt and Verstraete, 1999; Vanderhasselt et al. (1999a);
Anaerobic time	Shorter anaerobic Anaerobic reactor < 10%	Longer anaerobic time	Deflocculation at long anaerobic time Filament growth at large anaerobic zone	Wilén, 1999; Cooper et al., 1995;
Anoxic reactor outlet nitrite	Low NO_2 concentration	High NO_2 concentration (>1 to 2 mg NO_2/ℓ)	Bulking sludge due to high nitrite concentration Control the a- recycle according to denitrification potential	Lilley et al., 1997;
Bactericide	Chlorine, hydrogen peroxide, ozone Lower SVI and effluent suspended solids, higher settling velocity	Overdosing of bactericide: effluent SS increase, Floc formers can be affected Introduction of new constituents	Non-specific bulking control by filament killing Temporary solution High cost 2 to 8 mg Cl_2/(gMLSS.d) for 19 days reduces DSVI from 230 to 48 mℓ/g	Seka et al., 2001; Van Leeuwen and Pretorius; 1988; Wentzel et al., 1988;
DO concentration	DO = 2 mg/ℓ over 24 hr in whole aerobic reactor (ideally), or minimum 1 mg/ℓ over 24 hours in all sections of aerobic reactor	Over aeration (DO>3 mg/ℓ) Under aeration (DO <1 mg/ℓ) in zones or certain times, Oxygen limitation (DO< 0.5 mg/ℓ) Intermittent or alternating aeration	Increase DO: mechanical or point source aerators turbulence will shear sensitive flocs, Filament dominance, Deflocculation, irregular weak flocs, low ECP production; low adsorption colloids; porous flocs; anaerobic period determines deflocculation, Diffusional limitation inside flocs at a low DO, DO according to organic loading [2 mg/ℓ DO for 0.5 kg COD/kg MLVSS/d], Higher DO (>2 mg/ℓ) create large stable compact flocs, High DO and over-aeration cause foams; High DO in a-recycle to anoxic zone reduces BNR efficiency.	Jones and Franklin, 1985; Kabouris and Georgakakos, 1990; Kjellerup et al., 2001; Martins et al., 2003; Tandoi et al., 2006; Wilén, 1999; Wilén and Balmér, 1999; Pitman, 1991;
Organic loading	Organic loading high	Organic loading low Organic loading overload (long-term)	Filament dominance at low substrate, larger surface: volume Floc formers have higher substrate utilisation rates Floc formers cannot absorb too high substrate loading: break up Diffusional resistance inside flocs for high loading: break up Size of flocs increase with increased loading	Jones and Franklin, 1985; Tandoi et al., 2006; Barbusiński and Kościelniak, 1995; Pitman, 1975;
Plant stability	Start-up	Steady state	Start up unstable, microorganisms need period of a few sludge ages to acclimatise Bioflocs flocculate poorly in log growth phase when compared to declining growth phase	Kolmetz et al., 2003;
RAS recycle rates	High RAS recycle (>1)	Low RAS recycle (<1)	High contact for flocculation; Prevent clarifier denitrification	Cloete and Muyima, 1997;
Sludge age (SRT)	SRT high (>15 days for EPBNR)	SRT low (< 10 to 15 days EPBNR), or very high	High sludge age (15 to 20 days): Biofloc more stable, compact, floc surface more hydrophobic, less negatively charged, less hydrated, large ECP layer gives smoother surface and protective coat; Higher life forms scavenge effluent dispersed fragments; High sludge age: Filament dominance at very high sludge age; Low sludge age: weak buoyant floc shear easily no structure;	Liss et al., 2002; Liao et al., 2001; Akça et al., 1993; Kaewpipat and Grady, 2002; Nakhla and Lugowski, 2003; Gerardi, 2002;

11.7.5 Settleability failure identification

Table 11-11 Settleability failure identification guidelines

(adapted from Jenkins *et al.*, 1986)

Name of problem	Nature of problem / alternative names	Characterization of problem	Reasons for problem
Dispersed floc	Flocs do not aggregate, small clumps (10 to 20 µm) or single cells (Dispersed growth, straggler flocs)	Turbid effluent No or very low zone settling velocity Low sludge age from loss of sludge in settling tank	Low amount of ECP High organic loading Start-up of plant or low sludge age Toxicity event
Filamentous floc	Strong, large flocs Filaments extend from flocs into bulk solution, interfloc bridging Interfere with settling and compression Filaments cause foaming (*Norcadia* or *Microthrix parvicella*) (filamentous bulking)	Clear effluent Poor thickening and low RAS concentration Increased sludge blanket High SVI and high SV_{30}	Nutrient deficiency High organic loading / shock load Low DO concentration Low pH Septicity or high sulphide levels
Floating flocs	Bio surfactants or surface active agents, from foam forming filaments Floating foams from hydrophobic filaments, accumulate on surfaces Bacteria causing foams dominate	Foams visible in aerator and settling tank, aesthetic Carryover cause high nutrient content in effluent Low density billowy foam or heavy dense foam	Internal circulation of material and not removed from system Low temperature or seasonal changes Low sludge age Low DO concentration High organic shock load Industrial surface active agents
Non-filamentous floc	Sludge flocs become more hydrated and reduce density Bound water in sludge flocs due to hydrophilic biopolymers Exocellular slime or jelly-like characteristics of sludge solids (viscous bulking, hydrous zoogloeal bulking, non-filamentous bulking)	Low settling velocity Low compression and low RAS concentration Increased sludge blanket High SVI	Low sludge age Nutrient deficiency High organic loading / shock load Low DO concentration
Pin floc	Compact dense flocs settle rapidly, leaving lighter flocs in suspension Weak, small flocs Break up of large flocs (Pin-point floc, unsettleable floc)	Cloudy turbid effluent with fine particles High zone settling velocity Few filaments Low SVI	High DO concentration High turbulence from aerators or hydraulic jumps High shear High sludge age Low organic loading Absence of filaments
Rising flocs	Gas entrainment or gas release gives buoyancy to flocs Bubble aeration MLSS supersaturated with air Denitrification of nitrate in blanket with insoluble nitrogen gas release Long retention in settling tank make sludge anaerobic with gas release	Settle rapidly and compact well Flocs or clumps of flocs rise rapidly to surface, within 30 minutes to interfere with SVI test	Low RAS flow rate High sludge blanket or tank floor accumulation Reactor denitrification incomplete

11.7.6 Settleability impacts due to filamentous micro-organism dominance

Table 11-12 *Microthrix parvicella* dominance and settling effects in a NDBEPR process

(adapted from Tandoi *et al.*, 2006)

Parameter	*Microthrix parvicella* compared to floc-formers	*Microthrix parvicella* dominance impact on settling
Biocides	20 to 200 kgCl$_2$/kgSS effective for *Microthrix parvicella*; 2 kg Cl$_2$/kg SS normal dosing for other filaments	Hydrophobic cell wall prevents penetration to reduce *Microthrix parvicella* dominance
Cell wall	*Microthrix parvicella* hydrophobic	Supports formation of stable foams, Scum and bulking in same reactor attributed to *Microthrix parvicella*
Electron acceptors	*Microthrix parvicella* uses DO, NO$_3$, NO$_2$	All reactor zone grower (anaerobic, anoxic, aerobic) and related settleability deterioration
Maintenance energy	*Microthrix parvicella* has lower requirements, and can adapt and withstand environmental stress	Advantage under starvation conditions (low substrate loading such as C, N, O) leads to proliferation and related settleability deterioration
Oxygen affinity	*Microthrix parvicella* has high affinity	Advantage during micro-aerobic conditions During low DO concentration or plant overload More prevalent in surface aeration with low DO concentration sections
pH	Stimulated *Microthrix parvicella* growth alkaline pH (>8)	NDBEPR recovers alkalinity for resulting higher pH, and related settleability deterioration
Slowly biodegradable substrate	*Microthrix parvicella* grows well with SBCOD, and also a specialised lipid consumer	Kinetic selectors are not effective to reduce *Microthrix parvicella* dominance
Sludge age	Enhanced *Microthrix parvicella* growth at long sludge ages (>10 days)	NDBEPR process sludge age above 15 days, and related settleability deterioration
Strains	Numerous	Contradictory information; Difficult to isolate and cultivate
Symptoms	Varied indications makes identification difficult	Bulking and scum formation in same reactor
Temperature	Enhanced *Microthrix parvicella* growth at 12- 15°C (winter temperatures) *Microthrix parvicella* growth stops above 20°C (summer temperatures)	Seasonal / periodic dominance, and related long-term changes in settleability
Volatile fatty acids	Enhanced *Microthrix parvicella* growth with LCVFA in anaerobic reactor zones	LCVFA enriched settled sewage feed from prefermenters; *Microthrix parvicella* proliferation from anaerobic reactor in NDBEPR process and related settleability deterioration

Appendix H: Summary of regression model variable results

Table 11-13 Regression variable results

Parameter	Residual sum of squares (absolute)	Standard error of estimate	Proportion of variance explained [%]	variable	Value	Standard error	t-ratio	p value	95% confidence interval		
									95% (+/-)	Lower limit	Upper limit
SVI	33051.9430	20.0767	71.0372	a	872.4200	159.1041	5.48	0	316.5058	555.9142	1188.9258
				b	-4624176.0614	445895.8905	-10.37	0	887020.6949	-5511196.7563	-3737155.3665
				c	4823.4020	1611.5791	2.99	0.0037	3205.9143	1617.4878	8029.3163
t_umax	2419.6831	5.4322	70.2409	a	239.5624	43.0489	5.56	0	85.6372	153.9252	325.1996
				b	-1290679.9382	120646.3577	-10.70	0	240001.7994	-1530681.7375	-1050678.1388
				c	939.9347	436.0461	2.16	0.034	867.4264	72.5082	1807.3611
u_max	7.7978	0.3084	58.9421	a	-9.30	2.44	-3.81	0.0003	4.86	-14.16	-4.44
				b	57454.30	6848.89	8.39	0	13624.50	43829.76	71078.76
				c	-39.8603	24.75	-1.61	0.11	49.24	-89.10	9.38
u_ave	0.3879	0.0688	75.5813	a	-2.89	0.55	-5.31	0	1.08	-3.98	-1.81
				b	18433.81	1527.63	12.07	0	3038.92	15394.90	21472.74
				c	-15.18	5.52	-2.74	0.007	10.98	-26.16	-4.20
h	94532.14	33.9535	76.0927	a	1793.96	269.07	6.67	0	535.27	1258.69	2329.23
				b	-9200670.30	754092.67	-12.20	0	1500116.54	-10700786.85	-7700553.76
				c	7744.02	2725.48	2.84	0.006	5421.80	2322.23	13165.82
u1	2.4349	0.1723	32.0137	a	-1.1851	1.3656	-0.86	0.388	2.7166	-3.9018	1.5315
				b	14418.7348	3827.1866	3.77	0.0003	7613.4223	6805.31	22032.1571
				c	-31.9946	13.8324	-2.31	0.023	27.5168	-59.5115	-4.4778
u2	4.2432	0.2275	59.0884	a	-2.6708	1.8027	-1.4815	0.1423	3.5861	-6.2570	0.9153
				b	33145.3653	5052.1882	6.5606	0	10050.3181	23095.0472	43195.6834
				c	-74.7660	18.2598	-4.0946	0.0001	36.3244	-111.0903	-38.4416
u3	1.4572	0.1333	62.3507	a	-3.6732	1.0564	-3.4770	0.00081	2.1016	-5.7748	-1.5717
				b	25152.0675	2960.7089	8.4953	0	5889.7381	19262.3293	1041.8057
				c	-26.7192	10.7007	-2.4969	0.0145	21.2870	-48.0062	-5.4322
u4	0.6809	0.0911	59.5538	a	-4.1828	0.7222	-5.7921	0	1.4366	-5.6194	-2.7462
				b	19564.9547	2023.8724	9.6671	0	4026.09	15538.8655	23591.0440
				c	3.4218	7.3148	0.4678	0.6411	14.5513	-11.1295	17.9731
u5	0.5620	0.0838	33.6828	a	-3.3897	0.6561	-5.1666	0	1.3051	-4.6948	-2.0846
				b	11822.7573	1838.6975	6.4300	0	3657.7208	8165.0364	15480.4781
				c	18.7500	6.6455	2.8215	0.006	13.2199	5.5301	31.9700
u6	0.3475	0.0651	29.5519	a	-2.6835	0.5159	-5.2019	0	1.0262	-3.7097	-1.6573
				b	8411.5793	1445.7612	5.8181	0	2876.0528	5535.5265	11287.6321
				C	18.8984	5.2253	3.6167	0.00051	10.3948	8.5037	29.2932